OPTIMIZATION OF SINGLE REFRIGERANT CONOCOPHILLIPS LNG CASCADE PROCESS

Naken Saetang

A Thesis Submitted in Partial Fulfilment of the Requirements
for the Degree of Master of Science
The Petroleum and Petrochemical College, Chulalongkorn University
in Academic Partnership with
The University of Michigan, The University of Oklahoma,
Case Western Reserve University, and Institut Français du Pétrole
2018

Thesis Title: Optimization of Single Refrigerant ConocoPhillips LNG Cascade Process

By: Naken Saetang

Program: Petroleum Technology

Thesis Advisors: Asst. Prof. Uthaiporn Suriyapraphadilok

Prof. Miguel J. Bagajewicz

Accepted by The Petroleum and Petrochemical College, Chulalongkorn University, in partial fulfilment of the requirements for the Degree of Master of Science.

.... College Dean

(Prof. Suwabun Chirachanchai)

Thesis Committee:

....

(Asst. Prof. Uthaiporn Suriyapraphadilok)

....

(Prof. Miguel J. Bagajewicz)

....

(Prof. Thirasak Rirksomboon)

....

(Asst. Prof. Chanin Panjapornpon)

ABSTRACT

An LNG cascade process operates under high pressure and extremely low temperature to liquefy natural gas, requiring very high work input to the compressors. This thesis performed the optimization of the single refrigerant ConocoPhillips LNG process by a global optimization technique based on the domain and image partitioning methodology (Faria and Bagajewicz, 2012) to minimize work input to the system. The procedure consists of an NLP upper bound and MILP lower bound models. The lower bound model was formulated by discretizing and linear relaxation of the upper bound non-linear equations by assigning new integer variables and a set of linear constraints. To guarantee the global optimum, the difference between objective function of the upper and lower bound model must be small. The ConocoPhillips LNG process consists of three liquefaction loops which are propane, ethylene and methane loops. Thermodynamic properties prediction model consisted of a metamodel based on quadratic polynomials regressed from Peng-Robinson EOS. Several minimum approach temperatures were performed and the results showed that the lowest approach temperature of 3 K was the most efficient case that gave the lowest refrigerant flowrates, and the lowest total work input to the compressors. A simple cost analysis was performed both CAPEX and OPEX. The problem was solved in GAMS and the results were verified by PRO/II simulation software.

บทคัดย่อ

นเดนทร์ แซ่ตั้ง : การเพิ่มประสิทธิภาพของระบบหล่อเย็นแก๊สธรรมชาติของระบบทา
ความเย็นที่ใช้สารทำความเย็นแบบเดี่ยว (Optimization of Single Refrigerant ConocoPhillips
LNG Cascade Process) อ. ที่ปรึกษา : ผู้ช่วยศาสตราจารย์ ดร. อุทัยพร สุริยประภาดิลก และ
ศาสตราจารย์ ดร. มิเกล เจ บากาเจวิซ 125 หน้า

ระบบทำความเย็นของแก๊สธรรมชาติเหลวเป็นระบบที่ดำเนินการในสภาวะความดัน
สูงและอุณหภูมิต่ำ ส่งผลให้ต้องใช้งานปริมาณสูงในการ วิทยานิพนธ์ฉบับนี้นำเสนอการหาค่าที่
เหมาะสมของระบบทำความเย็นแก๊สธรรมชาติเหลวโคโนโคฟิลลิปส์ (ConocoPhillips) ด้วย
วิธีการแบ่งช่วง (Domain and Image Partitioning Method) เพื่อหางานที่ต่ำที่สุด วิธีการนี้ประ
ด้วยแบบจำลองขอบบน (Upper Bound model) เป็นแบบจำลองการโปรแกรมที่ไม่เป็นเชิงเส้น
และแบบจำลองขอบล่าง (Lower Bound Model) เป็นแบบจำลองการโปรแกรมเชิงเส้นผสมซึ่ง
สร้างมาจากการนำสมการไม่เชิงเส้นของแบบจำลองขอบบนมาแบ่งช่วงตัวแปรและแปลงเป็น
สมการเชิงเส้นผสมด้วยการกำหนดตัวแปรจำนวนเต็ม (Interger Variables) และเพิ่มเติม
สมการกำหนดขอบเขตชนิดเส้นตรง การหาคำตอบของแบบจำลองขอบบนและขอบล่าง
นำมาใช้เพื่อเป็นการยืนยันคำตอบว่าเป็นคำตอบที่ดีที่สุดที่แท้จริง (Global Optimum Solution)
โดยความต่างระหว่างคำตอบของแบบจำลองขอบบน และแบบจำลองขอบล่างจะต้องมีค่า
ใกล้เคียงกัน ระบบทำความเย็นแก๊สธรรมชาติเหลวโคโนโคฟิลลิปส์ประกอบด้วยระบบทำความ
เย็นสามระบบได้แก่ ระบบโพ-รเพน ระบบเอธีลีน และระบบมีเทน แบบจำลองเป็นแบบจำลอง
ของระบบสมการกำลังสองที่ได้มาจากสมการถดถอยซึ่งมีค่าอ้างอิงจากสมการสภาวะของ
Peng-Robinson การเปลี่ยนผลต่างอุณหภูมิที่ต่ำที่สุดถูกนำมาใช้เป็นกรณีศึกษา และผลลัพธ์
จากแบบจำลองแสดงให้เห็นว่าค่าผลต่างอุณภูมิที่ต่ำที่สุดที่ 3 เคลวิน จะทำให้ระบบมีสภาวะ
การดำเนินงานที่ดีที่สุดและมีอัตราการไหลของสารทำความเย็นที่ต่ำที่สุด ส่งผลให้งานที่ใช้ใน
ระบบมีค่าต่ำที่สุด กรณีศึกษาต่าง ๆ จะถูกนำมาคำนวณต้นทุน และค่าใช้จ่ายในการดำเนินการ
ผลลัพธ์ถูกคำนวณด้วยโปรแกรม GAMS และนำมาตรวจสอบความถูกต้องด้วยโปรแกรม
จำลอง PRO/II

GRAPHICAL ABSTRACT

```
                    ┌──────────────┐
                    │    Start     │
                    └──────────────┘
                           │
                           ▼
          ┌──────────────────────────────────┐
          │       Quadratic Regression        │
          └──────────────────────────────────┘
                           │
                           ▼
          ┌──────────────────────────────────┐
          │   Construct NLP Upper Bound Model │
          └──────────────────────────────────┘
                           │
                           ▼
          ┌──────────────────────────────────┐
          │        Linear Relaxation          │
          └──────────────────────────────────┘
                           │
                           ▼
          ┌──────────────────────────────────┐
          │       Set Number of Intervals     │◄─────┐
          └──────────────────────────────────┘      │
                           │                         │
                           ▼                         │
          ┌──────────────────────────────────┐      │
          │     Run MILP Lower Bound Model    │      │
          └──────────────────────────────────┘      │
                           │                         │
                           ▼                         │
          ┌──────────────────────────────────┐      │
          │  Initialize Upper Bound Model by  │      │
          │    Lower Bound Model solution     │      │
          └──────────────────────────────────┘      │
                           │                         │
                           ▼                         │
                      ◆ Gap between ◆                │
                   ◆ objective function ◆            │
                  ◆  of UB & LB less    ◆   No   ┌──────────────┐
                   ◆  than tolerance  ◆ ────────►│  Increase    │
                      ◆            ◆              │ number of    │
                           │                     │  intervals   │
                          Yes                    └──────────────┘
                           ▼
          ┌──────────────────────────────────┐
          │    Obtain global optimum solution │
          └──────────────────────────────────┘
                           │
                           ▼
          ┌──────────────────────────────────┐
          │          Verify Result            │
          └──────────────────────────────────┘
                           │
                           ▼
                    ┌──────────────┐
                    │     End      │
                    └──────────────┘
```

ACKNOWLEDGEMENTS

TABLE OF CONTENTS

LIST OF TABLES

LIST OF FIGURES

CHAPTER I
INTRODUCTION

Natural gas has gained more popularity in the past decade because of its low cost and clean energy. To transport natural gas where no gas pipeline network is unavailable, liquefaction of natural is the most economical solution. The condensation of natural gas can reduce volume to 600 times which make natural gas transportable to any places. To cool down natural gas to a liquid, namely liquefied natural gas (LNG) it requires large cooling systems and involves with several refrigerants, which can be single or mixed refrigerant. The combination of multiple loops cooling cycle is called a cascade cooling system. Conoco-Phillips process is one of the LNG cascade systems employing three types of refrigerant including propane, ethylene and methane. The liquefaction process requires a high work input to the compressors and an optimization is needed to reduce work input and suggests an optimal set of operating pressure to those compressors.

Optimization is a method which is used to obtain the desirable solution by solving a set of equations subject to constraints. Equations can be in any form such as linear or non-linear equations. Faria *et al.* (2011) developed an optimization methodology by using a bound contraction method. By substituting non-linear equations with a new variable and adding new constraints, a linear model was developed. The solution of the linear model is used as a lower bound of the problem and the solution of the problem is from the original non-linear or the upper bound model of the problem. When the gap between the upper and lower bound models is acceptable, the problem can reach optimal condition. Ounahasaree *et al.* (2016) and Saeneewong NaAyutthaya *et al.* (2016) demonstrated the bound contraction techniques through the systems of gasoline blending and heavy oil blending problems.

The main objective in this research is to optimize work input of a single and mixed refrigerant LNG cascade processes by using partitioning methodology which is one of the global optimization methods. Partitioning methodology is applied with binary variables to improve lower bound and upper bound of the system. Improvement of bound will lead to an optimal solution. Mathematical model is introduced by energy and entropy balances which are based on thermodynamics laws. The models are

optimized by General Algebraic Modeling System (GAMS). GAMS will provide the minimum work input within the best possible solution. LNG process is simulated in Simsci PRO/II to verify the GAMS solution.

CHAPTER II
THEORETICAL BACKGROUND AND LITERATURE REVIEW

2.1 Liquefied Natural Gas

Nowadays fossil fuel is the main energy resource around the world. Natural gas, one type of the fossil fuels, has been increasing in demand around the global due to its low price and clean combustion. To transport natural gas if a pipeline system is not available, liquefying natural gas to a liquid state is necessary. As a liquid, the volume of natural gas is reduced about 600 times of its volume at a standard condition. Not only is volume affected but energy density of natural gas also increases. In the liquid form, natural gas can be transportable to any places in the world. The liquefied natural gas is called LNG

2.2 LNG Process
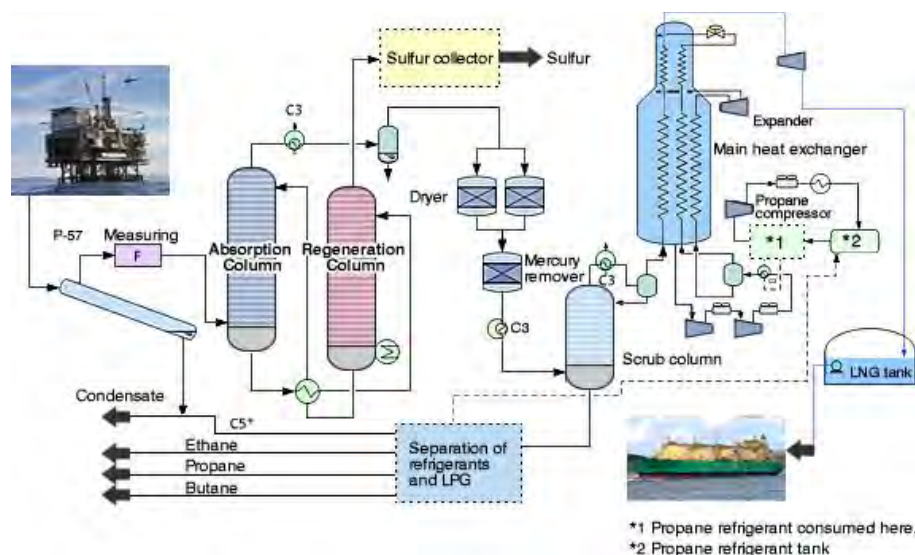
Figure 2.1 The schematic of liquefied natural gas process (Corporation, 2009).

Figure 2.1 shows the schematic of liquefied natural gas process. There are many units involved in the liquefied natural gas process. Most LNG plants contain 4 steps to produce LNG. First, pretreatment process. Natural gas from the production wells goes directly to a pretreatment process which will remove any undesired substances especially mercury. Second, an acid gas removal process is used after pretreatment process which will remove environmental pollutants such as carbon dioxide and hydrogen sulfide. These pollutants do not only cause pollution also have ability to corrode equipment. Third, a dehydration process is used to remove water from natural gas since water can be frozen and plug the process. Finally, the liquefaction process is the main process in the plant and it is used to liquefied natural gas into liquid. Liquefied natural gas is sent to storage and the temperature is maintained at its boiling point before transporting to customers. This work focuses on an optimization of commercial liquefaction processes (Austbø *et al.*, 2014). Specifications for LNG are tabulated in Table 2.1.

Table 2.1 The specification of LNG (www.uniongas.com, 2017)

Component	Range (mole %)
Methane	87.0 - 97.0
Ethane	1.50 - 9.00
Propane	0.10 - 1.50
iso - Butane	0.01 - 0.30
normal - Butane	0.01 - 0.30
iso - Pentane	trace - 0.04
normal - Pentane	trace - 0.04
Hexanes plus	trace - 0.06
Nitrogen	0.20 - 5.50
Carbon Dioxide	0.05 - 1.00
Oxygen	trace - 0.1
Hydrogen	trace - 0.02
Total	100

2.2.1 Commercial LNG Process

2.2.1.1 ConocoPhillips LNG Cascade Process

The ConocoPhillips LNG cascade process consists of three section which are propane loop, ethylene loop and methane loop as illustrated in Figure 2.2. At propane loop, propane is used to cool compressed ethylene, methane and natural gas to -42 °C. Only ethylene is condensed where methane and natural gas are in the vapor phase. At ethylene loop, ethylene is used as refrigerant to condense compressed methane and natural gas to -95 °C. Finally, methane loop, methane is used as refrigerant in the last loop where natural gas is subcooled to -155 °C. High pressure LNG is sent to expander and separator unit to decrease pressure and separate vaporized liquid before sending to storage (Company, 2017).
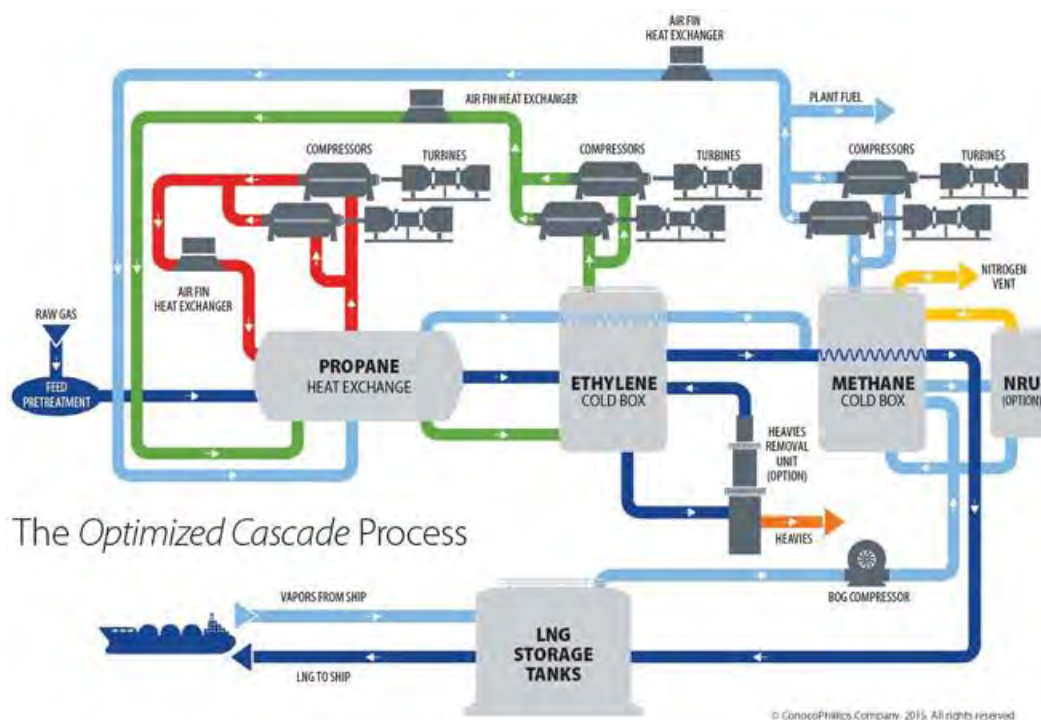
Figure 2.2 The schematic of ConocoPhillips liquefied natural gas process (Company, 2017).

2.2.1.2 Air Products LNG Process

The air products LNG process consists of two parts which are C3 pre-cooling loop and mixed refrigerant loop (see Figure 2.3). In pre-cooling loop, propane is compressed to high pressure stage and used as refrigerant in this loop. Natural gas is cooled down to -35 °C in this step. Next, cooled natural gas goes to mixed refrigerant cycle. Mixed refrigerant is compressed to high pressure stage and fed to shell of shell and tube heat exchanger. The final temperature of the natural gas is between -150°C and -162°C. AP-X is an upgrade version of normal air products system. The process is based on the integration of LNG sub-coolers with nitrogen coolant.
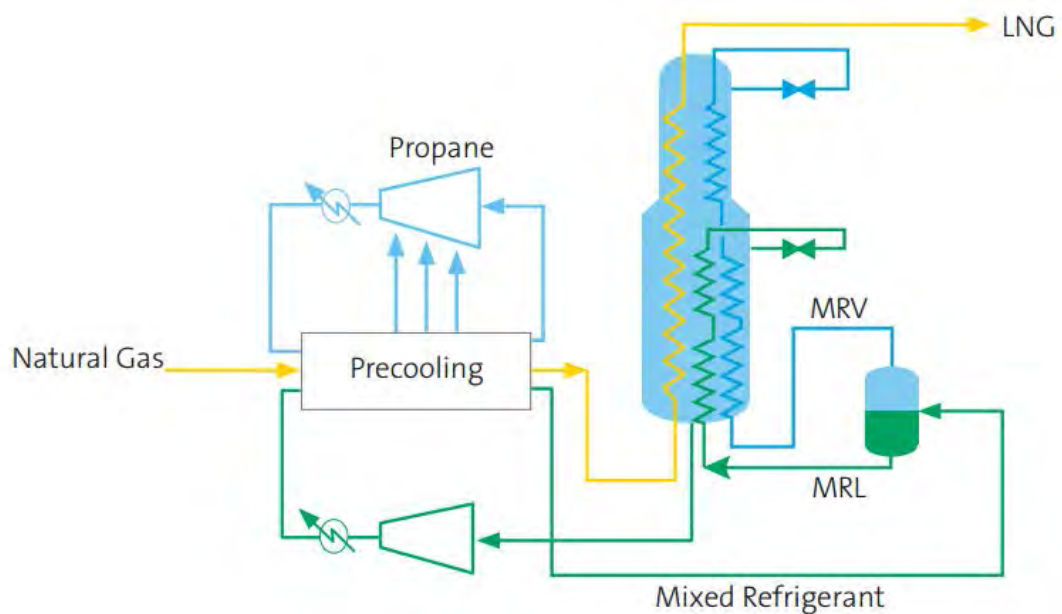
Figure 2.3 The schematic of air products liquefied natural gas process (Air Products and Chemicals, 2017).

2.3 Fundamental Concept

      2.3.1 <u>Thermodynamic Concept</u>

            2.3.1.1 First Law of Thermodynamics

            The first law of thermodynamics is also known as the conservation of energy principle. Energy can be neither created nor destroyed during a process. It can only change its forms. It can be described by the following equation (Cengel *et al.*, 2015).

$$\Delta U = Q + W \qquad\qquad \text{Eq. 2.1}$$

Where ΔU is the change of internal energy in the system

      Q is net quantity of heat transfer in the system

      W is total work done to system

            2.3.1.2 Second Law of Thermodynamics

            Only first law of thermodynamics cannot ensure that the process will actually take place. Second law will ensure the occurrence and explain direction of the process. The second law of thermodynamics states that the total entropy of an isolated system can only increase over time. It can remain constant in ideal cases where the system is in a steady state or undergoing a reversible process. It can be described by the following equation.

$$\Delta S = S_2 - S_1 = \int_1^2 \left(\frac{\delta Q}{T}\right)_{reversible} \qquad\qquad \text{Eq. 2.2}$$

            Not only entropy but second law can also express in other ways. Kelvin-Planck also stated the second law of thermodynamics as follows: "It is impossible for any device that operates on a cycle to receive heat from a single reservoir and produce a net amount of work."

            This statement is widely used in designing a heat engine. Carnot also has his statement on the second law of thermodynamics. This statement is used in the calculation of Carnot engine. "The efficiency of a quasi-static or reversible

Carnot cycle depends only on the temperatures of the two heat reservoirs, and is the same, whatever the working substance. The efficiency of an irreversible heat engine is always less than the efficiency of a reversible one operating between the same two reservoirs."

2.3.1.3 Third Law of Thermodynamics

Third law of thermodynamic is used to provide the absolute reference point of entropy. The entropy of a pure crystalline substance at absolute zero temperature is zero. This statement is feasible for pure crystalline substances. This is because the non-pure crystalline has more than one molecular configuration which leads to uncertainty of microscopic state of matter.

2.3.1.4 Diagram

A pressure enthalpy diagram is used to show a relationship between pressure and enthalpy of each substance. This diagram is widely used in a refrigeration system.
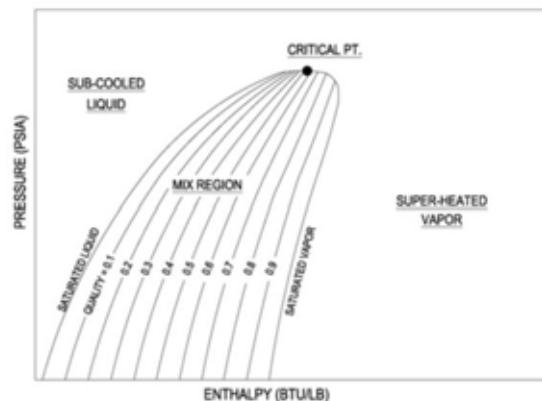
Figure 2.4 Pressure enthalpy diagram (Cengel *et al.*, 2015).

Figure 2.4 shows the structure of a Ph diagram. An envelope separates the diagram into three regions. First, the sub cooled liquid region represents a liquid state of the substance. Second, the liquid vapor mixed region takes place inside the envelope of the diagram. It represents the occurrence of both liquid and vapor in

the system. The mixed region is the phase change region, where any addition of enthalpy will cause additional liquid to vaporize instead of increasing the temperature. Lines in between the envelope represent the amount of liquid existed in the system. Third, the superheated vapor region represents the vapor state of the substance.

The temperature-entropy diagram is used to show a relationship between temperature and entropy of each substance.
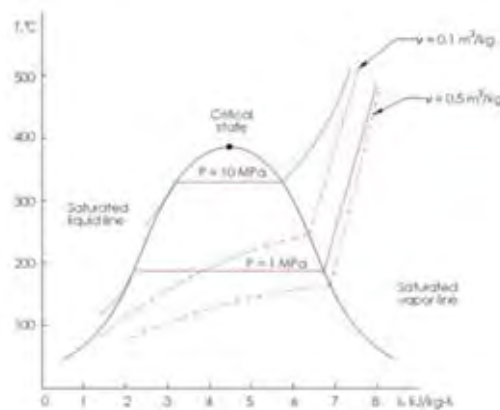
Figure 2.5 Temperature entropy diagram (Cengel *et al.*, 2015).

Figure 2.5 shows the structure of a Ts diagram. This diagram is used to show how a change in entropy can affect the temperature of a pure substance when that substance is kept at a constant pressure or specific volume. The area under the curve represent the heat transfer that took place during the process.

A cooling curve is a line that shows the change in phase of a matter. It can be changed from a solid phase to a gas phase or a liquid phase to a solid phase, as illustrated in Figure 2.6.
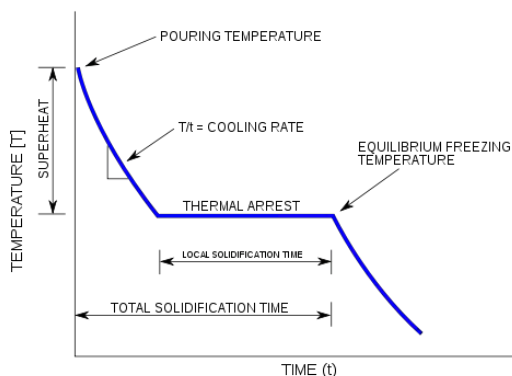
Figure 2.6 Cooling curve (Cengel *et al.*, 2015).

A cooling curve is plotted between the temperature of a matter and time. An initial point of the curve stats at pouring temperature which is a starting temperature of the matter. Slope of the graph is called a cooling rate which is change of temperature corresponding to time. Phase change occurs at the thermal arrest zone where the temperature is constant. Solidification or the liquid fraction is complete when temperature start to drop again.

2.3.2 Vapor Compression Refrigeration System

Typically, heat will transfer to direction of a decreasing temperature, from a high temperature zone to a low temperature zone. This heat transfer process occurs naturally without any devices. The use of this process is not popular in industry because it does not give a significant amount of energy. Many industries need to go beyond what a natural heat transfer can do. A reversed heat transfer process is introduced to carry out these jobs. However, a reversed process cannot occur by itself. The transfer of heat from a low temperature zone to a high temperature zone requires a specific device which is called refrigeration process.

The refrigeration process is a process which is used to transfer heat from a low temperature zone to a high temperature zone. This process uses refrigerant as a heat transfer medium. Refrigerant is a fluid which has low bubble point temperature.
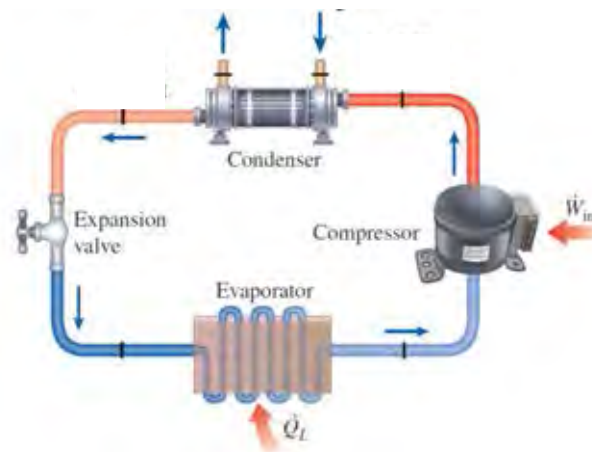
Figure 2.7 Refrigeration process (Cengel *et al.*, 2015).

Figure 2.7 shows a flow pattern of refrigerant in ideal compression refrigeration cycle. First, the heat transfers from a cold environment to an evaporator of the refrigeration process. Then, refrigerant accepts heat from the evaporator by vaporization. Vapor refrigerant is compressed and it reaches the bubble point temperature of the refrigerant. After that, refrigerant passes through a condenser which will cool down the refrigerant to a saturated liquid state. Finally, the saturated refrigerant is expanded by an expansion valve. At this stage, the refrigerant decreases in temperature and pressure before goes back to the evaporator again.

The performance of a refrigerator can be expressed in term of the coefficient of performance (COP) which can be defined as the following equation

$$COP = \frac{Cooling\ effect}{Work\ input} = \frac{Q_L}{W_{net,in}} \qquad \text{Eq. 2.3}$$

Where Q_L is heat input at an evaporator

$W_{net,in}$ is total work input at a compressor

Refrigeration process can be categorized according to the number of stages in a process such as a single stage, multi stages and a cascade process.

2.3.3 Mathematical Concept

A mathematical model is used in a commercial program to achieve the solution. There are several types of models which are used for different kinds of function. These following models are widely used in the chemical engineering field.

2.3.3.1 Linear Programming (LP)

Linear programing is a method to achieve the best outcome in mathematical model which is represented by a linear relationship. Normally, a linear programing is used to optimize the objective function subjected to linear equality and linear inequality constraints. The linear program can be expressed as follows.

$$Maximize\ or\ minimize\ \ cx$$
$$subject\ to\qquad\qquad Ax\ \alpha\ b$$
$$L \leq x \leq U,$$

2.3.3.2 Nonlinear Programming (NLP)

Nonlinear programing is usually found in many situations. Normally, equations come in terms of nonlinear equations. It is the process of solving an optimization problem defined by a system of equalities and inequalities where some of the constraints or the objective function are nonlinear. It is the sub-field of mathematical optimization that deals with non-linear problems. In some cases, nonlinear equations can be relaxed to linear function which is the method to handle a nonlinear model.

$$Maximize\ or\ minimize\ \ f(x)$$
$$subject\ to\qquad\qquad g(x)\ \alpha\ 0$$
$$L \leq x \leq U,$$

2.3.3.3 Nonlinear Programming with Discontinuous Derivatives

(DNLP)

This model uses the same concept as the nonlinear programing, except that the equation can be a discontinuous function. This model is more difficult to solve than a regular NLP model.

$$Maximize\ or\ minimize\ \ f(x)$$
$$subject\ to\ \ \ \ \ \ \ \ \ \ \ \ \ g(x)\ \alpha\ 0$$
$$L \leq x \leq U,$$

2.3.3.4 Mixed Integer Nonlinear Programming (MINLP)

This kind of the model uses for optimization with continuous and discrete variables and the nonlinear function appears in the objective function or constraints. This model can be applied with binary variables to select the best possible scenario in an optimization process.

$$Maximize\ or\ minimize\ \ f(x) + Dy$$
$$subject\ to\ \ \ \ \ \ \ \ \ \ \ \ \ g(x) + Hy\ \alpha\ 0$$
$$L \leq x \leq U$$
$$y = \{0,1,2,...\},$$

2.4 Global Optimization

Global optimization is employed to obtain the best possible solution for LNG process. Global optimization relied on energy and entropy balance while exergy analysis based on exergy balance and pinch analysis.

Optimization of an LNG process is based on complex thermodynamics models. In most literatures, optimization of LNG uses advanced global optimization algorithm combining with a simplified process model or a local search method with rigorous process model. In some cases, the solution is not a global optimum but this method is rigorous enough in practice. These following models are used in a global

optimization method which can be applied to the LNG processes. There are several global optimization methods for solving a complex MINLP including bound contraction method, novel bound contraction method and moving boundary method.

2.4.1 Bound Contraction

Bound contraction is a method which is used to handle nonlinear equations by relaxation of the original nonlinear models. Intervals analysis is used as the main strategy in this work to handle bilinear and concave terms (Faria *et al.*, 2012).

The theoretical functions are written in MINLP models which are used as an upper bound model of the problem. Then, variables in the upper bound model are partitioned into several intervals and all equations that contain those partitioning variables are linearized. The partitioning method will create the linear lower bound models. The result of the lower bound model is used as initial guess for upper bound model to achieve the solution of the upper bound of the problem. The bound contraction technique is then used to reduce the gap between the solutions of the lower and upper bound models by eliminating the intervals that do not contain the possible solution. After the gap between the upper and lower bound models is less than the targeted tolerance, typically set as 1%, the results of the non-linear model are confirmed as the global optimum. In some cases, bound contraction and intervals elimination strategy cannot achieve the targeted tolerance. Increasing number of intervals or branch and bound strategy will take place in those cases.

2.4.1.1 Variable Definition

Variables in the model should be categorized in a proper category. In the bound contraction method, variables are separated into three categories.

2.4.1.2 Partitioning Variables

These variables are partitioned into several intervals which will be used to create linear relaxation of bilinear and concave terms. These variables are used in the mixed integer linear model as a result.

2.4.1.3 Bound Contracted Variables

These variables are partitioned into intervals but only for performing the bound contraction methodology. The intervals in the lower bound model are identified by these variables. By identification of the bound contraction variables, this information is used in the elimination procedure. These variables do not need to be the same as the partitioned variables.

2.4.1.4 Branch and Bound Variables

These variables are used only when the bound contraction method does not perform. In a normal situation, there is no need to declare these variables.

2.4.1.5 Partitioning Methodology

Partitioning method is used to separate range of a variable into sections. There are different methods used to handle different variables and different situation. Consider a case of bilinear equation where z is the product of two continuous variables x and y:

$$z = xy \qquad\qquad \text{Eq. 2.4}$$

Where both x and y are subjected to a certain bound

$$x^L \leq x \leq x^U \qquad\qquad \text{Eq. 2.5}$$
$$y^L \leq y \leq y^U \qquad\qquad \text{Eq. 2.6}$$

Variable y is partitioned by using D-1 intervals. The initial point of each interval is given by the following equation.

$$\hat{y}_d = y^L + (d - 1)\frac{(y^U - y^L)}{D-1} \qquad\qquad \text{Eq. 2.7}$$

The term d-1 is used to determine a position in the interval. These equations are used in both direct partitioning and convex envelope methods.

2.4.1.6 Direct Partitioning Method

This method starts with the substitution of variable y in the product term by its discrete bounds. Substitution will allow z to be inside of one of the intervals which is between two discrete values. A binary variable (v_d) is introduced to assure that only one interval is selected.

$$\sum_{d=1}^{D-1} \hat{y}_d \, v_d \leq y \leq \sum_{d=1}^{D-1} \hat{y}_{d+1} \, v_d \qquad \text{Eq. 2.8}$$

$$\sum_{d=1}^{D-1} v_d = 1 \qquad \text{Eq. 2.9}$$

$$z \leq x \sum_{d=1}^{D-1} \hat{y}_{d+1} \, v_d \qquad \text{Eq. 2.10}$$

$$z \geq x \sum_{d=1}^{D-1} \hat{y}_d \, v_d \qquad \text{Eq. 2.11}$$

Equation 2.8 shows that y falls inside the interval corresponding to the binary variable. If x is the bound contraction variable, then x should be partitioned in the same way of y. Equation 2.9 will force the binary variable to equal to one. Equation 2.10 and 2.11 are the bound of z variable corresponding to y in a given interval. Given w_d as a positive variable this leads to $w_d = x v_d$. Then, w_d is substituted into Equations 2.10 and 2.11.

$$z \leq \sum_{d=1}^{D-1} \hat{y}_{d+1} \, w_d \qquad \text{Eq. 2.12}$$

$$z \geq \sum_{d=1}^{D-1} \hat{y}_d w_d \qquad \text{Eq. 2.13}$$

Where w_d obtained from these following equations.

$$w_d - x^U v_d \leq 0 \qquad \text{Eq. 2.14}$$

$$(x - w_d) - x^U(1 - v_d) \leq 0 \qquad \text{Eq. 2.15}$$

$$x - w_d \geq 0 \qquad \text{Eq. 2.16}$$

Equation 2.14 gives w_d equal to zero, if v_d is zero. On the other hand, if v_d is equal to one, Equation 2.15 and 2.16 render w_d equal to x. This method will transform any mixed integer nonlinear programing into a mixed integer linear programing which is a lower bound of the original model.

2.4.1.7 McCormick Envelopes

The McCormick model is one of the method which can be used to linearize a nonlinear model. The set of equations is different from the direct partitioning method but the concept is still in the same way. Equations can be written as follows.

$$z \geq x^L y + \sum_{d=1}^{D-1} (x \hat{y}_d v_d - x^L \hat{y}_d v_d) \qquad \text{Eq. 2.17}$$

$$z \geq x^U y + \sum_{d=1}^{D-1} (x \hat{y}_{d+1} v_d - x^U \hat{y}_{d+1} v_d) \qquad \text{Eq. 2.18}$$

$$z \leq x^L y + \sum_{d=1}^{D-1} (x \hat{y}_{d+1} v_d - x^L \hat{y}_{d+1} v_d) \qquad \text{Eq. 2.19}$$

$$z \leq x^U y + \sum_{d=1}^{D-1} (x \hat{y}_d v_d - x^U \hat{y}_d v_d) \qquad \text{Eq. 2.20}$$

These equations show that z falls inside the interval subject to the continuous and binary variables. Given w_d as a positive variable which is equal to the product of the continuous and binary variables ($w_d = xv_d$). This set of equations will transform into the following form.

$$z \geq x^L y + \sum_{d=1}^{D-1} (\hat{y}_d w_d - x^L \hat{y}_d v_d) \qquad \text{Eq. 2.21}$$

$$z \geq x^U y + \sum_{d=1}^{D-1} (\hat{y}_{d+1} w_d - x^U \hat{y}_{d+1} v_d) \qquad \text{Eq. 2.22}$$

$$z \leq x^L y + \sum_{d=1}^{D-1} (\hat{y}_{d+1} w_d - x^L \hat{y}_{d+1} v_d) \qquad \text{Eq. 2.23}$$

$$z \leq x^U y + \sum_{d=1}^{D-1} (\hat{y}_d w_d - x^U \hat{y}_d v_d) \qquad \text{Eq. 2.24}$$

where w_d is obtained from the following equations.

$$w_d - x^U v_d \leq 0 \qquad \text{Eq. 2.25}$$
$$(x - w_d) - x^U (1 - v_d) \leq 0 \qquad \text{Eq. 2.26}$$
$$x - w_d \geq 0 \qquad \text{Eq. 2.27}$$

As in the case of the direct partitioning, when substitution into the original mixed integer nonlinear programing, those equations will transform into a mixed integer linear programing model which is the lower bound of the original model.

In some cases, both bilinear terms can be partitioned. Partitioning both variables may improve the lower bound model of the system. On the other hand, the computational time is increased.
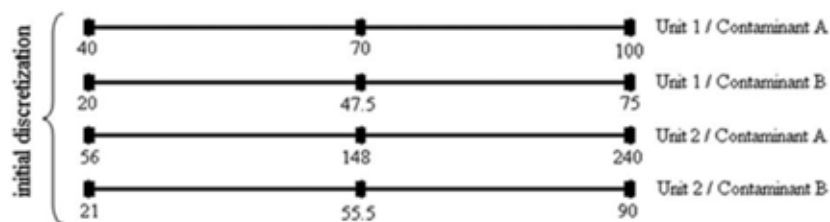
Figure 2.8 Partitioning of variables (Faria *et al.*, 2012).

2.4.1.8 Interval Elimination Strategy

The lower bound model is obtained after linear relazation of the nonlinear upper bound model. The solution of the lower bound model will be used as an initial guess to solve the upper bound problem. Once both upper bound and lower bound solutions have been found, elimination of interval will take place in the next step. The lower bound solution can be used as a guide to eliminate certain intervals. The method used for elimination is called one pass with one forbidden interval elimination. Elimination process takes place only one variable for each interval. This method can be used in several options which will explain in the next section.
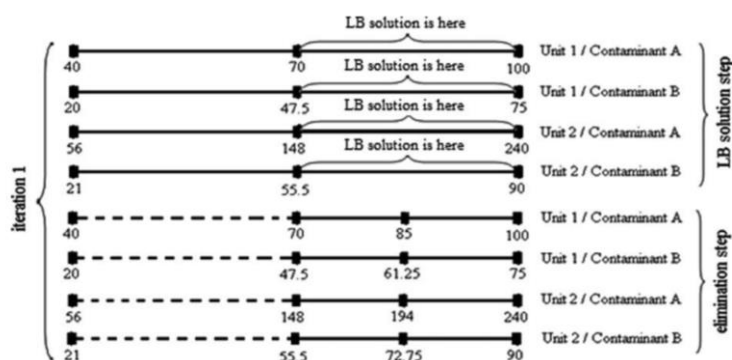
Figure 2.9 Interval elimination (Faria *et al.*, 2012).

In the case of all variables are considered for bound contraction. First, in the one pass elimination process, each variable will be visited only one time before a new lower bound is obtained. Second, in the cyclic elimination

process, after all variables have been visited, the elimination procedure will be started again until no more bound contraction is achieved.

There are several options when each variable is bound contracted. First, in the exhaustive elimination, the elimination process will be repeated again when each variable is contracted. The repeated process is used for that variable until no more bound contraction takes place. Second, the nonexhaustive elimination is the method where no variable is eliminated consecutively in the same iteration. Once a variable is contracted, the elimination process moves to the next variable. Third, the active upper bound, this method will calculate the upper bound model again when the elimination takes place. This process will improve the feasibility of the solution. Fourth, active lower bound is the method that obtains a new lower bound when the elimination process takes place. In some cases, no elimination takes place in all intervals which will lead to partitioning of all interval again. The elimination process can be terminated when the tolerance of a gap between the lower and the upper bound models is accepted.

There are several options related to forbidden interval. First, the single interval forbidding takes place when only one interval is forbidden and that interval should bracket the solution. Second, the extended interval forbidding is the process that forbids the identified interval plus the contiguous ones. This process is more reliable when a large number of intervals are used to obtain the lower bound model. In some cases, the contiguous intervals are not forbidden. Those intervals will render the lower bound which are lower than the current upper bound and lead to the non-elimination. Forbidden them will force other intervals to be picked. Those intervals will render unacceptable lower bound and leads to the elimination.

When no interval is eliminated but the gap between the lower bound and upper bound models is still unacceptable. Extended interval forbidden is applied by increasing the number of intervals. Increasing the number of interval will select a smaller part of feasible range of each variable. So, increasing the number of interval will provide tighter bounds and significantly increase the running time. If increasing the number of intervals cannot achieve an acceptable gap. Branch and bound procedure will be applied to achieve the solution.
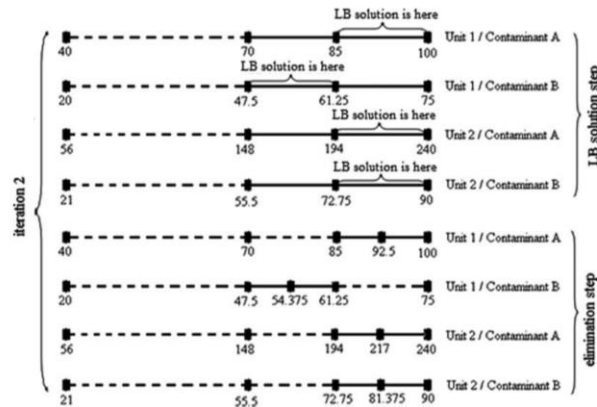
Figure 2.10 Partitioning and elimination of second iteration (Faria *et al.*, 2012)

2.4.1.9 Application of Bound Contraction

Not only the optimization of water management, bound contraction can also be applied to other fields of optimization, for example an optimization of gasoline blending (Ounahasaree *et al.*, 2016), an optimization of heavy fuel blending (Ayutthaya *et al.,* 2016).

2.4.1.10 Global optimum solution of bound contraction

Bound contraction is used to obtain a global optimum solution. A non-linear model provide an upper bound of objective function. A linearized model provides a lower bound of objective function. The linear model provides only one set of solution to meet the objective function which in turn helps in eliminating parts of the original feasible region where the global optimum does not lie. This step can be performed at every node of the Branch and Bound tree so as to reduce the search space, and to tighten the under- and over-estimators for the non-convex terms in the relaxation, so that the search is accelerated (Karuppiah, 2005).

Partitioning method provides a chance to contract the objective function between the upper bound and lower bound models. Binary variables are used to select the best possible interval of each variable. Increasing number of intervals decreases possible result in the interval which model can provide more accurate solution.

2.4.2 <u>Novel Bound Contraction</u>

Faria *et al.* (2011) introduced a novel bound contraction method as a solution strategy of a non-linear programing problem in a water management system. Difference from general bound contraction, this method does not need additional binary variables to identify in which interval the lower bound solution lies. Starting from the relaxation methodology, variables are set as follows.

$$z_{ij} = x_i y_j \qquad \text{Eq. 2.28}$$

Where both x and are continuous variables which are subject to a certain bound.

$$x_i^L \leq x_i \leq x_i^U \qquad \text{Eq. 2.29}$$
$$y_i^L \leq y_i \leq y_i^U \qquad \text{Eq. 2.30}$$

After substitution of boundaries into Equation 2.28, it can be written as follows.

$$z_{ij} \geq y_j \bar{x}_i^L \qquad \text{Eq. 2.31}$$
$$z_{ij} \leq y_j \bar{x}_i^U \qquad \text{Eq. 2.32}$$

To make the problem easier, x_i^{ref} is used as an estimator along with the bound departure which can be defined as follows.

$$d_i^L = x_i^{ref} - \bar{x}_i^L \qquad \text{Eq. 2.33}$$
$$d_i^U = \bar{x}_i^U - x_i^{ref} \qquad \text{Eq. 2.34}$$

Where d refer to the distance between the reference point to the boundary. Another assumption is the shorter distance between the lower bound to the reference point to the distance between the upper and the reference point. Then the auxiliary linear model can be defined by the following equations.

$$z_{rj} \geq \alpha_r^L y_j \qquad\qquad \text{Eq. 2.35}$$

$$\alpha_r^L = x_r^{ref} + sd_r^U \qquad\qquad \text{Eq. 2.36}$$

Where s can be varied from 0 to 1. The auxiliary linear model is used as bilinear constraints for all variables. It can be used by increasing the value of s until the solution reaches infeasible region or the lower bound is higher than the current upper bound. The solution is obtained when the difference between lower bound and upper bound is with in tolerance. Once the bound contraction cannot go any further, branch and bound is used to progress forward.

2.4.3 Branch and Bound Algorithm

Branch and bound strategy is used in a tree structure to explore the search space. Number of branches needed depends on how tightness of the intervals between the lower and the upper bounds. It can be separated into two strategies which are branching strategies and bounding strategies (Abdelsadek *et al.*, 2015).

2.4.3.1 Branching Strategies

In branching step, domain is divided into subdomains and fix decision variables in each subdomain. Branching strategy uses a concept of binary variable which means that in each step there are two possible situations occurred. Moreover, the depth first search (DFS) can be used for quickly achieved feasible solution. To avoid non-feasible solution, all overlap subdomains are removed when one subdomain is selected. The node with the greatest upper bound will be the most promising branch in this strategy.

2.4.3.2 Bounding Strategy

In this research, algorithm of branch and bound is a set to take the lower bound from the greatest value between the lower bound 1 and lower bound 2. Conversely, the upper bound is taken from the smallest value between the upper bound 1 and upper bound 2. Where the lower bound 1, lower bound 2, upper bound 1 and upper bound 2 come from the greedy search algorithm and the genetic algorithm which will not be explained in this report.

2.4.4 Moving Boundary Method

Not only the bound contraction method can be used to optimize the process the moving boundary is also one of the optimization methods. This example is based on the balance of heat exchanger in the system. Heat exchangers are divided into a few control volumes corresponding to each refrigerant state. A moving boundary approach is used to capture the dynamic of multiple fluid phase heat exchanger while conserving the simplicity of the model. Further the development of the moving boundary method allows some control volumes to disappear and reappear without simulation issues which is called switched moving boundary model.

Bejarano *et al.* (2017) demonstrated the optimization of a refrigeration system by the moving boundary method. Their research is focused on the optimization of a one-stage, one-load demand cycle. They found that the key factors to optimize the system are modelling, optimization and control.

2.4.4.1 Modelling

The moving boundary method is used to obtain the dynamic model for a condenser and an evaporator. The set of equations for the evaporator and condenser are defined by a steady state model of a complete cycle which is non-linear. The remaining elements of the cycle are defined by statically modelled. The effectiveness-NTU method is used to calculate the partial thermal power.

$$\dot{Q}_{e,sh} = \varepsilon_{e,sh}\left(\dot{m}c_p\right)_{min}(T_{e,sec,in} - T_e) \qquad \text{Eq. 2.37}$$

$$\dot{Q}_{e,tp} = \varepsilon_{e,tp}\left(\dot{m}c_p\right)_{min}(T_{e,sec,mid} - T_e) \qquad \text{Eq. 2.38}$$

$$\dot{Q}_{c,sh} = \varepsilon_{c,sh}\left(\dot{m}c_p\right)_{min}(T_{c,in} - T_{c,sec,in}) \qquad \text{Eq. 2.39}$$

$$\dot{Q}_{c,tp} = \varepsilon_{c,tp}\left(\dot{m}c_p\right)_{min}(T_c - T_{c,sec,in}) \qquad \text{Eq. 2.40}$$

2.4.4.2 Global Optimization

The optimization is relied on the cooling load by using COP as the energy efficiency of metrics. The optimization process focuses on the reduction of variables one-stage, one-load demand cycle is applied. Bejarano *et al.* (2017) also provide the method to reduce the number of variables to three variables. The candidate cycles are evaluated by a non-linear steady-state model. It is used to evaluate the

feasibility of the cycles by using some techniques and operational constraints. However, the result does not give the minimum degree of superheating for all cooling demand ranges. This leads to the use of control strategy which can improve the energy efficiency and drive the cycle to an optimum solution.

2.4.4.3 Control Strategy

The control strategy in this study is focused on the simplified condenser. Some problems are assigned to be under control, since the control problem can be excluded to drive a condenser to the optimum state. Consequently, excluding the controlled problems will reduce manipulated variables where the problem appear to be underactuated. Not only that the controllability study was conducted, this method can also suggest the controllable of the system which system can be controlled or not. This system is not completely controllable which lead to some difficulties to drive system to optimum.

These three strategies lead to the optimization of the cycle. Eventhough this process is uncontrollable, the sub optimal cycle can be achieved by projecting the optimal cycle from three degree of freedom optimization space to two degree of freedom control space. Not only projection is needed but the initial points are also important. They are working on nonlinear underactuated control strategy which will drive the process to an optimum condition.

2.4.5 Genetic Algorithm

Genetic algorithm is a mathematical method which apply biological genetic to mathematical model. This method is used in several optimization researches. Model concept based on stochastic method which relies on variable randomness. This method can be used to solve any kinds of model but this method is time consuming and dose not give the same result when the recalculation is done. The optimization method of LNG process by Genetic algorithm is provided by (Sun *et al.*, 2016).

2.4.5.1 Generate Initial Population

The initial population of the model is generated by randomness. The population size depends on the nature of the problem which cover the whole range of the possible solutions. The set of the initial population is called chromosome.

2.4.5.2 Evaluation

The initial population is evaluated by fitness function. The chromosome is evaluated individually and sorted by descending fitness values. The fitter solutions are typically more likely to be selected. The selected chromosome is used in the next section.

2.4.5.3 Genetic Operation

This step is used to select and generate the next generation of chromosome. Based on genetic theory, a pair of parent chromosome is crossed over or mutated to generate next generation. Selection is a process where chromosome is selected by ranking. Crossing over is a process which two chromosomes exchange some data between chromosome.

The last process is mutation process. In this process, a data in chromosome is changed to a difference value which can be called single point mutation. Crossing over and mutation process occur to random chromosome where the rest of the chromosome are passed through the next generation.

2.4.5.4 Termination

The evaluation process is repeated until the fitness value or the number of generation is reach terminate point. The final solution is used as global optimum solution. The process of genetic algorithm is shown in Figure 2.11.
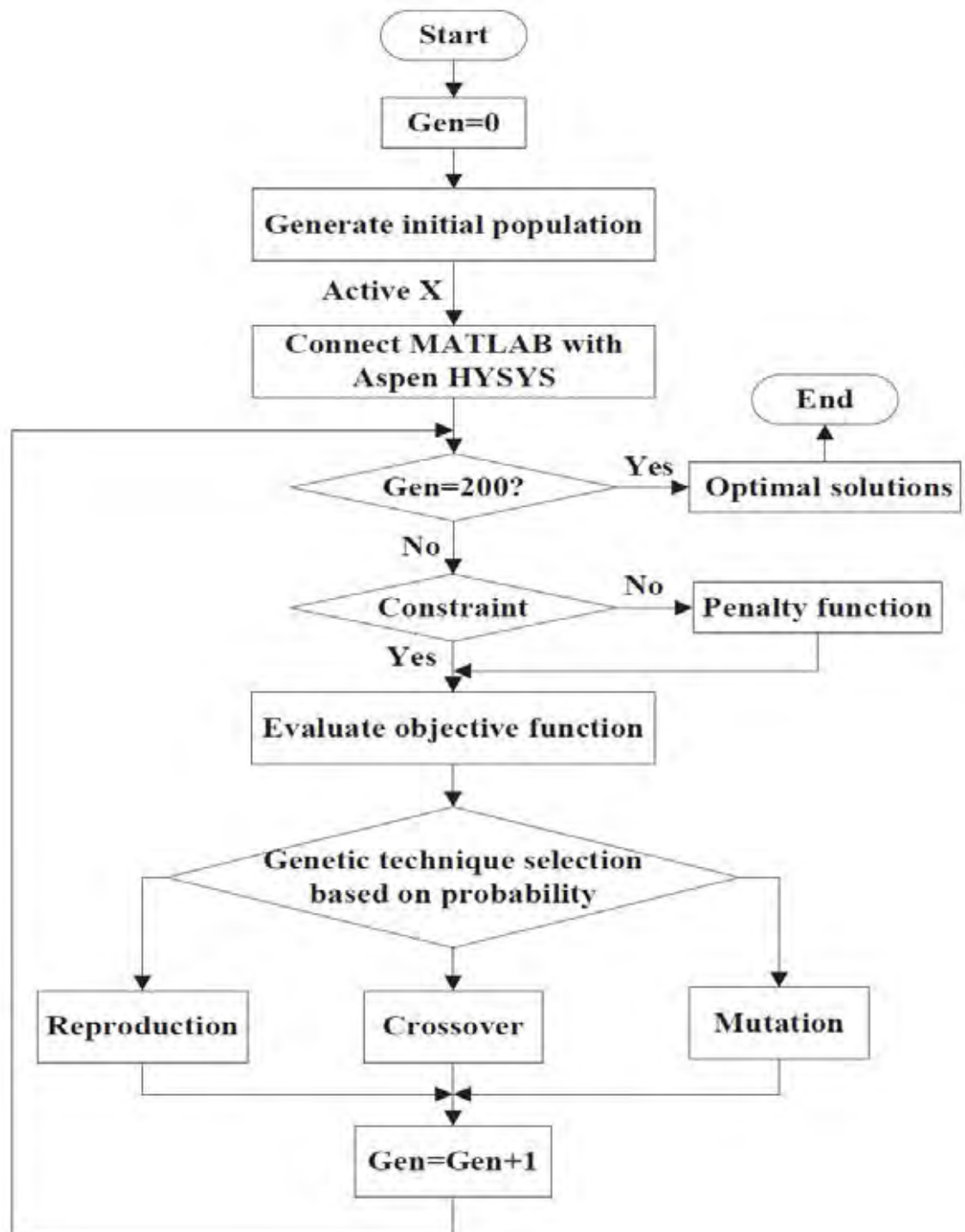
Figure 2.11 Genetic algorithm flow charts (Sun *et al.*, 2016).

2.4.6 Box Optimization Method

Box optimization is a sequential search technique which is used to find the near optimal solution. This method is a gradient free methodology which is used to handle non-linear function. The model is evaluated by direct function evaluation (Khan *et al.*, 2016).

2.4.6.1 Generate starting point

The feasible starting point is given to the model where the box model generates a complex of N+1 points around given value. These N+1 points are used in the objective function where $f(X)$ is calculated. The final value (N+1) is set as a first solution. The solutions are used in the next section.

2.4.6.2 Box operation

The solution is evaluated passthrough replacement, expansion and contraction. First, the solutions are re-arranged from the lowest to the highest. The trial point is generated by following equation.

$$X_t = \bar{X} + \alpha(\bar{X} - X_{n+1})$$
Eq. 2.41

The trial point is used to calculate solution in objective function where the solution $(f(X))$ is used in the rest of the process.

I. Replacement

If the solution of trial point fall between maximum and minimum solution, the X_{n+1} is replaced by X_t. The solution of X_t is used in the next section.

II. Expansion

If the solution of trial point is lower than minimum solution, the expansion process is occurred by generating X_e.

$$X_e = X_t + \beta(X_t - \bar{X})\,\grave{}$$
Eq. 2.42

This process occurs when the solution is good enough to keep looking the same direction. Solution from X_e is calculated and compared with X_t. If X_e solution is less than X_t solution, replace X_{n+1} by X_e. Otherwise, replace X_{n+1} by X_e and recalculation process is occurred. The solution of X_e is used in the next section.

III. Contraction

If the solution of trial point is greater than maximum solution, the contraction process is occurred by generating X_c.

$$X_c = X_t + \gamma(X_{n+1} - \bar{X}) \qquad \text{Eq. 2.43}$$

Contraction process perform when the solution is too large. X_c solution is calculated and compared with X_t. If X_c solution is less than X_{n+1} solution, replace X_{n+1} by X_c. Otherwise, re-calculate the contraction process again. The solution of X_c is used in the next section.

2.4.6.3 Constraints Satisfied

Solution from box optimization technique is evaluated in this section. If the solution satisfied the constraints, the process is stopped and the optimization solution is obtained.
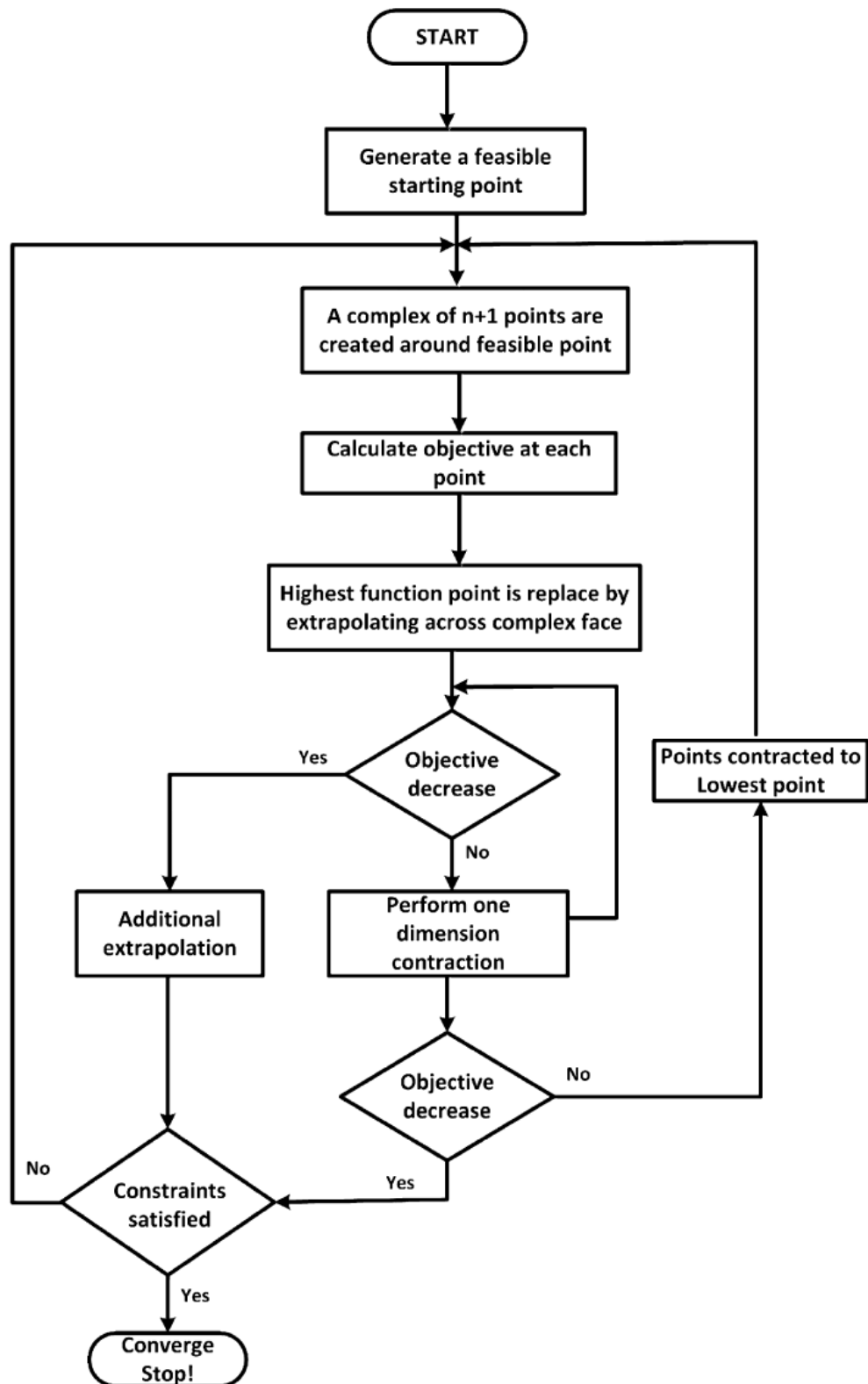
Figure 2.12 Box optimization technique flow charts (Khan *et al.*, 2016).

2.5 Computational Tools

2.5.1 <u>General Algebraic Modeling System (GAMS)</u>

GAMS is designed by incorporating relational database theory and mathematical programing. This information is merged to achieve the needs of modelers. Relational database theory offers a structured framework for developing general data organization and transformation capabilities. The mathematical programming guides a way of describing a problem and provides the methodology to solve it.

GAMS consists of solvers which can solve many kinds of equations such as linear model, nonlinear, etc. Modeler can also introduce a new method or new implementation of the existing method without changing the existing model. GAMS is commonly used to solve the optimization problems. GAMS is specifically designed for modeling linear, nonlinear and mixed integer optimization problems. (Rosenthal, 2013)

2.5.2 <u>Simsci Process Simulation PRO/II</u>

PRO/II is a process simulation program. It can be used for a process design or an operational analysis or engineering studies. PRO/II can offer a wide range of thermodynamic models and various types of substances which cover most of chemical processes. Not only for engineering analysis, PRO/II also has economic analysis which is used for optimizing cost of the process, both capital and operating cost.

2.6 MOTIVATION

Natural gas is one of the cleanest and cheapest fuel in the world. It is a decent fuel used in several industries and its demand has increased in the past decade. Transportation of the natural gas in a gaseous form is not appropriate for a long-distance transportation. A liquefaction process is required to liquefy natural gas in a boiling liquid form or LNG before shipping. Liquefaction of natural gas can reduce its volume to $1/600^{th}$ times when compared to the gas phase. This process also requires

high energy supply. The largest energy consumption is at compressors because the liquefaction process is operated under high pressure condition. The optimization of work in an LNG process can reduce the energy consumption and leads to the reduction of the operating cost. Partitioning method was selected as an optimization method to obtain global optimization of an LNG process (Faria *et al.*, 2012). The calculation was based on a basic thermodynamic and non-linear programing concept. The operating parameters of each process configuration were optimized and the optimum configuration providing the minimum amount of work input to system was expected.

2.7 OBJECTIVE

To optimize the shaft work of the commercial single and mixed refrigerant LNG cascade processes.

2.8 SCOPE OF RESEARCH

1.   GAMS is employed to optimize the single and mixed refrigerant system of the desired LNG process by the partitioning method (Faria *et al.*, 2012).

2.   The LNG processes include the ConocoPhillips LNG cascade process.

3.   Simsci PRO/II is employed to simulate the ConocoPhillips LNG cascade process for GAMS solution verification.

4.   Methane, ethylene and propane are used as refrigerant is this research.

5.   The mixed refrigerant is a combination of methane, ethylene and propane in optimal proportion.

CHAPTER III

METHODOLOGY

3.1 Materials and Equipment

3.1.1 Equipment

Personal computer model: Intel® Core™ i7-8700 CPU at 3.20GHz, Installed memory (RAM) 32.00 GB and 64-bit operating system.

3.1.2 Software

1.   General Algebraic Modeling System (GAMS)

2.   Simsci simulation software PRO/II version 10.0

3.   Microsoft office version 2016

4.   Minitab version 18

3.2 Methodology

This work was divided into three phases as follows.

3.2.1 Data Preparation

a. Generate enthalpy equations of methane, ethylene and propane based on pressure and temperature by a linear regression program.

b. Generate heat of vaporization and heat of condensation equations of methane, ethylene and propane based on pressure and temperature by a linear regression program.

c. Generate entropy equations of methane, ethylene and propane based on pressure and temperature by a linear regression program.

3.2.2 Process Simulation

a. Optimize shaft work of the single refrigerant in the selected commercial LNG processes by GAMS.

b. Optimize shaft work of difference minimum temperature approach.

c. Calculate total annual cost of process.

3.2.3 Verification

a. Simulate single refrigerant commercial LNG processes in PRO/II.

b. Compare optimization result between GAMS and PRO/II.

c. Compare optimization result between GAMS and PRO/II with optimizer.
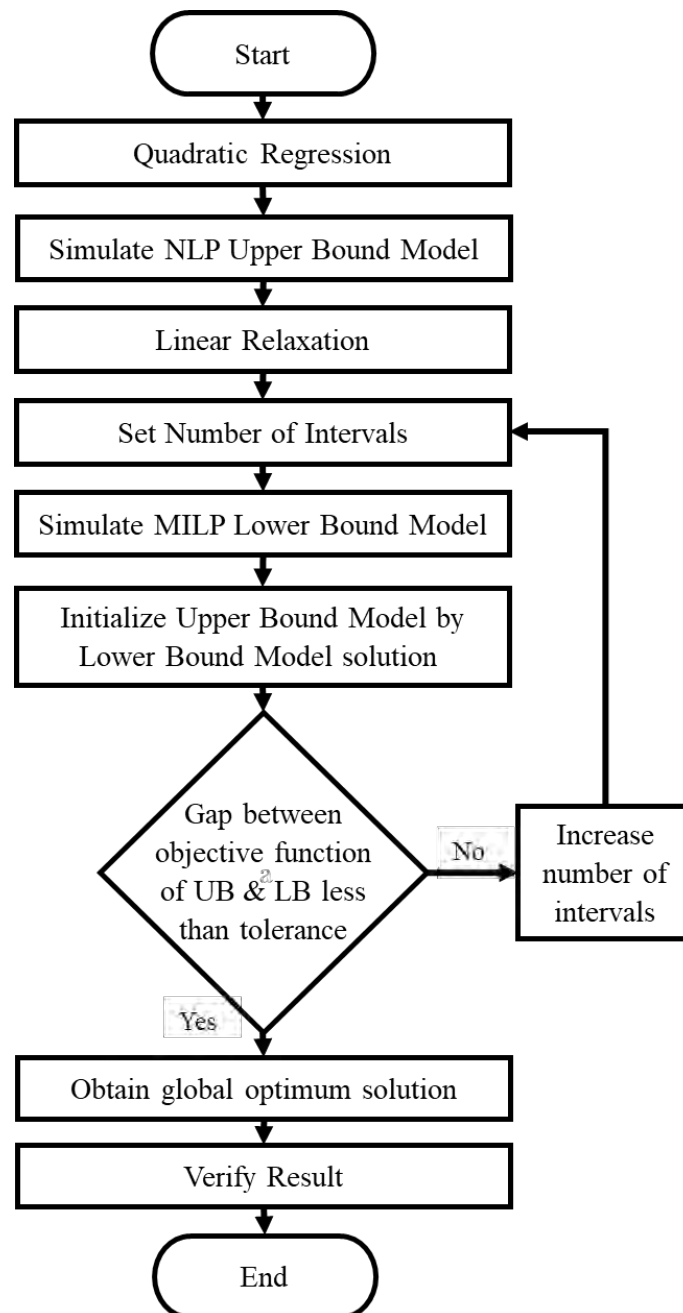
Figure 3.1 Process flow diagram.

CHAPTER IV
LIQUEFACTION MODEL OF SINGLE REFRIGERANT CONOCO-
PHILLIPS PROCESS

4.1 Nomenclature

4.1.1 <u>Sets</u>

k	Stage (1, 2, 3)
	Stage 1 for propane loop
	Stage 2 for ethylene loop
	Stage 3 for methane loop
i	Stream position (1, 2, 2I, 2P, 3, 3P, 4, V)
	Stream 1 for saturated vapor stream at low pressure
	Stream 2 for superheated vapor stream
	Stream 13 and 23 for saturated liquid stream
	Stream 33 for superheated vapor stream
	Stream 34 for saturated liquid stream
	Stream P for saturated vapor stream at high pressure
	Stream V for mixed phase stream
f	Number of flow rate intervals
j	Number of pressure intervals
r	Number of temperature intervals
Cn	Number of carbon component n (C1, C2, C3)

4.1.2 <u>Parameters</u>

η_k	Efficiency of compressor in the real system
ΔT_{min}	Minimum temperature approach
$\hat{F}^L$	Natural gas flow rate
$\hat{H}^{L,1}$	Natural gas enthalpy at feed condition
$\hat{F}^k_{max}$	Upper bound flow rate at each stage
$\hat{F}^k_{min}$	Lower bound flow rate at each stage

$\hat{P}_{max}$	Upper bound pressure of boundary
$\hat{P}_{min}$	Lower bound pressure of boundary
$\hat{T}_{max}$	Upper bound temperature of boundary
$\hat{T}_{min}$	Lower bound temperature of boundary
Γ	Large number
K	CAPCOST Constant

4.1.3 <u>Variables</u>

W^k	Compression work at each stage
F^k	Flow rate at each stage
$H^{k,i}$	Enthalpy of stream i at each stage
$H^{V,Cn}$	Enthalpy of vaporization of carbon component n at evaporator
$H^{C,Cn}$	Enthalpy of condensation of carbon component n at condenser
$R^{k,i}$	Heat flow of stream i at each stage
$M^{k,i}$	Product of enthalpy and phase quality of stream i at each stage
O^k	Product of Heat flow and quality of stream i at stage V
$S^{k,i}$	Entropy of stream i at each stage
$N^{k,i}$	Entropy function of stream i at each stage
f_H^k	Enthalpy function at each stage
f_S^k	Entropy function at each stage
$P^{k,i}$	Pressure of stream i at each stage
$T^{k,i}$	Temperature of stream i at each stage
$\theta^{k,i}$	Phase quality of stream i at each stage
$QB^{k,1}$	Heat of propane at each stage
$QB^{k,2}$	Heat of ethylene at each stage
$QB^{k,3}$	Heat of methane at each stage
$QB^{k,NG}$	Heat of natural gas at each stage

$\hat{F}^k_{dF_k}$ 　　　　Partitioned flow rate at intervals dF$_k$

$\hat{P}_{dP_j}$ 　　　　Partitioned pressure at intervals dP$_j$

$\hat{T}_{dT_r}$ 　　　　Partitioned temperature at intervals dT$_r$

$\hat{\theta}^{k,V}_{dF_k}$ 　　　　Partitioned phase fraction at intervals dF$_k$

$\hat{S}_{dS_f}$ 　　　　Partitioned entropy at intervals dS$_f$

H^* 　　　　Partitioned enthalpy at intervals dP$_j$ and dT$_r$

C^0_P 　　　　Capital cost of equipment in USD

A 　　　　Size parameter of the equipment

I 　　　　Chemical engineering cost index in USD

C_{elect} 　　　　Electricity cost in \$/kW

OPEX 　　　　Operating expense in 1 year

CAPEX 　　　　Capital expenditure

TAC 　　　　Total annual cost

4.1.4. <u>Binary Variables</u>

$y^k_{dF_k}$ 　　　　Flow rate partitioning binary variable

$y^k_{dP_j}$ 　　　　Pressure partitioning binary variable

$z^k_{dT_r}$ 　　　　Temperature partitioning binary variable

$\rho^k_{dP_j}$ 　　　　Enthalpy and entropy partitioning binary variable

$y\theta^{k,V}_{d\theta_k}$ 　　　　Quality partitioning binary variable for heat of vaporization

$\gamma\theta^{k,V}_{d\theta_k}$ 　　　　Product of quality partitioning binary variable and product of enthalpy and flow rate ($R^{k,i}$).

4.2 Global Optimization

4.2.1 ConocoPhillips LNG Cascade process

In the global optimization of cascade liquefaction process, the sets of equations are separated into upper bound and lower bound models with the objective function of minimizing shaft work requirement. The flow diagram of the cascade process which is used in this research is presented in Figure 4.1.
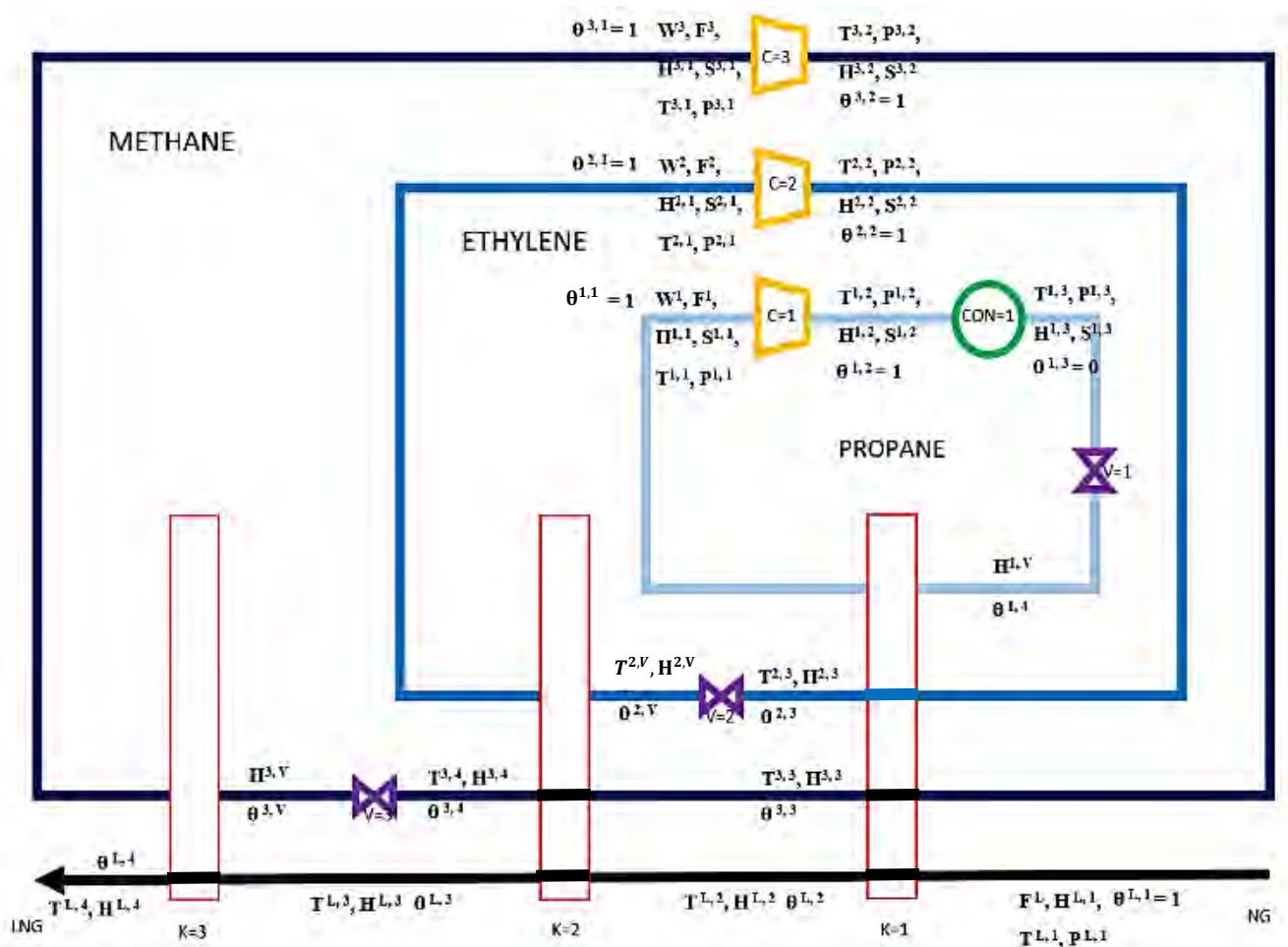
Figure 4.1 Simplified ConocoPhillips cascade process flow diagram.

4.2.2 Energy Balance
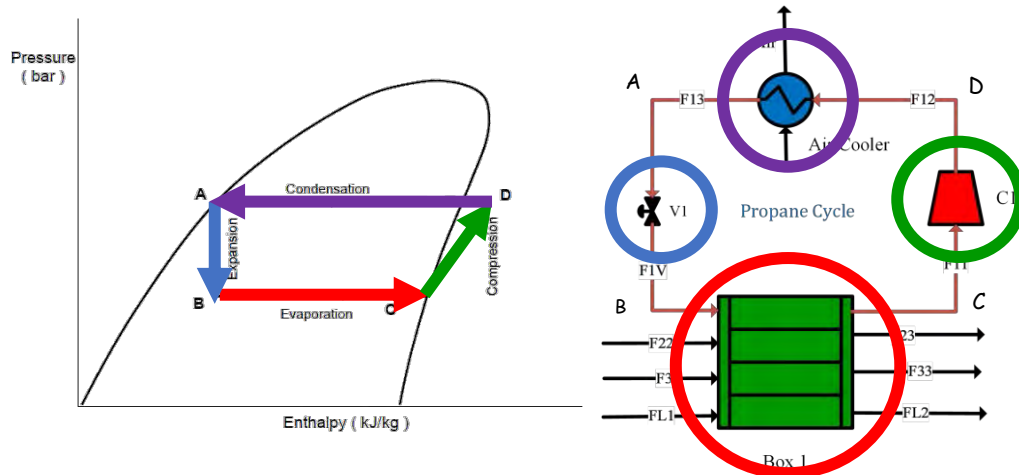
Figure 4.2 Pressure-Enthalpy diagram and propane cooling cycle.

An ideal energy balance is used to transform the cooling cycle into sets of equations. Figure 4.2 shows a pressure-enthalpy or PH diagram of the propane cooling cycle. From point A to B, liquid propane passes through an expansion valve by an isenthalpic expansion process. After the expansion valve, pressure of liquid propane decreases to 0.11 MPa which makes propane become a mixed pahse fluid. From point B to C, the mixed phase propane provides cooling to ethylene, methane and natural gas, and in turn, this same amount of heat transfer is received by propane and vaporizes all liquid portion of the mixed phase. Hence, all the liquid portion in the mixed phase fluid vaporizes to a saturated vapor phase. From point C to D, saturated vapor propane is compressed by isentropic compression to superheated state.From point D to A, superheated propane releases heat to an air cooler. At this state, propane becomes a saturated liquid stream. Apply all these energy balances, constraints and operating condition , the sets of equatios can be constructed in 4.2.3.

4.2.3 Upper Bound Model

4.2.3.1 Objective Function

$$\text{Min} \sum_k W^k$$

Where W^k is the power of the compressor in stage k (W^1, W^2, W^3). Base on the first law of thermodynamics, W^k is written as:

$$W^k = F^k[H^{k,2} - H^{k,1}] \qquad k=1,2,3 \qquad \text{Eq. 4.1}$$

The enthalpy and entropy balance of each equipment is used to obtain the work balance the system. The equations of each equipment can be set as follows.

4.2.3.2 Compressor Equations

In turn, entropy and enthalpy are calculated by a set of equation of state (e.g. Peng-Robinson, SRK, etc.) represented by ($f_S^k(P^{k,i}, T^{k,i}, \theta^k)$, $f_H^k(P^{k,i}, T^{k,i}, \theta^k)$), where θ^k is the quality (θ^k=1 for vapor/gas, θ^k=0 for pure liquid and $0 < \theta^k < 1$ for mixture of liquid and vapor. Then entropy and enthalpy equations are as follows:

$$S^{k,1} = f_S^k(P^k, T^k, \theta^k) \qquad k=1,2,3 \qquad \text{Eq. 4.2}$$
$$H^{k,1} = f_H^k(P^k, T^k, \theta^k) \qquad k=1,2,3 \qquad \text{Eq. 4.3}$$
$$S^{k,2} = f_S^k(P^{k,2}, T_{ideal}^{k,2}, \theta^{k,2}) \qquad k=1,2,3 \qquad \text{Eq. 4.4}$$
$$H^{k,2} = f_H^k(P^{k,2}, T^{k,2}, \theta^{k,2}) \qquad k=1,2,3 \qquad \text{Eq. 4.5}$$
$$H_{ideal}^{k,2} = f_H^k(P^{k,2}, T_{ideal}^{k,2}, \theta^{k,2}) \qquad k=1,2,3 \qquad \text{Eq. 4.6}$$

Isentropic compression is the compression in a compressor with 80% efficiency of compressor (M. Roberts, 2015). Thus,

$$S_{ideal}^{k,2} = S^{k,1} \qquad k=1,2,3 \qquad \text{Eq. 4.7}$$

Then, ideal enthalpy is used to find non-ideal enthalpy in non-isentropic compression process.

$$[H_{ideal}^{k,2} - H^{k,1}] = \eta_k[H^{k,2} - H^{k,1}] \qquad k=1,2,3 \qquad \text{Eq. 4.8}$$

4.2.3.3 Cooler Equations

The energy balances are:

$$Q^1 = F^1[H^{1,3} - H^{1,2}] \qquad \text{Eq. 4.9}$$

$$Q^1 = F^1[(H^{1,2} - H^{1,2P} - (H^{C,C3}\theta^{12})] \qquad \text{Eq. 4.10}$$

where
$$H^{1,3} = f_H^{k,v}(P^{1,3}, T^{1,3}, \theta^{1,3}) \qquad \text{Eq. 4.11}$$

$$H^{C,C3} = f_H^{1,3}(P^{1,3}, T^{1,3}, \theta^{1,3}) \qquad \text{Eq. 4.12}$$

$$H^{1,2P} = f_H^{1,2P}(P^{1,2}, T^{1,2P}, \theta^{1,2}) \qquad \text{Eq. 4.13}$$

$$T^{1,3} \geq T_{cooling}^{ref} + \Delta T_{min} \qquad \text{Eq. 4.14}$$

$$T^{1,3} = T^{1,2P} \qquad \text{Eq. 4.15}$$

$$P^{1,3} = P^{1,2} \qquad \text{Eq. 4.16}$$

4.2.3.4 Valve Equations

Valves are the equipment used for cooling the temperature of refrigerant and the energy balance equations and are represented as follows:

$$H^{1,v} = H^{1,3} \qquad \text{Eq. 4.17}$$

$$H^{1,v} = f_H^1(P^{1,v}, T^{1,v}, \theta^{1,v}) \qquad \text{Eq. 4.18}$$

$$H^{2,v} = H^{2,3} \qquad \text{Eq. 4.19}$$

$$H^{2,v} = f_H^2(P^{2,v}, T^{2,v}, \theta^{2,v}) \qquad \text{Eq. 4.20}$$

$$H^{3,v} = H^{3,4} \qquad \text{Eq. 4.21}$$

$$H^{3,v} = f_H^3(P^{3,v}, T^{3,v}, \theta^{3,v}) \qquad \text{Eq. 4.22}$$

4.2.3.5 Box Equations

Boxes or evaporators of each stage in the refrigeration cycle are used for transferring the heat between natural gas and refrigerant that can be calculated as follows:

At stage k = 1

$$QB^{1,1} = F^1[H^{1,1} - H^{1,v}] \qquad \text{Eq. 4.23}$$

$$QB^{1,1} = F^1 \; x \; H^{V,C3} \; x \; (1 - \theta^{1,v}) \qquad \text{Eq. 4.24}$$

$$QB^{1,2} = F^2[H^{2,2} - H^{2,3}] \qquad \text{Eq. 4.25}$$

$$QB^{1,2} = F^2[H^{2,2} - H^{2,2P} - H^{C,C2}] \qquad \text{Eq. 4.26}$$

$$QB^{1,3} = F^3[H^{3,2} - H^{3,3}] \qquad \text{Eq. 4.27}$$

$$QB^{1,C3} = QB^{1,C2} + QB^{1,C1} + QB^{1,NG} \qquad \text{Eq. 4.28}$$

$$H^{2,2P} = f_H^{2,2P}(P^{2,2}, T^{2,2P}, \theta^{2,2}) \qquad \text{Eq. 4.29}$$

$$H^{2,3} = f_H^{2,3}(P^{2,3}, T^{2,3}, \theta^{2,3}) \qquad \text{Eq. 4.30}$$

$$H^{3,3} = f_H^{3,3}(P^{3,3}, T^{3,3}, \theta^{3,3}) \qquad \text{Eq. 4.31}$$

$$H^{C,C2} = f_H^{C,C2}(P^{2,2}) \qquad \text{Eq. 4.32}$$

$$H^{V,C3} = f_H^{V,C3}(P^{1,V}) \qquad \text{Eq. 4.33}$$

$$T^{1,1} = T^{1,V} \qquad \text{Eq. 4.34}$$

$$T^{2,2P} = T^{1,3} \qquad \text{Eq. 4.35}$$

$$P^{1,1} = P^{1,V} \qquad \text{Eq. 4.36}$$

$$P^{2,2} = P^{2,3} \qquad \text{Eq. 4.37}$$

$$P^{3,2} = P^{3,3} \qquad \text{Eq. 4.38}$$

At stage k = 2

$$QB^{2,2} = F^2[H^{2,1} - H^{2,v}] \qquad \text{Eq. 4.39}$$

$$QB^{2,2} = F^2 \ x \ H^{V,C2} \ x \ (1 - \theta^{2,v}) \qquad \text{Eq. 4.40}$$

$$QB^{2,3} = F^3[H^{3,3} - H^{3,4}] \qquad \text{Eq. 4.41}$$

$$QB^{2,3} = F^3[H^{3,3} - H^{3,3P} - H^{C,C1}] \qquad \text{Eq. 4.42}$$

$$QB^{2,2} = QB^{2,3} + QB^{2,NG} \qquad \text{Eq. 4.43}$$

$$H^{3,3P} = f_H^{3,3P}(P^{3,3}, T^{3,3P}, \theta^{3,3}) \qquad \text{Eq. 4.44}$$

$$H^{3,4} = f_H^{3,4}(P^{3,4}, T^{3,4}, \theta^{3,4}) \qquad \text{Eq. 4.45}$$

$$H^{V,C2} = f_H^{V,C2}(P^{2,V}) \qquad \text{Eq. 4.46}$$

$$H^{C,C1} = f_H^{C,C1}(P^{3,3}) \qquad \text{Eq. 4.47}$$

$$T^{2,1} = T^{2,V} \qquad \text{Eq. 4.48}$$

$$T^{3,3P} = T^{3,4} \qquad \text{Eq. 4.49}$$

$$P^{2,1} = P^{2,V} \qquad \text{Eq. 4.50}$$

$$P^{2,1} = P^{3,4} \qquad \text{Eq. 4.51}$$

At stage k = 3

$$QB^{3,3} = F^3[H^{3,1} - H^{3,v}] \qquad \text{Eq. 4.52}$$

$$QB^{3,3} = F^3 \ x \ H^{V,C1} \ x \ (1 - \theta^{3,v}) \qquad \text{Eq. 4.53}$$

$$QB^{3,3} = QB^{3,NG} \qquad \text{Eq. 4.54}$$

$$H^{V,C1} = f_H^{V,C1}(P^{3,V}) \qquad \text{Eq. 4.55}$$

$$T^{3,1} = T^{3,V} \qquad \text{Eq. 4.56}$$

$$P^{3,1} = P^{3,V} \qquad \text{Eq. 4.57}$$

4.2.4 Lower Bound Model

Firstly, starting to relax non-linear equation to be linear equations by partitioning the parameters in the non-linear equations.

4.2.4.1 Flow rate partitioning

$$\hat{F}_{dF_k}^k = \hat{F}_{min}^k + \frac{ord(dF_k)-1}{card(dF_k)-1}[\hat{F}_{max}^k - \hat{F}_{min}^k]$$

$$F^k \geq \sum_{dF_k} \hat{F}_{dF_k}^k \ y_{dF_k}^k \qquad \text{Eq. 4.58}$$

$$F^k \leq \sum_{dF_k} \hat{F}_{dF_k+1}^k \ y_{dF_k}^k \qquad \text{Eq. 4.59}$$

Where

$$\sum_{dF_k} y_{dF_k}^k = 1 \qquad \text{Eq. 4.60}$$

Then the non-linear equations are substituted by the set of linear equations as following:

$$W^k = F^k[H^{k,2} - H^{k,1}] \qquad \text{Eq. 4.1}$$

$$W^k = [R^{k,2} - R^{k,1}] \qquad \text{Eq. 4.61}$$

Where

$$R^{k,i} = F^k \ x \ H^{k,i} \qquad \text{Eq. 4.62}$$

Instead of using the product $F^k \ x \ H^{k,i}$ to calculate $R^{k,i}$, a linear estimator of $R^{k,i}$ is introduced as follows:

$$R^{k,i} \geq \sum_{dF_k} \hat{F}_{dF_k}^k \gamma_{dF_k}^{k,i} \qquad \text{Eq. 4.63}$$

$$R^{k,i} \leq \sum_{dF_k} \hat{F}^k_{dF_k+1} \gamma^{k,i}_{dF_k} \qquad \text{Eq. 4.64}$$

Where, i =1,2,3 and v.

$$\gamma^{k,i}_{dF_k} - \Gamma y^k_{dF_k} \leq 0 \qquad \text{Eq. 4.65}$$

$$\gamma^{k,i}_{dF_k} \geq 0 \qquad \text{Eq. 4.66}$$

$$[H^{k,i} - \gamma^{k,i}_{dF_k}] - \Gamma[1 - y^k_{dF_k}] \leq 0 \qquad \text{Eq. 4.67}$$

$$[H^{k,i} - \gamma^{k,i}_{dF_k}] \geq 0 \qquad \text{Eq. 4.68}$$

where Γ is a large number.

In the partitioning of flow rate, one can also linearize the equation of condenser Eq. 4.9 and boxes equation Eq. 4.23, Eq. 4.25 and Eq. 4.27 as follows:

For the condenser Eq. 4.9 becomes.

$$Q^k = [R^{k,3} - R^{k,2}]$$

Eqs 4.23, 4.25 and 4.27 then become.

$$QB^{1,C3} = [R^{1,1} - R^{1,v}] \qquad \text{Eq. 4.69}$$

$$QB^{1,C2} = [R^{2,2} - R^{2,3}] \qquad \text{Eq. 4.70}$$

$$QB^{1,C1} = [R^{3,2} - R^{3,3}] \qquad \text{Eq. 4.71}$$

Eqs 4.39, 4.41 and 4.52 are then linearized to

$$QB^{2,C2} = [R^{2,1} - R^{2,v}] \qquad \text{Eq. 4.72}$$

$$QB^{2,C1} = [R^{3,3} - R^{3,4}] \qquad \text{Eq. 4.73}$$

$$QB^{3,C1} = [R^{3,1} - R^{3,v}] \qquad \text{Eq. 4.74}$$

Enthalpy, a function of temperature, pressure and quality, can be linearized as follows:

From
$$H^* = f_H(P^*, T^*, \theta^*)$$

Where * is replaced for any (k, 1), (k, 2), etc.

4.2.4.2 Pressure partitioning

$$\hat{P}_{dP_j} = \hat{P}_{min} + \frac{ord(dP_k)-1}{card(dP_k)-1}[\hat{P}_{max} - \hat{P}_{min}]$$

$$P^* \geq \sum_{dP_j} \hat{P}_{dP_j} \, yp^*_{dP_j} \qquad\qquad \text{Eq. 4.75}$$

$$P^* \leq \sum_{dP_j} \hat{P}_{dP_j+1} \, yp^*_{dP_j} \qquad\qquad \text{Eq. 4.76}$$

Where

$$\sum_{dP_j} y^*_{dP_j} = 1 \qquad\qquad \text{Eq. 4.77}$$

The extended pressure partitioning of pressure at each stream of each refrigerant cycle is represented as follows:

Propane Cycle:

(1,1) $\hat{P}_{dP_1} = \hat{P}_{min} + \frac{ord(dP_1)-1}{card(dP_1)-1}[\hat{P}_{max} - \hat{P}_{min}]$

$$P^{(1,1)} \geq \sum_{dP_1} \hat{P}_{dP_1} \, yp^{(1,1)}_{dP_1} \qquad\qquad \text{Eq. 4.78}$$

$$P^{(1,1)} \leq \sum_{dP_1} \hat{P}_{dP_1+1} \, yp^{(1,1)}_{dP_1} \qquad\qquad \text{Eq. 4.79}$$

Where

$$\sum_{dP_1} y^{(1,1)}_{dP_1} = 1 \qquad\qquad \text{Eq. 4.80}$$

(1,2) $\hat{P}_{dP_2} = \hat{P}_{min} + \frac{ord(dP_1)-1}{card(dP_1)-1}[\hat{P}_{max} - \hat{P}_{min}]$

$$P^{(1,2)} \geq \sum_{dP_2} \hat{P}_{dP_2} \, yp^{(1,2)}_{dP_2} \qquad\qquad \text{Eq. 4.81}$$

$$P^{(1,2)} \leq \sum_{dP_2} \hat{P}_{dP_2+1} \, yp^{(1,2)}_{dP_2} \qquad\qquad \text{Eq. 4.82}$$

Where

$$\sum_{dP_2} y^{(1,2)}_{dP_2} = 1 \qquad\qquad \text{Eq. 4.83}$$

(1,3) $\hat{P}_{dP_3} = \hat{P}_{min} + \frac{ord(dP_1)-1}{card(dP_1)-1}[\hat{P}_{max} - \hat{P}_{min}]$

$$P^{(1,3)} \geq \sum_{dP_3} \hat{P}_{dP_3} \, yp_{dP_3}^{(1,3)} \qquad \text{Eq. 4.84}$$

$$P^{(1,3)} \leq \sum_{dP_3} \hat{P}_{dP_3+1} \, yp_{dP_3}^{(1,3)} \qquad \text{Eq. 4.85}$$

Where

$$\sum_{dP_3} y_{dP_3}^{(1,3)} = 1 \qquad \text{Eq. 4.86}$$

Ethylene Cycle:

(2,1) $\hat{P}_{dP_1} = \hat{P}_{min} + \frac{ord(dP_2)-1}{card(dP_2)-1}[\hat{P}_{max} - \hat{P}_{min}]$

$$P^{(2,1)} \geq \sum_{dP_1} \hat{P}_{dP_1} \, yp_{dP_1}^{(2,1)} \qquad \text{Eq. 4.87}$$

$$P^{(2,1)} \leq \sum_{dP_1} \hat{P}_{dP_1+1} \, yp_{dP_1}^{(2,1)} \qquad \text{Eq. 4.88}$$

Where

$$\sum_{dP_1} y_{dP_1}^{(2,1)} = 1 \qquad \text{Eq. 4.89}$$

(2,2) $\hat{P}_{dP_2} = \hat{P}_{min} + \frac{ord(dP_2)-1}{card(dP_2)-1}[\hat{P}_{max} - \hat{P}_{min}]$

$$P^{(2,2)} \geq \sum_{dP_2} \hat{P}_{dP_2} \, yp_{dP_2}^{(2,2)} \qquad \text{Eq. 4.90}$$

$$P^{(2,2)} \leq \sum_{dP_2} \hat{P}_{dP_2+1} \, yp_{dP_2}^{(2,2)} \qquad \text{Eq. 4.91}$$

Where

$$\sum_{dP_2} y_{dP_2}^{(2,2)} = 1 \qquad \text{Eq. 4.92}$$

(2,3) $\hat{P}_{dP_3} = \hat{P}_{min} + \frac{ord(dP_2)-1}{card(dP_2)-1}[\hat{P}_{max} - \hat{P}_{min}]$

$$P^{(2,3)} \geq \sum_{dP_3} \hat{P}_{dP_3} \, yp_{dP_3}^{(2,3)} \qquad \text{Eq. 4.93}$$

$$P^{(2,3)} \leq \sum_{dP_3} \hat{P}_{dP_3+1} \, yp_{dP_3}^{(2,3)} \qquad \text{Eq. 4.94}$$

Where

$$\sum_{dP_3} y_{dP_3}^{(2,3)} = 1 \qquad \text{Eq. 4.95}$$

Methane Cycle:

$(3,1)$ $\hat{P}_{dP_1} = \hat{P}_{min} + \frac{ord(dP_3)-1}{card(dP_3)-1}[\hat{P}_{max} - \hat{P}_{min}]$

$$P^{(3,1)} \geq \sum_{dP_1} \hat{P}_{dP_1} \, yp_{dP_1}^{(3,1)} \qquad \text{Eq. 4.96}$$

$$P^{(3,1)} \leq \sum_{dP_1} \hat{P}_{dP_1+1} \, yp_{dP_1}^{(3,1)} \qquad \text{Eq. 4.97}$$

Where

$$\sum_{dP_1} y_{dP_1}^{(3,1)} = 1 \qquad \text{Eq. 4.98}$$

$(3,2)$ $\hat{P}_{dP_2} = \hat{P}_{min} + \frac{ord(dP_3)-1}{card(dP_3)-1}[\hat{P}_{max} - \hat{P}_{min}]$

$$P^{(3,2)} \geq \sum_{dP_2} \hat{P}_{dP_2} \, yp_{dP_2}^{(3,2)} \qquad \text{Eq. 4.99}$$

$$P^{(3,2)} \leq \sum_{dP_2} \hat{P}_{dP_2+1} \, yp_{dP_2}^{(3,2)} \qquad \text{Eq. 4.100}$$

Where

$$\sum_{dP_2} y_{dP_2}^{(3,2)} = 1 \qquad \text{Eq. 4.101}$$

$(3,3)$ $\hat{P}_{dP_3} = \hat{P}_{min} + \frac{ord(dP_3)-1}{card(dP_3)-1}[\hat{P}_{max} - \hat{P}_{min}]$

$$P^{(3,3)} \geq \sum_{dP_3} \hat{P}_{dP_3} \, yp_{dP_3}^{(3,3)} \qquad \text{Eq. 4.102}$$

$$P^{(3,3)} \leq \sum_{dP_3} \hat{P}_{dP_3+1} \, yp_{dP_3}^{(3,3)} \qquad \text{Eq. 4.103}$$

Where

$$\sum_{dP_3} y_{dP_3}^{(3,3)} = 1 \qquad \text{Eq. 4.104}$$

$(3,4)$ $\hat{P}_{dP_4} = \hat{P}_{min} + \frac{ord(dP_3)-1}{card(dP_3)-1}[\hat{P}_{max} - \hat{P}_{min}]$

$$P^{(3,4)} \geq \sum_{dP_4} \hat{P}_{dP_4} \, yp_{dP_4}^{(3,4)} \qquad \text{Eq. 4.105}$$

$$P^{(3,4)} \leq \sum_{dP_4} \hat{P}_{dP_4+1} \, yp_{dP_4}^{(3,4)} \qquad \text{Eq. 4.106}$$

Where

$$\sum_{dP_4} y_{dP_4}^{(3,4)} = 1 \qquad \text{Eq. 4.107}$$

4.2.4.3 Temperature partitioning

$$\hat{T}_{dT_r} = \hat{T}_{min} + \frac{ord(dP_k)-1}{card(dP_k)-1}[\hat{T}_{max} - \hat{T}_{min}]$$

$$T^* \geq \sum_{dT_r} \hat{T}_{dT_r} z^*_{dT_r} \qquad \text{Eq. 4.108}$$

$$T^* \leq \sum_{dT_r} \hat{T}_{dT_r+1} z^*_{dT_r} \qquad \text{Eq. 4.109}$$

Where

$$\sum_{dT_r} z^*_{dT_r} = 1 \qquad \text{Eq. 4.110}$$

The extended temperature partitioning of temperature at each stream of each refrigerant cycle is represented as follows:

Propane Loop:

(1,2) $\hat{T}_{dT_2} = \hat{T}_{min} + \frac{ord(dP_1)-1}{card(dP_1)-1}[\hat{T}_{max} - \hat{T}_{min}]$

$$T^{(1,2)} \geq \sum_{dT_2} \hat{T}_{dT_2} z^{(1,2)}_{dT_2} \qquad \text{Eq. 4.111}$$

$$T^{(1,2)} \leq \sum_{dT_2} \hat{T}_{dT_2+1} z^{(1,2)}_{dT_2} \qquad \text{Eq. 4.112}$$

Where

$$\sum_{dT_2} z^{(1,2)}_{dT_2} = 1 \qquad \text{Eq. 4.113}$$

(1,2P) $\hat{T}_{dT_{2P}} = \hat{T}_{min} + \frac{ord(dP_1)-1}{card(dP_1)-1}[\hat{T}_{max} - \hat{T}_{min}]$

$$T^{(1,2P)} \geq \sum_{dT_{2P}} \hat{T}_{dT_{2P}} z^{(1,2P)}_{dT_{2P}} \qquad \text{Eq. 4.114}$$

$$T^{(1,2P)} \leq \sum_{dT_{2P}} \hat{T}_{dT_{2P}+1} z^{(1,2P)}_{dT_{2P}} \qquad \text{Eq. 4.115}$$

Where

$$\sum_{dT_{2P}} z^{(1,2P)}_{dT_{2P}} = 1 \qquad \text{Eq. 4.116}$$

(1,3) $\hat{T}_{dT_3} = \hat{T}_{min} + \frac{ord(dP_1)-1}{card(dP_1)-1}[\hat{T}_{max} - \hat{T}_{min}]$

$$T^{(1,3)} \geq \sum_{dT_3} \hat{T}_{dT_3} z^{(1,3)}_{dT_3} \qquad \text{Eq. 4.117}$$

$$T^{(1,3)} \leq \sum_{dT_3} \hat{T}_{dT_3+1} z^{(1,3)}_{dT_3} \qquad \text{Eq. 4.118}$$

Where

$$\sum_{dT_3} z^{(1,3)}_{dT_3} = 1 \qquad \text{Eq. 4.119}$$

$$(1,\text{V}) \ \hat{T}_{dT_V} = \hat{T}_{min} + \frac{ord(dP_1)-1}{card(dP_1)-1}[\hat{T}_{max} - \hat{T}_{min}]$$

$$T^{(1,\text{V})} \geq \sum_{dT_V} \hat{T}_{dT_V} z_{dT_V}^{(1,\text{V})} \qquad \text{Eq. 4.120}$$

$$T^{(1,\text{V})} \leq \sum_{dT_V} \hat{T}_{dT_V+1} z_{dT_V}^{(1,\text{V})} \qquad \text{Eq. 4.121}$$

Where

$$\sum_{dT_V} z_{dT_V}^{(1,\text{V})} = 1 \qquad \text{Eq. 4.122}$$

Ethylene Loop:

$$(2,2) \ \hat{T}_{dT_2} = \hat{T}_{min} + \frac{ord(dP_1)-1}{card(dP_1)-1}[\hat{T}_{max} - \hat{T}_{min}]$$

$$T^{(2,2)} \geq \sum_{dT_2} \hat{T}_{dT_2} z_{dT_2}^{(2,2)} \qquad \text{Eq. 4.123}$$

$$T^{(2,2)} \leq \sum_{dT_2} \hat{T}_{dT_2+1} z_{dT_2}^{(2,2)} \qquad \text{Eq. 4.124}$$

Where

$$\sum_{dT_2} z_{dT_2}^{(2,2)} = 1 \qquad \text{Eq. 4.125}$$

$$(2,2\text{P}) \ \hat{T}_{dT_{2P}} = \hat{T}_{min} + \frac{ord(dP_1)-1}{card(dP_1)-1}[\hat{T}_{max} - \hat{T}_{min}]$$

$$T^{(2,2\text{P})} \geq \sum_{dT_{2P}} \hat{T}_{dT_{2P}} z_{dT_{2P}}^{(2,2\text{P})} \qquad \text{Eq. 4.126}$$

$$T^{(2,2\text{P})} \leq \sum_{dT_{2P}} \hat{T}_{dT_{2P}+1} z_{dT_{2P}}^{(2,2\text{P})} \qquad \text{Eq. 4.127}$$

Where

$$\sum_{dT_{2P}} z_{dT_{2P}}^{(2,2\text{P})} = 1 \qquad \text{Eq. 4.128}$$

$$(2,\text{V}) \ \hat{T}_{dT_V} = \hat{T}_{min} + \frac{ord(dP_1)-1}{card(dP_1)-1}[\hat{T}_{max} - \hat{T}_{min}]$$

$$T^{(2,\text{V})} \geq \sum_{dT_V} \hat{T}_{dT_V} z_{dT_V}^{(2,\text{V})} \qquad \text{Eq. 4.129}$$

$$T^{(2,\text{V})} \leq \sum_{dT_V} \hat{T}_{dT_V+1} z_{dT_V}^{(2,\text{V})} \qquad \text{Eq. 4.130}$$

Where

$$\sum_{dT_V} z_{dT_V}^{(2,\text{V})} = 1 \qquad \text{Eq. 4.131}$$

Methane Loop:

(3,2) $\hat{T}_{dT_2} = \hat{T}_{min} + \frac{ord(dP_1)-1}{card(dP_1)-1}[\hat{T}_{max} - \hat{T}_{min}]$

$$T^{(3,2)} \geq \sum_{dT_2} \hat{T}_{dT_2} z_{dT_2}^{(3,2)} \qquad \text{Eq. 4.132}$$

$$T^{(3,2)} \leq \sum_{dT_2} \hat{T}_{dT_2+1} z_{dT_2}^{(3,2)} \qquad \text{Eq. 4.133}$$

Where

$$\sum_{dT_2} z_{dT_2}^{(3,2)} = 1 \qquad \text{Eq. 4.134}$$

(3,3P) $\hat{T}_{dT_{3P}} = \hat{T}_{min} + \frac{ord(dP_1)-1}{card(dP_1)-1}[\hat{T}_{max} - \hat{T}_{min}]$

$$T^{(3,3P)} \geq \sum_{dT_{3P}} \hat{T}_{dT_{3P}} z_{dT_{3P}}^{(3,3P)} \qquad \text{Eq. 4.135}$$

$$T^{(3,3P)} \leq \sum_{dT_{3P}} \hat{T}_{dT_{3P}+1} z_{dT_{3P}}^{(3,3P)} \qquad \text{Eq. 4.136}$$

Where

$$\sum_{dT_{3P}} z_{dT_{3P}}^{(3,3P)} = 1 \qquad \text{Eq. 4.137}$$

(3,V) $\hat{T}_{dT_V} = \hat{T}_{min} + \frac{ord(dP_1)-1}{card(dP_1)-1}[\hat{T}_{max} - \hat{T}_{min}]$

$$T^{(3,V)} \geq \sum_{dT_V} \hat{T}_{dT_V} z_{dT_V}^{(3,V)} \qquad \text{Eq. 4.138}$$

$$T^{(3,V)} \leq \sum_{dT_V} \hat{T}_{dT_V+1} z_{dT_V}^{(3,V)} \qquad \text{Eq. 4.139}$$

Where

$$\sum_{dT_V} z_{dT_V}^{(3,V)} = 1 \qquad \text{Eq. 4.140}$$

To make sure the phases are easily distinguished. Thus, $f_H(P^*, T^*, \theta^*)$ is rewritten as follows:

$f_{H,liq}(P^*, T^*) *(1-\theta^*) + f_{H,vap}(P^*, T^*) * \theta^*$, where the phase is determined by fixing $\theta^* = 1$ for vapor and $\theta^* = 0$ for liquid. $f_{H,liq}\left(\hat{T}_{dT_r}, \hat{P}_{dP_j}\right)$ and $f_{H,vap}\left(\hat{T}_{dT_r}, \hat{P}_{dP_j}\right)$ are numbers (no longer functions), which are introduced as regressed equations, and are obtained directly from Pro/II software.

Then, $H^* = f_H(P^*, T^*, \theta^*)$ is replaced by:

$$\sum_{dP_j}\sum_{dT_r}\left[f_{H,liq}\left(\hat{T}_{dT_r},\hat{P}_{dP_j}\right)(1-\theta^*)+f_{H,vap}\left(\hat{T}_{dT_r},\hat{P}_{dP_j}\right)\theta^*\right]z^*_{dT_r}y^*_{dP_j}\le H^*\le$$

$$\sum_{dP_j}\sum_{dT_r}\left[f_{H,liq}\left(\hat{T}_{dT_r+1},\hat{P}_{dP_{j+1}}\right)(1-\theta^*)+f_{H,vap}\left(\hat{T}_{dT_r+1},\hat{P}_{dP_{j+1}}\right)\theta^*\right]z^*_{dT_r}y^*_{dP_j}$$

Or

$$\sum_{dP_j}\sum_{dT_r}\left[f_{H,liq}\left(\hat{T}_{dT_r},\hat{P}_{dP_j}\right)(1-\theta^*)+f_{H,vap}\left(\hat{T}_{dT_r},\hat{P}_{dP_j}\right)\theta^*\right]\rho^*_{dT_r,dP_j}\le H^*\le$$

$$\sum_{dP_j}\sum_{dT_r}\left[f_{H,liq}\left(\hat{T}_{dT_r+1},\hat{P}_{dP_{j+1}}\right)(1-\theta^*)+f_{H,vap}\left(\hat{T}_{dT_r+1},\hat{P}_{dP_{j+1}}\right)\theta^*\right]\rho^*_{dT_r,dP_j}$$

where $\rho^*_{dT_r,dP_j}=z^*_{dT_r}*y^*_{dP_j}$ which is written in a relaxed

form as follows:

$$\rho^*_{dP_j}\le y^*_{dP_j} \qquad\qquad \text{Eq. 4.141}$$

$$\rho^*_{dP_j}\le z^*_{dT_r} \qquad\qquad \text{Eq. 4.142}$$

$$\rho^*_{dP_j}\ge y^*_{dP_j}+z^*_{dT_r}-1 \qquad\qquad \text{Eq. 4.143}$$

The extended of enthalpy at each stream of each refrigerant cycle is represented as following:

Propane Loop:

(1,1) $\qquad H^{(1,1)}\ge\sum_{dP_1}\sum_{dT_1}\left[f^{sat}_{H,vap}\left(\hat{T}_{dT_1},\hat{P}_{dP_1}\right)\right]\rho^{(1,1)}_{dT_1,dP_1}$ Eq. 4.144

$\qquad H^{(1,1)}\le\sum_{dP_1}\sum_{dT_1}\left[f^{sat}_{H,vap}\left(\hat{T}_{dT_1+1},\hat{P}_{dP_1+1}\right)\right]\rho^{(1,1)}_{dT_1,dP_1}$ Eq. 4.145

$$\rho^{(1,1)}_{dP_1}\le y^{(1,1)}_{dP_1} \qquad\qquad \text{Eq. 4.146}$$

$$\rho^{(1,1)}_{dP_1}\le z^{(1,1)}_{dT_1} \qquad\qquad \text{Eq. 4.147}$$

$$\rho^{(1,1)}_{dP_1}\ge y^{(1,1)}_{dP_1}+z^{(1,1)}_{dT_1}-1 \qquad\qquad \text{Eq. 4.148}$$

(1,2) $\qquad H^{(1,2)}\ge\sum_{dP_2}\sum_{dT_2}\left[f_{H,vap}\left(\hat{T}_{dT_2},\hat{P}_{dP_2}\right)\right]\rho^{(1,2)}_{dT_2,dP_2}$ Eq. 4.149

$\qquad H^{(1,2)}\le\sum_{dP_2}\sum_{dT_2}\left[f_{H,vap}\left(\hat{T}_{dT_2+1},\hat{P}_{dP_2+1}\right)\right]\rho^{(1,2)}_{dT_2,dP_2}$ Eq. 4.150

$$\rho^{(1,2)}_{dP_2}\le y^{(1,2)}_{dP_2} \qquad\qquad \text{Eq. 4.151}$$

$$\rho^{(1,2)}_{dP_2}\le z^{(1,2)}_{dT_2} \qquad\qquad \text{Eq. 4.152}$$

$$\rho_{dP_2}^{(1,2)} \geq y_{dP_2}^{(1,2)} + z_{dT_2}^{(1,2)} - 1 \qquad \text{Eq. 4.153}$$

(1,2P) $\qquad H^{(1,2\text{P})} \geq \sum_{dP_{2P}} \sum_{dT_{2P}} \left[f_{H,vap}^{sat}\!\left(\hat{T}_{dT_{2P}}, \hat{P}_{dP_2}\right) \right] \rho_{dT_{2P},dP_2}^{(1,2\text{P})}$ $\qquad$ Eq. 4.154

$$H^{(1,2\text{P})} \leq \sum_{dP_2} \sum_{dT_{2P}} \left[f_{H,vap}^{sat}\!\left(\hat{T}_{dT_{2P}+1}, \hat{P}_{dP_2+1}\right) \right] \rho_{dT_{2P},dP_2}^{(1,2\text{P})} \qquad \text{Eq. 4.155}$$

$$\rho_{dP_2}^{(1,2\text{P})} \leq y_{dP_2}^{(1,2)} \qquad \text{Eq. 4.156}$$

$$\rho_{dP_2}^{(1,2\text{P})} \leq z_{dT_{2P}}^{(1,2\text{P})} \qquad \text{Eq. 4.157}$$

$$\rho_{dP_2}^{(1,2\text{P})} \geq y_{dP_2}^{(1,2)} + z_{dT_{2P}}^{(1,2\text{P})} - 1 \qquad \text{Eq. 4.158}$$

(1,3) $\qquad H^{(1,3)} \geq \sum_{dP_3} \sum_{dT_3} \left[f_{H,liq}^{sat}\!\left(\hat{T}_{dT_3}, \hat{P}_{dP_3}\right) \right] \rho_{dT_3,dP_3}^{(1,3)}$ $\qquad$ Eq. 4.159

$$H^{(1,3)} \leq \sum_{dP_3} \sum_{dT_3} \left[f_{H,liq}^{sat}\!\left(\hat{T}_{dT_3+1}, \hat{P}_{dP_3+1}\right) \right] \rho_{dT_3,dP_3}^{(1,3)} \qquad \text{Eq. 4.160}$$

$$\rho_{dP_3}^{(1,3)} \leq y_{dP_3}^{(1,3)} \qquad \text{Eq. 4.161}$$

$$\rho_{dP_3}^{(1,3)} \leq z_{dT_3}^{(1,3)} \qquad \text{Eq. 4.162}$$

$$\rho_{dP_3}^{(1,3)} \geq y_{dP_3}^{(1,3)} + z_{dT_3}^{(1,3)} - 1 \qquad \text{Eq. 4.163}$$

(1,v) $\quad H^{(1,\text{V})} \geq \sum_{dP_V} \sum_{dT_V} \left[f_{H,liq}^{sat}\!\left(\hat{T}_{dT_V}, \hat{P}_{dP_V}\right)\left(1 - \theta^{(1,\text{V})}\right) \rho_{dT_V,dP_V}^{(1,\text{V})} \right]$

$$+ \sum_{dP_V} \sum_{dT_V} \left[f_{H,vap}^{sat}\!\left(\hat{T}_{dT_V}, \hat{P}_{dP_V}\right) \right] \theta^{(1,\text{V})} \rho_{dT_V,dP_V}^{(1,\text{V})} \qquad \text{Eq. 4.164}$$

$$H^{(1,\text{V})} \leq \sum_{dP_V} \sum_{dT_V} \left[f_{H,liq}^{sat}\!\left(\hat{T}_{dT_V+1}, \hat{P}_{dP_V+1}\right)\left(1 - \theta^{(1,\text{V})}\right) \rho_{dT_V,dP_V}^{(1,\text{V})} \right]$$

$$+ \sum_{dP_V} \sum_{dT_V} \left[f_{H,vap}^{sat}\!\left(\hat{T}_{dT_V+1}, \hat{P}_{dP_V+1}\right) \right] \theta^{(1,\text{V})} \rho_{dT_V,dP_V}^{(1,\text{V})} \qquad \text{Eq. 4.165}$$

$$\rho_{dP_V}^{(1,\text{V})} \leq y_{dP_V}^{(1,\text{V})} \qquad \text{Eq. 4.166}$$

$$\rho_{dP_V}^{(1,\text{V})} \leq z_{dT_V}^{(1,\text{V})} \qquad \text{Eq. 4.167}$$

$$\rho_{dP_V}^{(1,\text{V})} \geq y_{dP_V}^{(1,\text{V})} + z_{dT_V}^{(1,\text{V})} - 1 \qquad \text{Eq. 4.168}$$

Ethylene Loop:

(2,1) $\qquad H^{(2,1)} \geq \sum_{dP_1} \sum_{dT_1} \left[f_{H,vap}^{sat}\!\left(\hat{T}_{dT_1}, \hat{P}_{dP_1}\right) \right] \rho_{dT_1,dP_1}^{(2,1)}$ $\qquad$ Eq. 4.169

$$H^{(2,1)} \leq \sum_{dP_1} \sum_{dT_1} \left[f_{H,vap}^{sat}\!\left(\hat{T}_{dT_1+1}, \hat{P}_{dP_1+1}\right) \right] \rho_{dT_1,dP_1}^{(2,1)} \qquad \text{Eq. 4.170}$$

$$\rho_{dP_1}^{(2,1)} \leq y_{dP_1}^{(2,1)} \qquad \text{Eq. 4.171}$$

$$\rho_{dP_1}^{(2,1)} \leq z_{dT_1}^{(2,1)} \qquad \text{Eq. 4.172}$$

$$\rho_{dP_1}^{(2,1)} \geq y_{dP_1}^{(2,1)} + z_{dT_1}^{(2,1)} - 1 \qquad \text{Eq. 4.173}$$

(2,2)
$$H^{(2,2)} \geq \sum_{dP_2} \sum_{dT_2} \left[f_{H,vap}(\hat{T}_{dT_2}, \hat{P}_{dP_2}) \right] \rho_{dT_2,dP_2}^{(2,2)} \qquad \text{Eq. 4.174}$$

$$H^{(2,2)} \leq \sum_{dP_2} \sum_{dT_2} \left[f_{H,vap}(\hat{T}_{dT_2+1}, \hat{P}_{dP_2+1}) \right] \rho_{dT_2,dP_2}^{(2,2)} \qquad \text{Eq. 4.175}$$

$$\rho_{dP_2}^{(2,2)} \leq y_{dP_2}^{(2,2)} \qquad \text{Eq. 4.176}$$

$$\rho_{dP_2}^{(2,2)} \leq z_{dT_2}^{(2,2)} \qquad \text{Eq. 4.177}$$

$$\rho_{dP_2}^{(2,2)} \geq y_{dP_2}^{(2,2)} + z_{dT_2}^{(2,2)} - 1 \qquad \text{Eq. 4.178}$$

(2,2P)
$$H^{(2,2P)} \geq \sum_{dP_{2P}} \sum_{dT_{2P}} \left[f_{H,vap}^{sat}(\hat{T}_{dT_{2P}}, \hat{P}_{dP_2}) \right] \rho_{dT_{2P},dP_2}^{(2,2P)} \qquad \text{Eq. 4.179}$$

$$H^{(2,2P)} \leq \sum_{dP_2} \sum_{dT_{2P}} \left[f_{H,vap}^{sat}(\hat{T}_{dT_{2P}+1}, \hat{P}_{dP_2+1}) \right] \rho_{dT_{2P},dP_2}^{(2,2P)} \qquad \text{Eq. 4.180}$$

$$\rho_{dP_2}^{(2,2P)} \leq y_{dP_2}^{(2,2)} \qquad \text{Eq. 4.181}$$

$$\rho_{dP_2}^{(2,2P)} \leq z_{dT_{2P}}^{(2,2P)} \qquad \text{Eq. 4.182}$$

$$\rho_{dP_2}^{(2,2P)} \geq y_{dP_2}^{(2,2)} + z_{dT_{2P}}^{(2,2P)} - 1 \qquad \text{Eq. 4.183}$$

(2,3)
$$H^{(2,3)} \geq \sum_{dP_3} \sum_{dT_3} \left[f_{H,liq}^{sat}(\hat{T}_{dT_3}, \hat{P}_{dP_3}) \right] \rho_{dT_3,dP_3}^{(2,3)} \qquad \text{Eq. 4.184}$$

$$H^{(2,3)} \leq \sum_{dP_3} \sum_{dT_3} \left[f_{H,liq}^{sat}(\hat{T}_{dT_3+1}, \hat{P}_{dP_3+1}) \right] \rho_{dT_3,dP_3}^{(2,3)} \qquad \text{Eq. 4.185}$$

$$\rho_{dP_3}^{(2,3)} \leq y_{dP_3}^{(2,3)} \qquad \text{Eq. 4.186}$$

$$\rho_{dP_3}^{(2,3)} \leq z_{dT_3}^{(2,3)} \qquad \text{Eq. 4.187}$$

$$\rho_{dP_3}^{(2,3)} \geq y_{dP_3}^{(2,3)} + z_{dT_3}^{(2,3)} - 1 \qquad \text{Eq. 4.188}$$

(2,v)
$$H^{(2,V)} \geq \sum_{dP_V} \sum_{dT_V} \left[f_{H,liq}^{sat}(\hat{T}_{dT_V}, \hat{P}_{dP_V})(1 - \theta^{(2,V)}) \rho_{dT_V,dP_V}^{(2,V)} \right]$$

$$+ \sum_{dP_V} \sum_{dT_V} \left[f_{H,vap}^{sat}(\hat{T}_{dT_V}, \hat{P}_{dP_V}) \right] \theta^{(2,V)} \rho_{dT_V,dP_V}^{(2,V)} \qquad \text{Eq. 4.189}$$

$$H^{(2,\text{V})} \leq \sum_{dP_V} \sum_{dT_V} \left[f_{H,liq}^{sat}(\hat{T}_{dT_V+1}, \hat{P}_{dP_V+1})(1 - \theta^{(2,\text{V})})\rho_{dT_V,dP_V}^{(2,\text{V})} \right]$$

$$+ \sum_{dP_V} \sum_{dT_V} \left[f_{H,vap}^{sat}(\hat{T}_{dT_V+1}, \hat{P}_{dP_V+1}) \right] \theta^{(2,\text{V})}\rho_{dT_V,dP_V}^{(2,\text{V})} \qquad \text{Eq. 4.190}$$

$$\rho_{dP_V}^{(2,\text{V})} \leq y_{dP_V}^{(2,\text{V})} \qquad \text{Eq. 4.191}$$

$$\rho_{dP_V}^{(2,\text{V})} \leq z_{dT_V}^{(2,\text{V})} \qquad \text{Eq. 4.192}$$

$$\rho_{dP_V}^{(2,\text{V})} \geq y_{dP_V}^{(2,\text{V})} + z_{dT_V}^{(2,\text{V})} - 1 \qquad \text{Eq. 4.193}$$

Methane Loop:

(3,1)
$$H^{(3,1)} \geq \sum_{dP_1} \sum_{dT_1} \left[f_{H,vap}^{sat}(\hat{T}_{dT_1}, \hat{P}_{dP_1}) \right] \rho_{dT_1,dP_1}^{(3,1)} \qquad \text{Eq. 4.194}$$

$$H^{(3,1)} \leq \sum_{dP_1} \sum_{dT_1} \left[f_{H,vap}^{sat}(\hat{T}_{dT_1+1}, \hat{P}_{dP_1+1}) \right] \rho_{dT_1,dP_1}^{(3,1)} \qquad \text{Eq. 4.195}$$

$$\rho_{dP_1}^{(3,1)} \leq y_{dP_1}^{(3,1)} \qquad \text{Eq. 4.196}$$

$$\rho_{dP_1}^{(3,1)} \leq z_{dT_1}^{(3,1)} \qquad \text{Eq. 4.197}$$

$$\rho_{dP_1}^{(3,1)} \geq y_{dP_1}^{(3,1)} + z_{dT_1}^{(3,1)} - 1 \qquad \text{Eq. 4.198}$$

(3,2)
$$H^{(3,2)} \geq \sum_{dP_2} \sum_{dT_2} \left[f_{H,vap}(\hat{T}_{dT_2}, \hat{P}_{dP_2}) \right] \rho_{dT_2,dP_2}^{(3,2)} \qquad \text{Eq. 4.199}$$

$$H^{(3,2)} \leq \sum_{dP_2} \sum_{dT_2} \left[f_{H,vap}(\hat{T}_{dT_2+1}, \hat{P}_{dP_2+1}) \right] \rho_{dT_2,dP_2}^{(3,2)} \qquad \text{Eq. 4.200}$$

$$\rho_{dP_2}^{(3,2)} \leq y_{dP_2}^{(3,2)} \qquad \text{Eq. 4.201}$$

$$\rho_{dP_2}^{(3,2)} \leq z_{dT_2}^{(3,2)} \qquad \text{Eq. 4.202}$$

$$\rho_{dP_2}^{(3,2)} \geq y_{dP_2}^{(3,2)} + z_{dT_2}^{(3,2)} - 1 \qquad \text{Eq. 4.203}$$

(3,3)
$$H^{(3,3)} \geq \sum_{dP_3} \sum_{dT_3} \left[f_{H,vap}(\hat{T}_{dT_3}, \hat{P}_{dP_3}) \right] \rho_{dT_3,dP_3}^{(3,3)} \qquad \text{Eq. 4.204}$$

$$H^{(3,3)} \leq \sum_{dP_3} \sum_{dT_3} \left[f_{H,vap}(\hat{T}_{dT_3+1}, \hat{P}_{dP_3+1}) \right] \rho_{dT_3,dP_3}^{(3,3)} \qquad \text{Eq. 4.205}$$

$$\rho_{dP_3}^{(3,3)} \leq y_{dP_3}^{(3,3)} \qquad \text{Eq. 4.206}$$

$$\rho_{dP_3}^{(3,3)} \leq z_{dT_3}^{(3,3)} \qquad \text{Eq. 4.207}$$

$$\rho_{dP_3}^{(3,3)} \geq y_{dP_3}^{(3,3)} + z_{dT_3}^{(3,3)} - 1 \qquad \text{Eq. 4.208}$$

$(3,3\text{P})$ $\qquad H^{(3,3\text{P})} \geq \sum_{dP_{2P}} \sum_{dT_{2P}} \left[f_{H,vap}^{sat}\left(\hat{T}_{dT_{3P}}, \hat{P}_{dP_3}\right) \right] \rho_{dT_{3P},dP_3}^{(3,3\text{P})}$ $\qquad$ Eq. 4.209

$\qquad H^{(3,3\text{P})} \leq \sum_{dP_3} \sum_{dT_{3P}} \left[f_{H,vap}^{sat}\left(\hat{T}_{dT_{3P}+1}, \hat{P}_{dP_3+1}\right) \right] \rho_{dT_{3P},dP_3}^{(3,3\text{P})}$ $\qquad$ Eq. 4.210

$$\rho_{dP_3}^{(3,3\text{P})} \leq y_{dP_3}^{(3,3)} \qquad\qquad \text{Eq. 4.211}$$

$$\rho_{dP_3}^{(3,3\text{P})} \leq z_{dT_{3P}}^{(3,3\text{P})} \qquad\qquad \text{Eq. 4.212}$$

$$\rho_{dP_3}^{(3,3\text{P})} \geq y_{dP_3}^{(3,3)} + z_{dT_{3P}}^{(3,3\text{P})} - 1 \qquad\qquad \text{Eq. 4.213}$$

$(3,4)$ $\qquad H^{(3,4)} \geq \sum_{dP_4} \sum_{dT_4} \left[f_{H,liq}^{sat}\left(\hat{T}_{dT_4}, \hat{P}_{dP_4}\right) \right] \rho_{dT_4,dP_4}^{(3,4)}$ $\qquad$ Eq. 4.214

$\qquad H^{(3,4)} \leq \sum_{dP_4} \sum_{dT_4} \left[f_{H,liq}^{sat}\left(\hat{T}_{dT_4+1}, \hat{P}_{dP_4+1}\right) \right] \rho_{dT_4,dP_4}^{(3,4)}$ $\qquad$ Eq. 4.215

$$\rho_{dP_4}^{(3,4)} \leq y_{dP_4}^{(3,4)} \qquad\qquad \text{Eq. 4.216}$$

$$\rho_{dP_4}^{(3,4)} \leq z_{dT_4}^{(3,4)} \qquad\qquad \text{Eq. 4.217}$$

$$\rho_{dP_4}^{(3,4)} \geq y_{dP_4}^{(3,4)} + z_{dT_4}^{(3,4)} - 1 \qquad\qquad \text{Eq. 4.218}$$

$(3,v)$ $\quad H^{(3,V)} \geq \sum_{dP_V} \sum_{dT_V} \left[f_{H,liq}^{sat}\left(\hat{T}_{dT_V}, \hat{P}_{dP_V}\right)\left(1 - \theta^{(3,V)}\right)\rho_{dT_V,dP_V}^{(3,V)} \right]$

$\qquad + \sum_{dP_V} \sum_{dT_V} \left[f_{H,vap}^{sat}\left(\hat{T}_{dT_V}, \hat{P}_{dP_V}\right) \right] \theta^{(3,V)} \rho_{dT_V,dP_V}^{(3,V)}$ $\qquad$ Eq. 4.219

$$H^{(3,V)} \leq \sum_{dP_V} \sum_{dT_V} \left[f_{H,liq}^{sat}\left(\hat{T}_{dT_V+1}, \hat{P}_{dP_V+1}\right)\left(1 - \theta^{(3,V)}\right)\rho_{dT_V,dP_V}^{(3,V)} \right]$$

$\qquad + \sum_{dP_V} \sum_{dT_V} \left[f_{H,vap}^{sat}\left(\hat{T}_{dT_V+1}, \hat{P}_{dP_V+1}\right) \right] \theta^{(3,V)} \rho_{dT_V,dP_V}^{(3,V)}$ $\qquad$ Eq. 4.220

$$\rho_{dP_V}^{(3,V)} \leq y_{dP_V}^{(3,V)} \qquad\qquad \text{Eq. 4.221}$$

$$\rho_{dP_V}^{(3,V)} \leq z_{dT_V}^{(3,V)} \qquad\qquad \text{Eq. 4.222}$$

$$\rho_{dP_V}^{(3,V)} \geq y_{dP_V}^{(3,V)} + z_{dT_V}^{(3,V)} - 1 \qquad\qquad \text{Eq. 4.223}$$

When the phases are already declared $\hat{\theta}^*$ is a parameter, that is $\hat{\theta}^* = 1 \ or \ \hat{\theta}^* = 0$. If a fluid is a mixture of liquid and vapor, $0 < \theta^* < 1$

The heat of vaporization equations need to be linearized because it contains 3 variables. The linearization method is similar to the linearization of flow rate.

$$\hat{\theta}_{dF_k}^{k,V} = \hat{\theta}_{min}^{k,V} + \frac{ord(d\theta_k)-1}{card(d\theta_k)-1}[\hat{\theta}_{max}^{k,V} - \hat{\theta}_{min}^{k,V}]$$

$$\theta^{k,V} \geq \sum_{d\theta_k} \hat{\theta}_{d\theta_k}^{k,V} y\theta_{d\theta_k}^{k,V} \qquad \text{Eq. 4.224}$$

$$\theta^{k,V} \leq \sum_{d\theta_k} \hat{\theta}_{d\theta_k+1}^{k,V} y\theta_{d\theta_k}^{k,V} \qquad \text{Eq. 4.225}$$

Where

$$\sum_{d\theta_k} y\theta_{d\theta_k}^{k,V} = 1 \qquad \text{Eq. 4.226}$$

Then the non-linear equations are substituted by the set of linear equations as follows:

$$O^k = (1 - \theta^{k,V})R^{k,HV} \qquad \text{Eq. 4.227}$$

where $R^{k,HV} = F^k \; x \; H^{V,Cn}$

Instead of using the product of $(1 - \theta^{k,V})R^{k,HV}$ to calculate O^k, a linear estimator of O^k is introduced as follows:

$$O^k \geq \sum_{d\theta_k} \hat{\theta}_{d\theta_k}^{k,V} \gamma\theta_{d\theta_k}^{k,V} \qquad \text{Eq. 4.228}$$

$$O^k \leq \sum_{d\theta_k} \hat{\theta}_{d\theta_k+1}^{k,V} \gamma\theta_{d\theta_k}^{k,V} \qquad \text{Eq. 4.229}$$

$$\gamma\theta_{d\theta_k}^{k,V} - \Gamma y\theta_{d\theta_k}^{k,V} \leq 0 \qquad \text{Eq. 4.230}$$

$$\gamma\theta_{d\theta_k}^{k,V} \geq 0 \qquad \text{Eq. 4.231}$$

$$[R^{k,HV} - \gamma\theta_{d\theta_k}^{k,V}] - \Gamma[1 - y\theta_{d\theta_k}^{k,V}] \leq 0 \qquad \text{Eq. 4.232}$$

$$[R^{k,HV} - \gamma\theta_{d\theta_k}^{k,V}] \geq 0 \qquad \text{Eq. 4.233}$$

Since entropy is a function of temperature and pressure, it can be linearized as follows:

$$S^* = f_S(P^*, \; T^*),$$

Where $*$ $is \; replaced \; for \; any \; (k,1), (k,2), etc.$

$$\hat{S}_{dS_f} = \hat{S}_{min} + \frac{ord(dS_k)-1}{card(dS_k)-1}[\hat{S}_{max} - \hat{S}_{min}]$$

$$S^* \geq \sum_{dP_j} \sum_{dT_r} \left[f_S\left(\hat{T}_{dT_r}, \hat{P}_{dP_j}\right) \rho^*_{dT_r,dP_j} \right] \qquad \text{Eq. 4.234}$$

$$S^* \leq \sum_{dP_j} \sum_{dT_r} [f_S\left(\hat{T}_{dT_r+1}, \hat{P}_{dP_j+1}\right) \rho^*_{dT_r,dP_j}] \qquad \text{Eq. 4.235}$$

Where
$$\rho^*_{dT_r,dP_j} = y^*_{dP_j} z^*_{dT_r} \qquad \text{Eq. 4.236}$$

$$\sum_{dS_f} \rho^*_{dT_r,dP_j} = 1 \qquad \text{Eq. 4.237}$$

In this case, consider the conditions of temperature and pressure such that $\theta^* = 1$. The extended of enthalpy at each stream of each refrigerant cycle is represented as follows:

Propane Loop:

(1,1)
$$S^{(1,1)} \geq \sum_{dP_1} \sum_{dT_1} \left[f_S(\hat{T}_{dT_1}, \hat{P}_{dP_1}) \rho^{(1,1)}_{dT_1,dP_1} \right] \qquad \text{Eq. 4.238}$$

$$S^{(1,1)} \leq \sum_{dP_1} \sum_{dT_1} [f_S(\hat{T}_{dT_1+1}, \hat{P}_{dP_1+1}) \rho^{(1,1)}_{dT_1,dP_1}] \qquad \text{Eq. 4.239}$$

$$\rho^{(1,1)}_{dP_1} \leq y^{(1,1)}_{dP_1} \qquad \text{Eq. 4.240}$$

$$\rho^{(1,1)}_{dP_1} \leq z^{(1,1)}_{dT_1} \qquad \text{Eq. 4.241}$$

$$\rho^{(1,1)}_{dP_1} \geq y^{(1,1)}_{dP_1} + z^{(1,1)}_{dT_1} - 1 \qquad \text{Eq. 4.242}$$

(1,2)
$$S^{(1,2)} \geq \sum_{dP_2} \sum_{dT_2} [f_S(\hat{T}_{dT_2}, \hat{P}_{dP_2}) \rho^{(1,2)}_{dT_2,dP_2}] \qquad \text{Eq. 4.243}$$

$$S^{(1,2)} \leq \sum_{dP_2} \sum_{dT_2} [f_S(\hat{T}_{dT_2+1}, \hat{P}_{dP_2+1}) \rho^{(1,2)}_{dT_2,dP_2}] \qquad \text{Eq. 4.244}$$

$$\rho^{(1,2)}_{dP_2} \leq y^{(1,2)}_{dP_2} \qquad \text{Eq. 4.245}$$

$$\rho^{(1,2)}_{dP_2} \leq z^{(1,2)}_{dT_2} \qquad \text{Eq. 4.246}$$

$$\rho^{(1,2)}_{dP_2} \geq y^{(1,2)}_{dP_2} + z^{(1,2)}_{dT_2} - 1 \qquad \text{Eq. 4.247}$$

Ethylene Loop:

(2,1)
$$S^{(2,1)} \geq \sum_{dP_1} \sum_{dT_1} [f_S(\hat{T}_{dT_1}, \hat{P}_{dP_1}) \rho^{(2,1)}_{dT_1,dP_1}] \qquad \text{Eq. 4.248}$$

$$S^{(2,1)} \leq \sum_{dP_1} \sum_{dT_1} [f_S(\hat{T}_{dT_1+1}, \hat{P}_{dP_1+1}) \rho^{(2,1)}_{dT_1,dP_1}] \qquad \text{Eq. 4.249}$$

$$\rho^{(2,1)}_{dP_1} \leq y^{(2,1)}_{dP_1} \qquad \text{Eq. 4.250}$$

$$\rho_{dP_1}^{(2,1)} \leq z_{dT_1}^{(2,1)} \qquad \text{Eq. 4.251}$$

$$\rho_{dP_1}^{(2,1)} \geq y_{dP_1}^{(2,1)} + z_{dT_1}^{(2,1)} - 1 \qquad \text{Eq. 4.252}$$

(2,2) $\qquad S^{(2,2)} \geq \sum_{dP_2} \sum_{dT_2} [f_S(\hat{T}_{dT_2}, \hat{P}_{dP_2}) \rho_{dT_2, dP_2}^{(2,2)}] \qquad \text{Eq. 4.253}$

$$S^{(2,2)} \leq \sum_{dP_2} \sum_{dT_2} [f_S(\hat{T}_{dT_2+1}, \hat{P}_{dP_2+1}) \rho_{dT_2, dP_2}^{(2,2)}] \qquad \text{Eq. 4.254}$$

$$\rho_{dP_2}^{(2,2)} \leq y_{dP_2}^{(2,2)} \qquad \text{Eq. 4.255}$$

$$\rho_{dP_2}^{(2,2)} \leq z_{dT_2}^{(2,2)} \qquad \text{Eq. 4.256}$$

$$\rho_{dP_2}^{(2,2)} \geq y_{dP_2}^{(2,2)} + z_{dT_2}^{(2,2)} - 1 \qquad \text{Eq. 4.257}$$

Methane Loop:

(3,1) $\qquad S^{(3,1)} \geq \sum_{dP_1} \sum_{dT_1} \left[f_S(\hat{T}_{dT_1}, \hat{P}_{dP_1}) \rho_{dT_1, dP_1}^{(3,1)} \right] \qquad \text{Eq. 4.258}$

$$S^{(3,1)} \leq \sum_{dP_1} \sum_{dT_1} [f_S(\hat{T}_{dT_1+1}, \hat{P}_{dP_1+1}) \rho_{dT_1, dP_1}^{(3,1)}] \qquad \text{Eq. 4.259}$$

$$\rho_{dP_1}^{(3,1)} \leq y_{dP_1}^{(3,1)} \qquad \text{Eq. 4.260}$$

$$\rho_{dP_1}^{(3,1)} \leq z_{dT_1}^{(3,1)} \qquad \text{Eq. 4.261}$$

$$\rho_{dP_1}^{(3,1)} \geq y_{dP_1}^{(3,1)} + z_{dT_1}^{(3,1)} - 1 \qquad \text{Eq. 4.262}$$

(3,2) $\qquad S^{(3,2)} \geq \sum_{dP_2} \sum_{dT_2} [f_S(\hat{T}_{dT_2}, \hat{P}_{dP_2}) \rho_{dT_2, dP_2}^{(3,2)}] \qquad \text{Eq. 4.263}$

$$S^{(3,2)} \leq \sum_{dP_2} \sum_{dT_2} [f_S(\hat{T}_{dT_2+1}, \hat{P}_{dP_2+1}) \rho_{dT_2, dP_2}^{(3,2)}] \qquad \text{Eq. 4.264}$$

$$\rho_{dP_2}^{(3,1)} \leq y_{dP_2}^{(3,1)} \qquad \text{Eq. 4.265}$$

$$\rho_{dP_2}^{(3,1)} \leq z_{dT_2}^{(3,1)} \qquad \text{Eq. 4.266}$$

$$\rho_{dP_2}^{(3,1)} \geq y_{dP_2}^{(3,1)} + z_{dT_2}^{(3,1)} - 1 \qquad \text{Eq. 4.267}$$

4.2.4.4 Compressor Equations

The lower bound model is obtained after linearization by partitioning method of the upper bound equations are changed into linear upper bound model as follows.

$$W^k = R^{k,2} - R^{k,1} \qquad k=1,2,3 \qquad \text{Eq. 4.268}$$

In this work, we can divide the equation for optimization the objective function with each part of equipment

$$W^k = F^k[H^{k,2} - H^{k,1}] \qquad k=1,2,3 \qquad \text{Eq. 4.1}$$

In turn, entropy and enthalpy are calculated by a set of equation (Peng-Robinson, SRK, etc.) represented by ($f_S^k(P^{k,i}, T^{k,i}, \theta^k)$, $f_H^k(P^{k,i}, T^{k,i}, \theta^k)$), where θ^k is the quality ($\theta^k=1$ for vapor/gas, $\theta^k=0$ for pure liquid and $0 < \theta^k < 1$ for mixture of liquid and vapor. Then we write:

$$
\begin{aligned}
S^{k,1} &= f_S^k(P^k, T^k, \theta^k) & k=1,2,3 && \text{Eq. 4.2} \\
H^{k,1} &= f_H^k(P^k, T^k, \theta^k) & k=1,2,3 && \text{Eq. 4.3} \\
S^{k,2} &= f_S^k(P^{k,2}, T_{ideal}^{k,2}, \theta^{k,2}) & k=1,2,3 && \text{Eq. 4.4} \\
H^{k,2} &= f_H^k(P^{k,2}, T^{k,2}, \theta^{k,2}) & k=1,2,3 && \text{Eq. 4.5}
\end{aligned}
$$

Isentropic compression is the compression in a compressor with 80% efficiency of compressor. Thus,

$$S_{ideal}^{k,2} = S^{k,1} \qquad k=1,2,3 \qquad \text{Eq. 4.7}$$

Then, ideal enthalpy is used to find non-ideal enthalpy in non-isentropic compression process.

$$[H_{ideal}^{k,2} - H^{k,1}] = \eta_k[H^{k,2} - H^{k,1}] \qquad k=1,2,3 \qquad \text{Eq. 4.8}$$

4.2.4.5 Cooler Equations

The energy balance equations around a cooler are:

$$Q^1 = R^{1,3} - R^{1,2} \qquad \text{Eq. 4.269}$$

$$Q^1 = R^{1,2} - R^{1,2P} - R^{1,HC} \qquad \text{Eq. 4.270}$$

where $\qquad H^{1,3} = f_H^{k,v}(P^{1,3}, T^{1,3}, \theta^{1,3}) \qquad \text{Eq. 4.11}$

$$H^{C,C3} = f_H^{1,3}(P^{1,3}, T^{1,3}, \theta^{1,3}) \qquad\qquad \text{Eq. 4.12}$$

$$H^{1,2P} = f_H^{1,2P}(P^{1,2}, T^{1,2P}, \theta^{1,2}) \qquad\qquad \text{Eq. 4.13}$$

$$T^{1,3} = T^{1,2P} \qquad\qquad \text{Eq. 4.15}$$

$$P^{1,3} = P^{1,2} \qquad\qquad \text{Eq. 4.16}$$

4.2.4.6 Valve Equations

Valves are the equipment used for cooling the temperature of refrigerant and the energy balance equations are represented as follows:

$$H^{1,v} = H^{1,3} \qquad\qquad \text{Eq. 4.17}$$

$$H^{1,v} = f_H^1(P^{1,v}, T^{1,v}, \theta^{1,v}) \qquad\qquad \text{Eq. 4.18}$$

$$H^{2,v} = H^{2,3} \qquad\qquad \text{Eq. 4.19}$$

$$H^{2,v} = f_H^2(P^{2,v}, T^{2,v}, \theta^{2,v}) \qquad\qquad \text{Eq. 4.20}$$

$$H^{3,v} = H^{3,4} \qquad\qquad \text{Eq. 4.21}$$

$$H^{3,v} = f_H^3(P^{3,v}, T^{3,v}, \theta^{3,v}) \qquad\qquad \text{Eq. 4.22}$$

4.2.4.7 Box Equations

Boxes or evaporators of each stage in the refrigeration cycle are used for transferring the heat between natural gas and refrigerant that can be calculated as follows:

At stage k = 1

$$QB^{1,1} = R^{1,1} - R^{1,v} \qquad\qquad \text{Eq. 4.271}$$

$$QB^{1,1} = O^1 \qquad\qquad \text{Eq. 4.272}$$

$$QB^{1,2} = R^{2,2} - R^{2,3} \qquad\qquad \text{Eq. 4.273}$$

$$QB^{1,2} = R^{2,2} - R^{2,2P} - R^{2,HC} \qquad\qquad \text{Eq. 4.274}$$

$$QB^{1,3} = R^{3,2} - R^{3,3} \qquad\qquad \text{Eq. 4.275}$$

$$QB^{1,C3} = QB^{1,C2} + QB^{1,C1} + QB^{1,NG} \qquad\qquad \text{Eq. 4.28}$$

$$H^{2,2P} = f_H^{2,2P}(P^{2,2}, T^{2,2P}, \theta^{2,2}) \qquad\qquad \text{Eq. 4.29}$$

$$H^{2,3} = f_H^{2,3}(P^{2,3}, T^{2,3}, \theta^{2,3}) \qquad\qquad \text{Eq. 4.30}$$

$$H^{3,3} = f_H^{3,3}(P^{3,3}, T^{3,3}, \theta^{3,3}) \qquad\qquad \text{Eq. 4.31}$$

$$H^{C,C2} = f_H^{C,C2}(P^{2,2}) \qquad\qquad \text{Eq. 4.32}$$

$$H^{V,C3} = f_H^{V,C3}(P^{1,V}) \qquad \text{Eq. 4.33}$$

$$T^{1,1} = T^{1,V} \qquad \text{Eq. 4.34}$$

$$T^{2,2P} = T^{1,3} \qquad \text{Eq. 4.35}$$

$$P^{1,1} = P^{1,V} \qquad \text{Eq. 4.36}$$

$$P^{2,2} = P^{2,3} \qquad \text{Eq. 4.37}$$

$$P^{3,2} = P^{3,3} \qquad \text{Eq. 4.38}$$

At stage k = 2

$$QB^{2,2} = R^{2,1} - R^{2,v} \qquad \text{Eq. 4.276}$$

$$QB^{2,2} = O^2 \qquad \text{Eq. 4.277}$$

$$QB^{2,3} = R^{3,3} - R^{3,4} \qquad \text{Eq. 4.278}$$

$$QB^{2,3} = R^{3,3} - R^{3,3P} - R^{3,HC}] \qquad \text{Eq. 4.279}$$

$$QB^{2,2} = QB^{2,3} + QB^{2,NG} \qquad \text{Eq. 4.43}$$

$$H^{3,3P} = f_H^{3,3P}(P^{3,3}, T^{3,3P}, \theta^{3,3}) \qquad \text{Eq. 4.44}$$

$$H^{3,4} = f_H^{3,4}(P^{3,4}, T^{3,4}, \theta^{3,4}) \qquad \text{Eq. 4.45}$$

$$H^{V,C2} = f_H^{V,C2}(P^{2,V}) \qquad \text{Eq. 4.46}$$

$$H^{C,C1} = f_H^{C,C1}(P^{3,3}) \qquad \text{Eq. 4.47}$$

$$T^{2,1} = T^{2,V} \qquad \text{Eq. 4.48}$$

$$T^{3,3P} = T^{3,4} \qquad \text{Eq. 4.49}$$

$$P^{2,1} = P^{2,V} \qquad \text{Eq. 4.50}$$

$$P^{2,1} = P^{3,4} \qquad \text{Eq. 4.51}$$

At stage k = 3

$$QB^{3,3} = R^{3,1} - R^{3,v} \qquad \text{Eq. 4.280}$$

$$QB^{3,3} = O^3 \qquad \text{Eq. 4.281}$$

$$QB^{3,3} = QB^{3,NG} \qquad \text{Eq. 4.54}$$

$$H^{V,C1} = f_H^{V,C1}(P^{3,V}) \qquad \text{Eq. 4.55}$$

$$T^{3,1} = T^{3,V} \qquad \text{Eq. 4.56}$$

$$P^{3,1} = P^{3,V} \qquad \text{Eq. 4.57}$$

Mixed integer linear programming (MIP) is used as a method for solve the lower bound model. The result from the lower bound model is used to evaluate the reliability of the upper bound model. The difference of the objective function between upper bound and lower bound models should be less than 1% to affirm that upper solution is a global optimum solution.

4.2.5 Variable Model

Some equations are added to upper bound and lower bound model when fixed parameters become variables.

$$H^{k,NG} = f_H^k(P^k, T^k, \theta^k, C^N) \qquad \text{k=1,2,3,4} \qquad \text{Eq. 4.282}$$

$$QB^{k,NG} = F^{NG}[H^{k,NG} - H^{k-1,NG}] \quad \text{k=1,2,3,4} \qquad \text{Eq. 4.283}$$

$$T^{k+1,NG} = T^{k,1} + \Delta Tmin \quad \text{k=1,2,3,4} \qquad \text{Eq. 4.284}$$

$QB^{k,NG}$ is considered as variable depending on enthalpy of natural gas in each stage. C^N is a component of LNG which are defined as follows.

Table 4.1 Natural gas composition for base case model

Component	Natural Gas Component of base case model (mole %)	Range* (mole %)
Methane	90.460	87.0 - 97.0
Ethane	5.710	1.5 - 9.0
Propane	0.524	0.1 - 1.5
iso - Butane	0.103	0.01 - 0.3
normal - Butane	0.103	0.01 - 0.3
iso - Pentane	0.040	trace - 0.04
normal - Pentane	0.040	trace - 0.04
Hexanes plus	0.050	trace - 0.06
Nitrogen	1.660	0.2 - 5.5
Carbon Dioxide	1.310	0.05 - 1.5
Oxygen	0.000	trace - 0.1
Hydrogen	0.000	trace - 0.02
Total	100.000	

*The range of each component refer from table 2.1.

This composition is used in variables model which heat load on natural gas stream become variables.

4.2.6 Cost Estimation

In this thesis, the cost estimation is focused on major equipment and major operating cost of LNG process. The assumptions and equations are listed as follows.

4.2.6.1 Total Annualizes cost

Total annualized cost (TAC) is an annualized value of total cost which are capital cost and operating cost.

$$TAC = CAPEX + OPEX \qquad \text{Eq. 4.285}$$

CAPEX is capital expenditure which can be calculated by CAPCOST method (Turton *et al.*, 2009):

$$\log_{10} C_P^0 = K_1 + K_2 \log_{10}(A) + K_3 [\log_{10}(A)]^2 \qquad \text{Eq. 4.286}$$

where C_P^0 is the equipment cost in USD, K_i are constants of respective equipment, A is a size parameter of the equipment. The size parameters K_i depend on the type of equipment. For example, the size parameter of a heat exchanger is the heat exchanger area in square meter whereas work input was the size parameter of a compressor. The values of constant K_i of spiral wound heat exchangers and compressors are tabulated in Table 4.2. Since Equation 4.286 and all constants were the equipment cost based on the year 1969; hence, the Chemical engineering plant cost index (CEPCI) (Lozowski, 2018) was used to escalate the cost (Vatavul, 2002). The escalated equipment cost to current dollars in 2018 is calculated by:

$$C_{present} = C_{old} \frac{I_{present}}{I_{old}} = C_{old} \frac{119}{567.5} \qquad \text{Eq. 4.287}$$

where I is the chemical engineering cost index.

Table 4.2 Ki values (Turton *et al*., 2009)

Equipment	K1	K2	K3
Air Cooler	4.0336	0.2341	0.0497
Spiral Wound Heat Exchanger	3.9912	0.0668	0.2430
Compressor	2.2897	1.3604	-0.1027

OPEX is the operating expense which is calculated by the power consumption of the compressors. Electricity bill was referred from the Metropolitan Electricity Authority of Thailand which can be calculated as follows:

$$OPEX = 8760 C_{elect} W^k \qquad \text{Eq. 4.288}$$

where $OPEX$ is the operating expense in 1 year, C_{elect} is an electricity bill in \$/kW, and W^k is work of compressor in kW/h.

CHAPTER V
RESULTS AND DISCUSSION

5.1 Regression

Enthalpy and entropy functions in the model were generated by regression in Minitab 18. Enthalpy and entropy functions were set in quadratic form which is shown as follows.

$$H^{k,n} = aP^{k,n} + bT^{k,n} + c + d(P^{k,n})^2 + e(T^{k,n})^2 + fP^{k,n}T^{k,n} \qquad \text{Eq. 5.1}$$

$$S^{k,n} = aP^{k,n} + bT^{k,n} + c + d(P^{k,n})^2 + e(T^{k,n})^2 + fP^{k,n}T^{k,n} \qquad \text{Eq. 5.2}$$

where a, b, c, d, e and f are constant.

Heat of vaporization depends on one variable which is pressure. Linear form of heat of vaporization is shown as follows:

$$H^{k,n} = aP^{k,n} + b \qquad\qquad \text{Eq. 5.3}$$

where a and b are constant.

Enthalpy and entropy data were generated in PRO/II software by these assumptions.

1. Peng-Robinson thermodynamic package was used in methane and propane while Lee-Kesler-Pocker thermodynamic package was used to obtain the properties of ethylene. Peng-Robinson EOS is appropriate for light alkane while Lee-Kesler-Pocker EOS was the suggested thermodynamic package for an ethylene tower (Razifar, 2006).

2. Partitioning method cannot be used in negative enthalpy region. A value of 680 was added to all enthalpy values to obtain a positive enthalpy throughout the entire operating range in this study. This number was

obtained from the enthalpy of methane at 112.5 K and 0.11 MPa. The coefficients a, b, c, d, e, and f are defined in Appendix A.
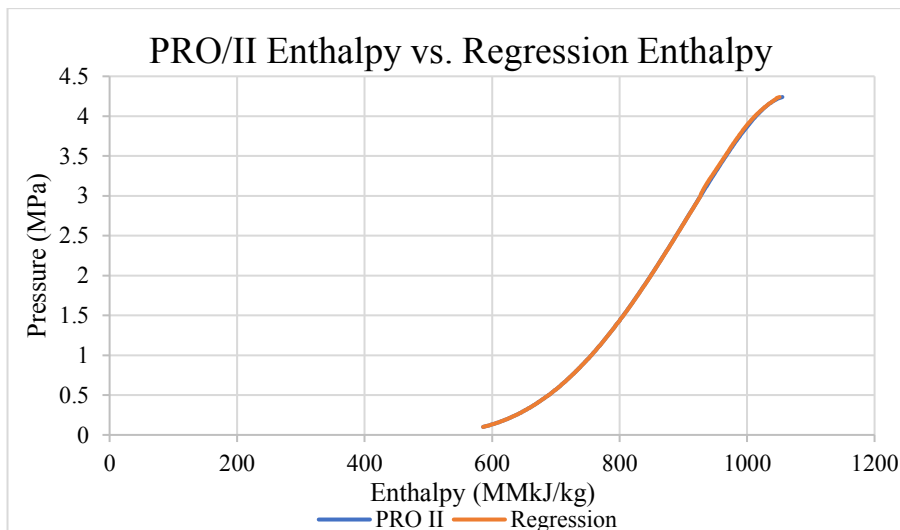
Figure 5.1 PRO/II and quadratic regression enthalpy of liquid propane.

The quadratic equation offers a better solution when compared to the regression by a linear equation. Quadratic equations could decrease an error between raw data and the regressed data to be within 1%.
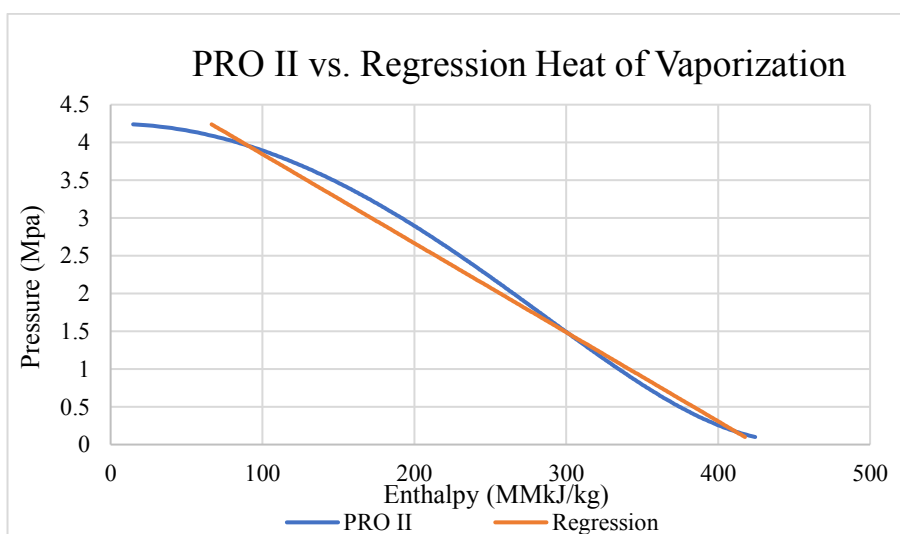
Figure 5.2 PRO/II and linear regression of propane heat of vaporization.

Heat of vaporization is appropriate in linear form because it depends on one variable which is pressure. Other comparison between the values obtain from PRO/II and the regressed values are shown in appendix A.

5.2 Base Case Model

The base case model was constructed based on a fixed operating condition of the Conoco-Phillips liquefaction process presented in Chapter 4. The purpose of the base case model was to verify if the developed model was mathematically correct. The fixed parameters are listed below.

1.   Fixed heat transfer from natural gas to refrigerant.
2.   Fixed outlet temperature of all box heat exchangers.
3.   Fixed the valve outlet pressure.
4.   Fixed cooling water of the propane loop at 303 K.
5.   Fixed efficiency of a compressor at 80%.
6.   Fixed approach temperature of all heat exchagers at 7 Kelvin.

The lower bound model was obtained by linearization of the upper bound model. All equations were listed in Chapter 4. To accomplish a global optimization, the partitioning approach from Faria *et al.* (2011) was applied. First the MILP lower bound model was solved by a given number of interval. The objective value of the lower bound model was kept as the first lower bound. CONOPT was the solver of the upper bound model. The solution of the lower bound model was used as initials in the NLP upper bound model to help finding a good solution. The objective value was kept as the first objective from the upper bound model. The gap between the upper and lower bound models was calculated. If the gap value was more than one percent difference, all procedure was repeated by increasing the number of intervals in the lower bound model. The procedure was then repeated until the gap between the two objectives was small enough (typically 1%). At this point the solution of the NLP upper bound was the answer of the problem and global optimum was reached. The solution of the NLP model was then validated by PRO/II by plugging in the result from GAMS into PRO/II and setting all equipment in the same order as those arranged in GAMS.

Table 5.1 shows the solution of the case study comparing with the converged values of the PRO/II run. The solutions from GAMS match well with those from PRO/II, giving the percentage error in an acceptable value of all variables.

Table 5.1 Optimization result of the upper bound model obtained from GAMS

Variable	PRO/II	GAMS	%Error
F1 [kg/h]	6881.224	6874.372	0.100
F2 [kg/h]	1541.560	1549.164	0.493
F3 [kg/h]	520.155	521.309	0.222
P11 [MPa]	0.110	0.110	0.000
P12 [MPa]	1.340	1.340	0.000
P13 [MPa]	1.340	1.340	0.000
P1V [MPa]	0.110	0.110	0.000
P21 [MPa]	0.110	0.110	0.000
P22 [MPa]	2.126	2.126	0.000
P23 [MPa]	2.126	2.126	0.000
P2V [MPa]	0.110	0.110	0.000
P31 [MPa]	0.110	0.110	0.000
P32 [MPa]	3.077	3.077	0.000
P33 [MPa]	3.077	3.077	0.000
P34 [MPa]	3.077	3.077	0.000
P3V [MPa]	0.110	0.110	0.000
W1 [kW]	282.126	282.075	0.018
W2 [kW]	108.519	108.495	0.022
W3 [kW]	51.879	51.876	0.006
W total [kW]	442.524	442.446	0.018
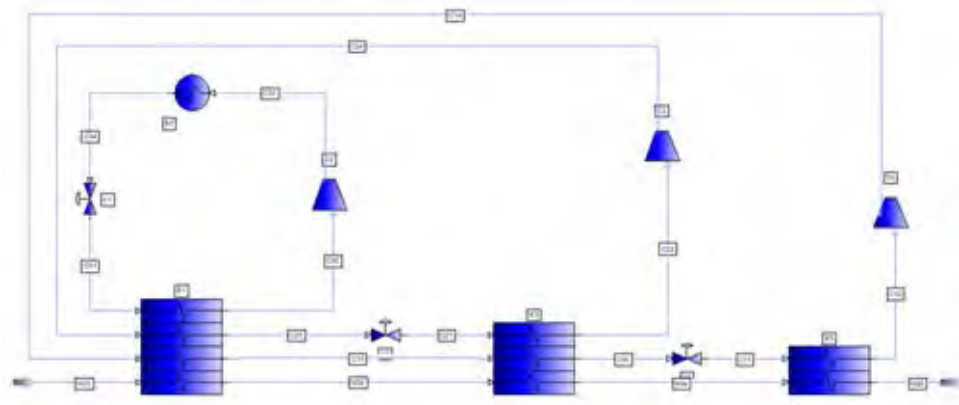
Figure 5.3 PRO/II simulation of ConocoPhillips LNG cascade process.

Figure 5.3 shows the simulation of ConocoPhillips LNG cascade process in PRO/II. Fixed operating conditions from GAMS were set in this simulation. Compressor was operated at 80% efficiency. Flow rate of each refrigerant was obtained by a controller in PRO/II by setting the controller to find the flowrate that gave all vapor feeding to the compressor. The outlet pressure of all throttling valves was fixed at 0.11 MPa.

Table 5.2 Optimization result of lower bound model

Intervals	Upper Bound Work (kW)	Lower Bound Work (kW)	Running Time (h)	% Error
50	442.446	416.019	0.020	5.973
100	442.446	428.013	0.398	3.262
150	442.446	433.167	2.246	2.097
200	442.446	435.686	2.062	1.528
250	442.446	436.920	10.384	1.249
300	442.446	438.056	17.986	0.990

Table 5.2 shows the total work input (objective function) to the system obtained from the lower bound model. The results show that increasing number of intervals can decrease the error between Upper Bound Model and Lower Bound Model. Moreover, running time also increased significantly. At 300 intervals, the error between upper bound model and lower bound model was 0.99% which is lower than 1%, confirming the global optimum solution of the upper bound model.

5.3 Variable Model

After validating the base case model with PRO/II simulator, almost all of the fixed parameters in the base case model were changed to variables and the model was called a variable model. The only fixed parameters in the variables model are listed below:

1. Fixed cooling water of the propane loop at 303 K.
2. Fixed efficiency of a compressor at 80%.
3. Fixed pressure of natural gas at 3.9 MPa

4.   Fixed component of natural gas as in Table 4.1.

5.   The approach temperature of all box heat exchangers was set at 7 K or greater.

The model was simulated in GAMS. Optimizer function in PRO/II was used to achieve the optimum solution and the solution was compared with GAMS solution.

Table 5.3 Comparison of optimized result of the variable upper bound model and PRO/II with optimizer

Variable	LB	UB	Optimized solution from GAMS	PRO/II with Optimizer	% Difference
F1 [kg/h]	1000	10000	6524.316	6557.107	0.503
F2 [kg/h]	100	5000	1483.545	1492.024	0.572
F3 [kg/h]	100	1000	479.850	485.685	1.216
P11 [MPa]	0.11	5.10	0.110	0.110	0.372
P12 [MPa]	0.11	5.10	1.310	1.310	0.000
P13 [MPa]	0.11	5.10	1.310	1.310	0.000
P1V [MPa]	0.11	5.10	0.110	0.110	0.372
P21 [MPa]	0.11	5.10	0.110	0.110	0.013
P22 [MPa]	0.11	5.10	2.060	2.060	0.000
P23 [MPa]	0.11	5.10	2.060	2.060	0.000
P2V [MPa]	0.11	5.10	0.110	0.110	0.013
P31 [MPa]	0.11	5.10	0.110	0.110	0.000
P32 [MPa]	0.11	5.10	3.069	3.070	0.033
P33 [MPa]	0.11	5.10	3.069	3.070	0.033
P34 [MPa]	0.11	5.10	3.069	3.070	0.033
P3V [MPa]	0.11	5.10	0.110	0.110	0.000
W1 [kW]	1	1000	266.319	265.876	0.166
W2 [kW]	1	1000	103.862	103.582	0.270
W3 [kW]	1	1000	47.989	48.393	0.842
W tot [kW]	1	1000	418.169	417.851	0.076

Table 5.3 shows the optimum result of the variable model. The minimum temperature approach of this model was 7 K or greater. GAMS result was compared with PRO/II simulation. Optimizer tool was applied in PRO/II to obtain the best solution using the same fixed parameters and approach temperature in GAMS. The result from GAMS and optimizer PRO/II simulation is resemble. The rest of variables are shown in comparison table which is in appendix B. Table 5.3 revealed that although

the upper and lower pressures of all loops were set as variables, the optimum solution obtained from GAMS gave the low pressure level of atmospheric pressure to all refrigeration loops.

Table 5.4 Optimization result of variable lower bound model with the approach temperature of 7 K

Intervals	Upper Bound Work (kW)	Lower Bound Work (kW)	Running Time (h)	% Error
50	418.169	398.805	0.008	4.630
100	418.169	400.897	0.127	4.130
150	418.169	407.561	1.597	2.537
200	418.169	415.414	6.068	0.659

To confirm the global optimum solution, the lower bound model was performed with increasing number of interval as shown in Table 5.4. At 200 number of intervals, the objective function the lower bound result of 415.414 kW, given the %Error of less than 1% when compared to the objective function of the upper bound model. Hence, the global optimum of the upper bound model was confirmed. The variable model required more running time when compared to the fixed model. The extra running time came from the larger number of variables in the variable model.

5.3.1 Case Study: Variation of Minimum Approach Temperature

The variable model was simulated using various minimum approach temperatures of 3, 5, 7 and 9 K. These conditions were run in both GAMS and PRO/II for a comparison. When the minimum approach temperature was lower, less power was consumed in the compressors as tabulated in Table 5.5. The lowering of approach temperature led to decrease of compressor outlet pressure. When pressure was decreased, work consume was decreased. The results of the lower bound model at different number of intervals are shown in Tables 5.6 to 5.8 for the approach temperatures of 3, 5 and 9, respectively. The objective function of all lower bound models gave %Error of less than 1% as compared to its respective upper bound model; hence, the global optimum of the upper bound model was confirmed. Cases 3K and

5K used less number of intervals to be converged than the 7K and 9K cases. In terms of running time, case 7K can reach solution faster than other cases following by 5K, 3K and 9K, respectively. The faster run time of the 5K and 7K cases probably causes by the operating conditions that were in the middle of the interested range. Whereas the 3K case was operated in a low pressure and temperature zone while the 9K case was operated in a high pressure and temperature zone. Optimizing the model at the regions close to the bounds of each variable may cause the run time to be longer.

The low pressure level of atmospheric pressure was the optimum operating condition in the cases of 7K and 9K approach temperature for all refrigeration loops as seen in Table 5.5. In the cases of 3K and 5K approach temperatures, the low pressure level of all refrigeration loops was slightly higher than the atmospheric pressure. Low pressure level can be changed due to the increasing of maximum boiling when approach temperature is decreased. High pressure level of all loops tend to decrease when the approach temperature is decreased. Decreasing of approach temperature can reduce the upper pressure of the system which allow pressure and temperature to decrease.

Table 5.5 Optimization result from the variable upper bound model using 3, 5, 7 and 9 K minimum approach temperature

Variable	*3 Kelvin*	*5 Kelvin*	*7 Kelvin*	*9 Kelvin*
F1 [kg/h]	6252.178	6340.582	6524.316	6761.240
F2 [kg/h]	1419.043	1471.722	1483.545	1546.116
F3 [kg/h]	493.173	513.696	479.850	520.301
P11 [MPa]	0.114	0.113	0.110	0.110
P12 [MPa]	1.253	1.247	1.310	1.300
P13 [MPa]	1.253	1.247	1.310	1.300
P1V [MPa]	0.114	0.113	0.110	0.110
P21 [MPa]	0.123	0.121	0.110	0.110
P22 [MPa]	1.882	1.976	2.060	2.163
P23 [MPa]	1.882	1.976	2.060	2.163
P2V [MPa]	0.123	0.121	0.110	0.110
P31 [MPa]	0.110	0.110	0.110	0.110
P32 [MPa]	3.029	3.118	3.069	3.260
P33 [MPa]	3.029	3.118	3.069	3.260
P34 [MPa]	3.029	3.118	3.069	3.260

P3V [MPa]	0.110	0.110	0.110	0.110
W1 [kW]	245.467	248.398	266.319	271.721
W2 [kW]	88.833	96.738	103.862	110.483
W3 [kW]	48.805	51.754	47.989	53.504
W tot [kW]	383.105	396.891	418.169	435.708

Table 5.6 Optimization result of 3K lower bound model

Intervals	Upper Bound Work (kW)	Lower Bound Work (kW)	Running Time (h)	% Error
50	383.105	372.871	0.783	2.671
100	383.105	376.293	13.150	1.778
150	383.105	380.928	45.414	0.568

Table 5.7 Optimization result of 5K lower bound model

Intervals	Upper Bound Work (kW)	Lower Bound Work (kW)	Running Time (h)	% Error
50	396.891	383.892	0.023	3.275
100	396.891	389.967	1.682	1.745
150	396.891	395.021	14.661	0.471

Table 5.8 Optimization result of 9K lower bound model

Intervals	Upper Bound Work (kW)	Lower Bound Work (kW)	Running Time (h)	% Error
50	437.834	421.471	0.018	3.737
100	437.834	424.056	2.086	3.147
150	437.834	428.797	14.190	2.064
200	437.834	436.509	47.463	0.303

5.3.2 <u>Case Study: Variation of LNG Heat Load on Each Refrigerant Loops</u>

The second case study was the variation of LNG heat load. The idea was to demonstrate the change in heat load of each exchanger box and observe the corresponding total work of the system. All 9 cases were performed as shown in Table 5.9. Case 1 of this study was the optimum case from 9 cases. The propane flow rate of Case 1 was 12 times higher than the methane flow rate. The 3K approach temperature was used in all 9 case studies.

Table 5.9 Proportion of LNG heat load on each stages

Case	% load of			Total Work (kW)
	Propane	**Ethylene**	**Methane**	
1	64%	24%	12%	383
2	60%	28%	12%	398
3	58%	30%	12%	575
4	64%	22%	14%	400
5	60%	26%	14%	420
6	58%	28%	14%	607
7	64%	20%	16%	530
8	60%	24%	16%	561
9	58%	26%	16%	721

Table 5.10 Optimization result of heat load variation cases 12% load on methane

12% Heat Load on Methane Loop			
Variable	**58% Load on Propane**	**60% Load on Propane**	**64% Load on Propane**
F1 [kg/h]	8739	7055	6252
F2 [kg/h]	4694	2576	1419
F3 [kg/h]	498	505	493
P11 [MPa]	0.538	0.342	0.114
P12 [MPa]	1.050	1.050	1.253
P21 [MPa]	0.110	0.110	0.123
P22 [MPa]	5.010	3.517	1.882
P31 [MPa]	0.110	0.110	0.123
P32 [MPa]	2.996	2.996	3.029
W1 [kW]	95	123	245
W2 [kW]	432	225	89
W3 [kW]	48	49	49
W total [kW]	575	398	383

Table 5.11 Optimization result of heat load variation cases 14% load on methane

14% Heat Load on Methane Loop			
Variable	**58% Load on Propane**	**60% Load on Propane**	**64% Load on Propane**
F1 [kg/h]	9297	7323	6449
F2 [kg/h]	5130	2827	1598
F3 [kg/h]	777	777	777
P11 [MPa]	0.520	0.340	0.110

P12 [MPa]	0.667	1.050	1.050
P21 [MPa]	0.245	0.258	0.198
P22 [MPa]	4.929	3.507	1.646
P31 [MPa]	0.110	0.110	0.110
P32 [MPa]	4.428	4.426	4.457
W1 [kW]	105	135	236
W2 [kW]	425	208	87
W3 [kW]	77	77	77
W total [kW]	607	420	400

Table 5.12 Optimization result of heat load variation cases 16% load on methane

16% Heat Load on Methane Loop			
Variable	**58% Load on Propane**	**60% Load on Propane**	**64% Load on Propane**
F1 [kg/h]	9793	8335	7936
F2 [kg/h]	7700	3509	1839
F3 [kg/h]	1530	1491	1405
P11 [MPa]	0.497	0.338	0.110
P12 [MPa]	1.102	1.102	1.105
P21 [MPa]	0.185	0.188	0.278
P22 [MPa]	5.006	3.568	2.008
P31 [MPa]	0.110	0.110	0.110
P32 [MPa]	3.633	3.633	3.633
W1 [kW]	35	155	275
W2 [kW]	506	226	91
W3 [kW]	180	180	165
W total [kW]	721	561	531

Tables 5.9 to 5.12 show the simulation results of LNG heat load variation model. Case 1 was result of optimum case from variable model (section 5.3.1). Table 5.9 shows that decreasing %heat load of propane loop while maintaining %heat load of methane resulted in increasing refrigerant flow rate, work input and pressure of ethylene loop. On the other hand, it was of interest to observe the effect of increasing %heat load of the methane loop. When the %heat load of methane increased from 12% to 16%, while maintaining the %heat load of propane loop at 64%, this resulted in increasing the overall refrigerant flow rate and work input. Propane loop was not only used for cooling down the natural gas but also used for pre-cooling others refrigerant. Increasing the heat load of methane loop led to the increase in methane

flow rate which gave more load on the propane loop; hence, the total work of the liquefaction process increased significantly. Therefore, the results of this section suggested that a given heat load of the propane loop must be the highest to pre-cool the natural gas and the other two refrigerants and the heat load of the methane loop was the lowest among all loops. When the load on propane loop was less than 58%, pressure of the propane loop exceeded the interested range. The ethylene loop plays an important role in converting natural gas from its gas phase to a liquid phase while the methane loop is to sub-cool natural gas. The results from this section also confirmed that the solution obtained from the variable model gave the optimum solution to the problem.

5.4 Scaled-Up Models

5.4.1 <u>Case Study: Variation of Minimum Temperature Approach</u>

The models in this case study were simulated using the same operating condition as the variable models but the flow rate of LNG was scaled up from 4.5 million kilograms per annum to 4.5 million tons per annum (MMTA). The upper bound and lower bound model were modeled and the solution from GAMS were compared with the results from PRO/II simulation and optimizer PRO/II simulation which shows in table B2, B3, B4 and B5.

Table 5.13 Optimization result of scaled up models

Variable	3K	5K	7K	9K
F1 [kg/h]	6252178	6340326	6524277	6784783
F2 [kg/h]	1419043	1472596	1484540	1551580
F3 [kg/h]	493173	513734	479884	527697
P11 [MPa]	0.114	0.113	0.110	0.110
P12 [MPa]	1.253	1.247	1.310	1.300
P13 [MPa]	1.253	1.247	1.310	1.300
P1V [MPa]	0.114	0.113	0.110	0.110
P21 [MPa]	0.143	0.121	0.110	0.110
P22 [MPa]	1.882	1.978	2.062	2.159
P23 [MPa]	1.882	1.978	2.062	2.159
P2V [MPa]	0.143	0.121	0.110	0.110

P31 [MPa]	0.110	0.110	0.110	0.110
P32 [MPa]	3.029	3.118	3.069	3.265
P33 [MPa]	3.029	3.118	3.069	3.265
P34 [MPa]	3.029	3.118	3.069	3.265
P3V [MPa]	0.110	0.110	0.110	0.110
W1 [kW]	245467	248259	266174	272889
W2 [kW]	88833	96821	103964	110640
W3 [kW]	48805	51758	47992	54306
W tot [kW]	383105	396838	418131	437834

Table 5.13 shows the simulation result of the scaled up model. The results were similar to the variable model except flow rate and work input. Work input and refrigerant flow rate increased 1000 times to achieve cooling duty of the new flow rate of natural gas. The model was checked with initial PRO/II and optimizer which the comparison tables show in appendix B.

Table 5.14 Optimization result of scaled up models of case 3K

Variable	Case 3K scaled-up	Case 3K
F1 [kg/h]	6252178	6252
F2 [kg/h]	1419043	1419
F3 [kg/h]	493173	493
P11 [MPa]	0.114	0.114
P12 [MPa]	1.253	1.253
P13 [MPa]	1.253	1.253
P1V [MPa]	0.114	0.114
P21 [MPa]	0.143	0.123
P22 [MPa]	1.882	1.882
P23 [MPa]	1.882	1.882
P2V [MPa]	0.143	0.123
P31 [MPa]	0.110	0.110
P32 [MPa]	3.029	3.029
P33 [MPa]	3.029	3.029
P34 [MPa]	3.029	3.029
P3V [MPa]	0.110	0.110
W1 [kW]	245467	245
W2 [kW]	88833	88
W3 [kW]	48805	48
W tot [kW]	383105	383

Table 5.14 show the comparison result between variable case 3K and scaled up model of case 3K. The result shows the similar number but scaled up case is 1000 times higher than base case. From this result, scale up flow rate of natural gas did not affect thermodynamic properties (pressure, temperature). The only parameters that were affected were flow rate of each refrigerant, leading to an increase in work input.

5.4.2 Total Annual Cost Calculation

This part covers the cost calculation of ConocoPhillips LNG process. The captical cost calculation method follows CAPCOST method which was used to estimate the equipment cost. The operating cost calculation was considered only compressor operating cost which was electricity bill. The scaled up cases were used as a study case in this section. Since all cost calculation was based on the same throughput and the purpose of this calculation was to compare the cases of different approach temperature, other equipments were assumed to remain the same. The calculation was done in a Microsoft Excel spreadsheet following these assumptions:

1.   Capital cost was calculated based on the equipment cost of the heat exchangers and compressors (see equations in Section 4.26).

2.   Operating cost was calculated from power consumption of compressor (see equations in Section 4.26).

3.   Operating period was 20 years with an interest rate of 1.5%.

4.   LMTD of each box heat exchanger was obtained from PRO/II.

5.   Overall heat transfer coefficient was obtained from Engineers Edge (2000) and the area of the box heat exchanger was calculated by

$$Q = UA\Delta T_{LM}$$

Eq.5.4

Table 5.15 Log mean temperature difference from PRO/II

Equipment	3T	5T	7T	9T
1st **Heat Exchanger**	18.72	22.28	26.63	29.82
2nd **Heat Exchanger**	9.69	12.26	14.35	16.81
3rd **Heat Exchanger**	22.29	25.05	27.48	30.50

Table 5.16 Equipment cost calculation of case 3K

Equipment	Heat Transfer [kJ/h]	LMTD	Area [m²]	Work [kW]	Cost [$]
1st **Exchanger**	1,430,615,000	18.722	23,585		850,043,834
2nd **Exchanger**	439,690,600	9.687	14,008		279,252,750
3rd **Exchanger**	114,744,300	22.287	1,589		4,955,768
Cooler	2,314,294,000	4.453	360,873		7,404,929
Compressor 1				245,466	4,351,143
Compressor 2				88,833	3,212,057
Compressor 3				48,805	2,572,569
Total Equipment Cost					1,151,793,053
Total Equipment Cost after consider Cost index					5,492,794,600

Table 5.17 Operating cost calculation of case 3K

Equipment	Work [kW/h]	Operating Cost [$]
Compressor 1	245,266	568,251
Compressor 2	88,833	205,815
Compressor 3	48,805	113,075
Total per hour	382,904	887,142
Total Operating Cost per year		7,771,369,421

Table 5.15 shows the result of capital cost calculation. The calculation requires some parameters which are Q, U and LMTD. Heat transfer (Q) was the result from GAMS simulation in kJ/h. Log mean temperature difference (LMTD) was obtained from the respective run using PRO/II simulation where the initial values came from the solution from GAMS. The overall heat transfer coefficient (U) was equal to 900 W/m² K as the coefficient between fluid and fluid Engineers Edge (2000). The

calculated heat exchanger area was then used to calculate the equipment cost in CAPCOST equation. The reference equation was based on the equipment cost in 1969. The Chemical Engineering Plant Cost Index (CEPCI) is then used as a correction factor to indicate the equipment cost in 2018.

Table 5.16 shows the operating cost of each compressor. The propane loop compressor requires higher work input than two others due to the high propane flow rate. Operating cost calculated from the work input and electricity bill which obtained from the Metropolitan Electricity Authority of Thailand. Total operating cost is annualized from billion USD per hour to billion USD per year Province Electricity Authority of Thailand (2015).

Table 5.17 Total cost comparison

	3K	5K	7K	9K
Capital Cost (CAPEX) [Billion USD]	5.49	3.89	2.72	2.24
Operating Cost (OPEX) [Billion USD/y]	7.77	8.05	8.49	8.89
Total Annualized Cost (TAC) [Billion USD/y]	8.09	8.28	8.64	9.02

Table 5.17 shows the comparison between cost of each cases. For the capital cost, the 3K case required the highest capital cost since the case 3K gave the largest area of heat exchanger among all cases. Vice vesa, the 9K case required less CAPEX because of its smallest heat exchange area. In term of operating cost, the 3K case required less operating cost than others cases due to the lowest work requirement. CAPEX was annualized into a yearly basis by assuming a 20-year life time with an interest rate of 1.5%. Table 5.17 indicates that the 3K case gave the lowest total annualized cost (TAC). The result showed the impact of operating cost which was significantly higher than the capital cost even though CAPEX of the 3K case was double from that of the 9K case.
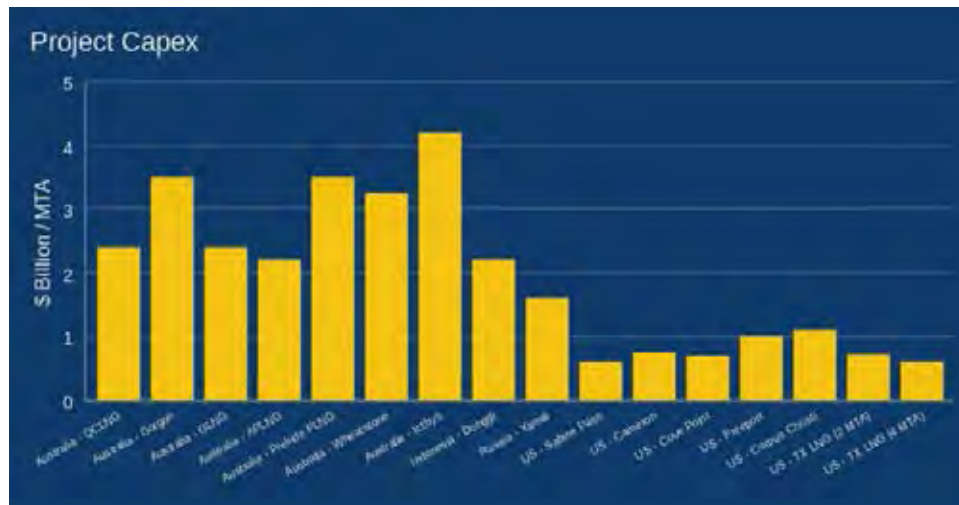
Figure 5.4 CAPEX of LNG processes (Chandra, 2017).

Chandra (2017) provided the estimated CAPEX of an LNG process from various locations around the globe as shown in Figure 5.4. The throughput of the scale-up case was 4.5 MMTA. CAPEX of simulated case was in the ranges of 0.50-1.22 billion USD/MMTA for all approach temperatures studied in this work. Although CAPEX of our study only estimated based on the compressors, box heat exchangers and coolers, these equipments are the majority portion of the purchased equipment cost of the project. If the purchased equipment cost was assumed to be 20% of the total CAPEX (Note: total CAPEX = fixed capital investment + working capital), the estimated CAPEX would be in the ranges of 2.5-6.1 billion USD/MMTA. Hence, our estimated CAPEX was still in the ballpark figure.

CHAPTER VI
CONCLUSION AND RECOMMENDATION

6.1 Conclusion

This thesis presents a new method of global optimization for LNG process. Partitioning method is a part of RYSIA ((Faria *et al.*, 2011, Faria *et al.*, 2012, Ounahasaree *et al.*, 2016)) which is comprehensive to bound contraction technique. The accuracy of metamodel is excellent when compared to PRO/II simulation. Several minimum approach temperature models were performed and the lowest approach temperature of 3K gave the lowest work input and total annual cost. The scale up of natural gas flow rate affected flow rate of refrigerant but not the thermodynamic properites. The benifit of metamodel over PRO/II simulation is that PRO/II optimizer requires a correct boundary to reach the optimum condition while GAMS model requires any value to make a non-zero variables.

6.2 Recommendation

- This thesis proves a partitioning method on single refrigerant system which can be applied to the mixed refrigerant system.
- Series of compressors should be considered to decrease compression ratio.

REFERENCES

Abdelsadek, Y., Herrmann, F., Kacem, I. and Otjacques, B. (2015) Branch-and-bound algorithm for the maximum triangle packing problem. Computers & Industrial Engineering 81, 147-157.

Austbø, B., Løvseth, S.W. and Gundersen, T. (2014) Annotated bibliography—Use of optimization in LNG process design and operation. Computers & Chemical Engineering 71, 391-414.

Bejarano, G., Alfaya, J.A., Ortega, M.G. and Vargas, M. (2017) On the difficulty of globally optimally controlling refrigeration systems. Applied Thermal Engineering 111, 1143-1157.

Cengel, Y.A. and Boles, M.A. (2015) Thermodynamics. Thermodynamics An Engineering Approach 8th Ed. 8, 1-996.

Chandra, V. (2017) Strategically located, realistically sized, and focused on low risk, low cost LNG production. Texas LNG 1, 1-13.

Faria, D.b.C. and Bagajewicz, M.J. (2011) Global Optimization of Water Management Problems Using Linear Relaxation and Bound Contraction Methods. Industrial & Engineering Chemistry Research 50(7), 3738-3753.

Faria, D.C. and Bagajewicz, M.J. (2011) Novel bound contraction procedure for global optimization of bilinear MINLP problems with applications to water management problems. Computers & Chemical Engineering 35(3), 446-455.

Faria, D.C. and Bagajewicz, M.J. (2012) A new approach for global optimization of a class of MINLP problems with applications to water management and pooling problems. AIChE Journal 58(8), 2320-2335.

Karuppiah, R. (2005) GLOBAL OPTIMIZATION FOR THE SYNTHESIS OF INTEGRATED WATER SYSTEMS IN CHEMICAL PROCESSES. M.S. Thesis, Department of Chemical Engineering, Carnegie Mellon University, USA.

Khan, M.S., Karimi, I.A. and Lee, M. (2016) Evolution and optimization of the dual mixed refrigerant process of natural gas liquefaction. Applied Thermal Engineering 96, 320-329.

M. Roberts, F.C., O. Saygi-arslan (2015) Brayton Refrigeration Cycyles for Small Sacle LNG Gas Processing, 27-32.

Ounahasaree, Y., Suriyapraphadilok, U. and Bagajewicz, M. (2016) Global Optimization of Gasoline Blending Model using Bound Contraction Technique. 26th European Symposium on Computer Aided Process Engineering: 1293-1298.

Rosenthal, R.E. (2013) GAMSUsersGuide. GAMS A User's Guide 1, 1-304.

Sun, H., He Ding, D., He, M. and Shoujun Sun, S. (2016) Simulation and optimisation of AP-X process in a large-scale LNG plant. Journal of Natural Gas Science and Engineering 32, 380-389.

Turton, R., Bailie, R.C., Whiting, W.B. and Shaeiwitz, J.A. (2009) Analysis Synthesis and Design of Chemical Processes 3, 1-1144.

Vatavul, W.M. (2002) Chemical Engineering Plant Cost Index 2002. Engineering Pratice 10, 62-70.

Air Products and Chemicals, I. "Air Products LNG Process." Air Product Process. 1 Nov 2017. 7 Nov 2017 <http://www.airproducts.com/industries/ energy/lng/lng-applications/product-list/natural-gas-liquefaction-lng.aspx?itemId=57A62244AC724328B90250DBF258805E>.

Company, C. (2017) "ConocoPhillips LNG Cascade Process." ConocoPhillips LNG Process. 20 Jan 2000. 24 Oct 2017. <http://lnglicensing.conocophillips.com /what-we-do/lng-technology/optimized-cascade-process/>.

Corporation, C. (2009, 2017) "LiquefactionTechnology." LNG Process. 15 Aug 2009. 21 Oct 2017. <https://www.chiyoda-corp.com/technology /en/lng/liquefaction.html>.

Engineers Edge, L. (2000, 2018) "Overall Heat Transfer Coefficient Table, Charts and Equations." Heat Trasfer Coefficient. 18 Jul 2000. 21 Apr 2018. <https://www.engineersedge.com/thermodynamics/overall_heat_transfer-table.htm>.

Lozowski, D. (2018) "Chemical Engineering Plant Cost Index" CEPCI 2018. 22 Mar 2018. 30 Mar 2018. <http://www.chemengonline.com/pci-home>.

Province Electricity Authority of Thailand. (2015) "Electricity Cost" Electricity Cost for Chemical Plant. 1 Nov 2015. 20 Mar 2018. <http://peane2.pea.co.th/kalasin/ckfinder/userfiles/files/kls/electricity_rate_ 11_58.pdf >

Razifar, M. (2006) "Property Package Descriptions". Thermodynamic Package. 21 Dec 2007. 2 Jun 2017. <http://www.razifar.com/cariboost_files/ Property_20Package_20Descriptions.pdf>.

APPENDICES

Appendix A Enthalpy and Entropy Regression

Regression of enthalpy and entropy of each refrigerant are shown in this section. Each figure shows the comparison between raw data (PRO/II) and regressed data.
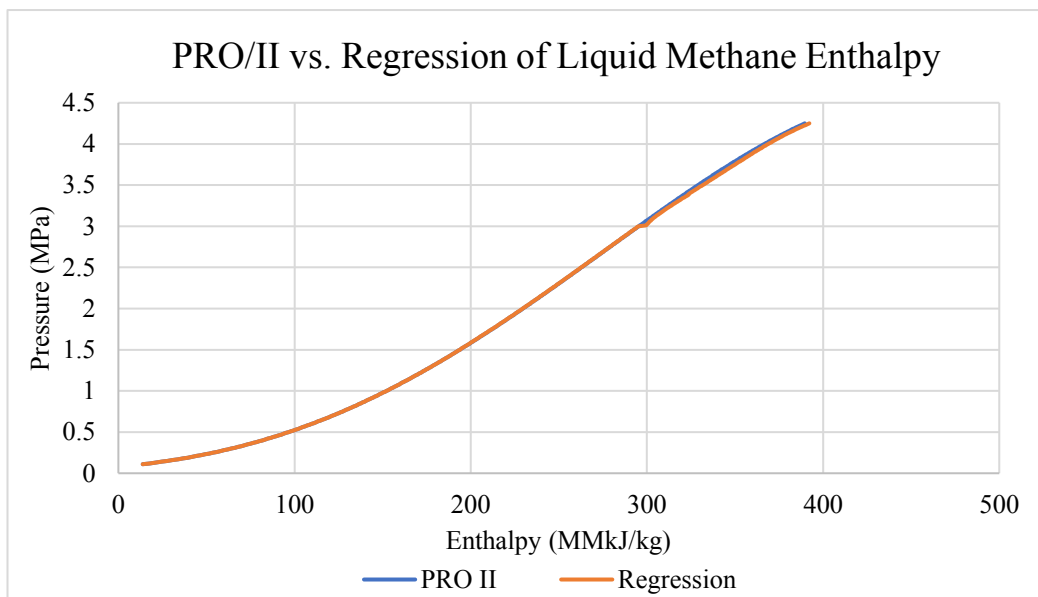
Figure A1 Comparison between PRO/II and regressed enthalpy of liquid methane.

Equation:

$$H^{3,1} = 7920P^{3,4} + 359.2^{3,4} - 20016.9 + 80.05(P^{3,4})^2 - 1.66(T^{3,4})^2 - 29.24P^{3,4}T^{3,4}$$

87
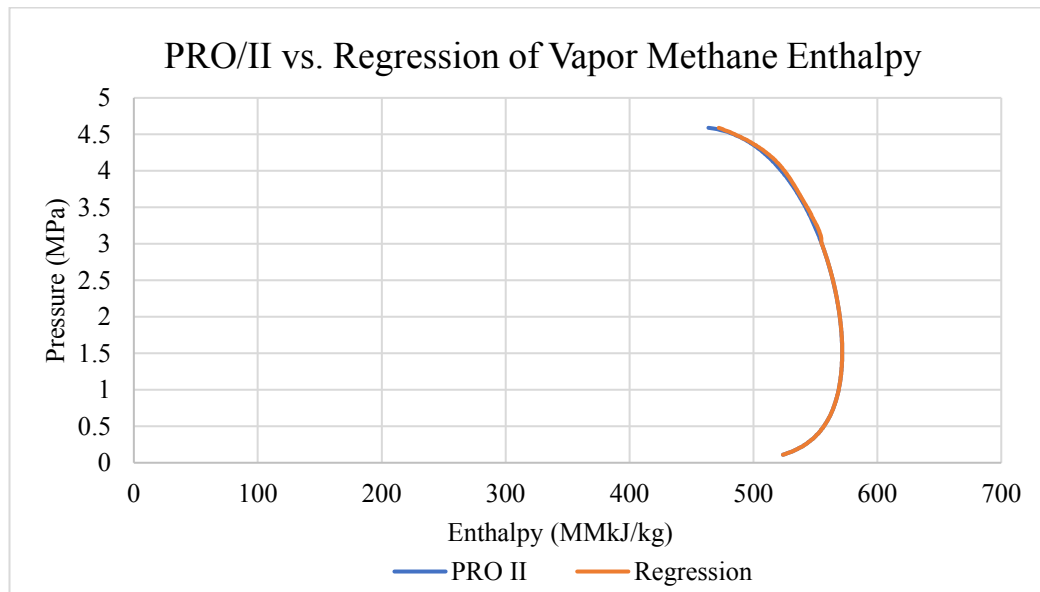
Figure A2 Comparison between PRO/II and regressed enthalpy of vapor methane.

Equation:

$$H^{3,1} = -7869P^{3,1} - 350.11T^{3,1} + 19745.9 - 79.612(P^{3,1})^2 + 1.649(T^{3,1})^2 + 29.05P^{3,1}T^{3,1}$$
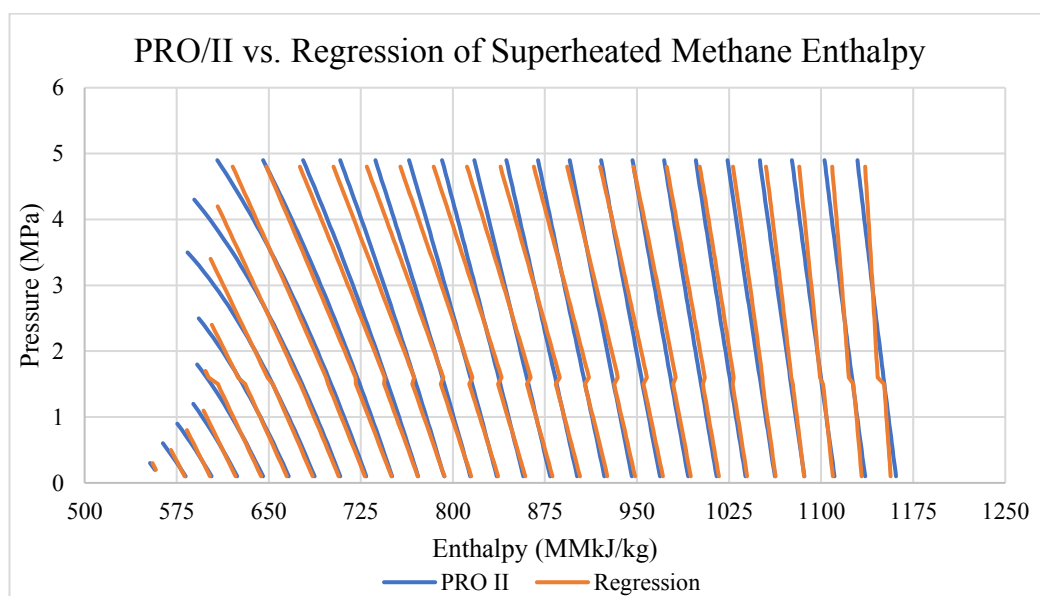
Figure A3 Comparison between PRO/II and regressed enthalpy of superheated methane.

Equation:

$$H^{3,2} = -45.85P^{3,2} + 2.27T^{3,2} + 263.05 - 0.116(P^{3,2})^2 - 0.00013(T^{3,2})^2 + 0.1085P^{3,2}T^{3,2}$$
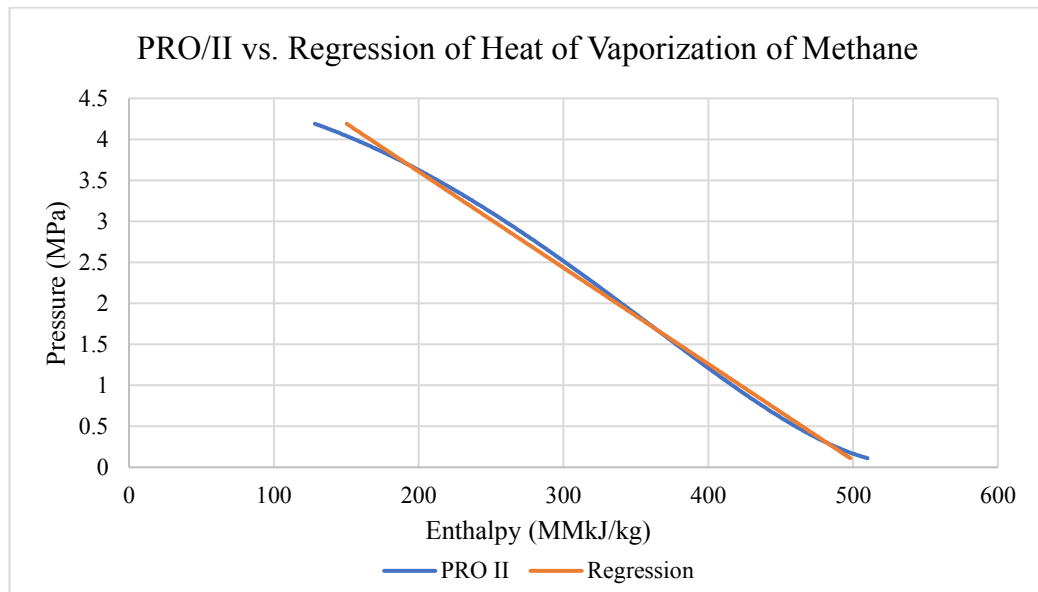
Figure A4 Comparison between PRO/II and regressed heat of vaporization of methane.

Equation:

$$H^{V,C1} = -85.2340P^{3,V} + 530.44526$$
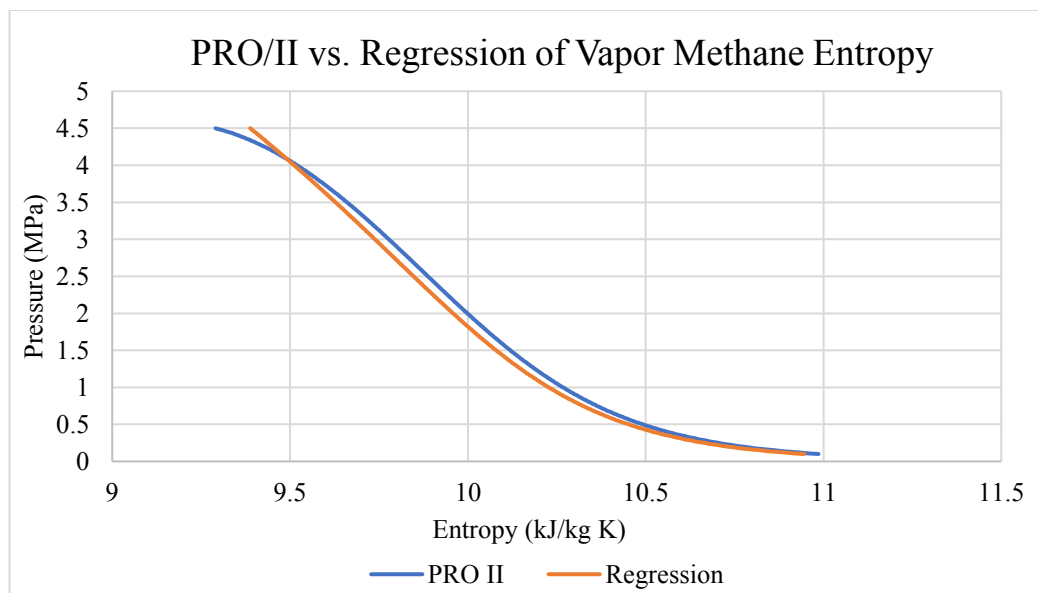
Figure A5 Comparison between PRO/II and regressed entropy of vapor methane.

Equation:

$$S^{3,1} = -2.69P^{3,1} - 0.148T^{3,1} + 20.13 - 0.0535(P^{3,1})^2 + 0.000602(T^{3,1})^2 + 0.01039P^{3,1}T^{3,1}$$
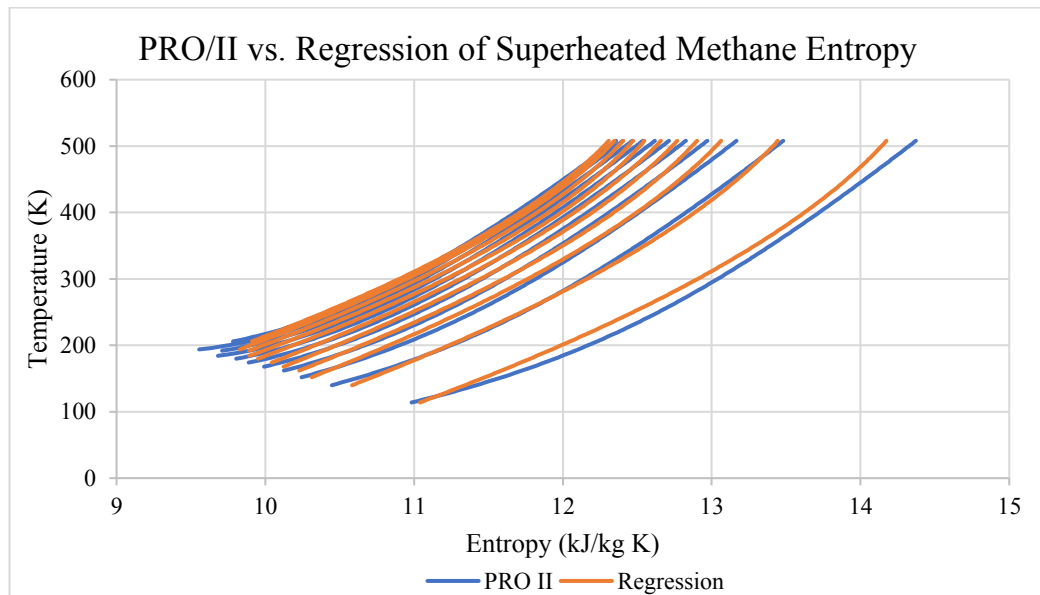
Figure A6 Comparison between PRO/II and regressed entropy of superheated methane.

Equation:

$$S^{3,2} = -0.574P^{3,2} + 0.0145T^{3,2} + 8.886 + 0.0507(P^{3,2})^2 - 0.0000107(T^{3,2})^2 + 0.00023P^{3,2}T^{3,2}$$
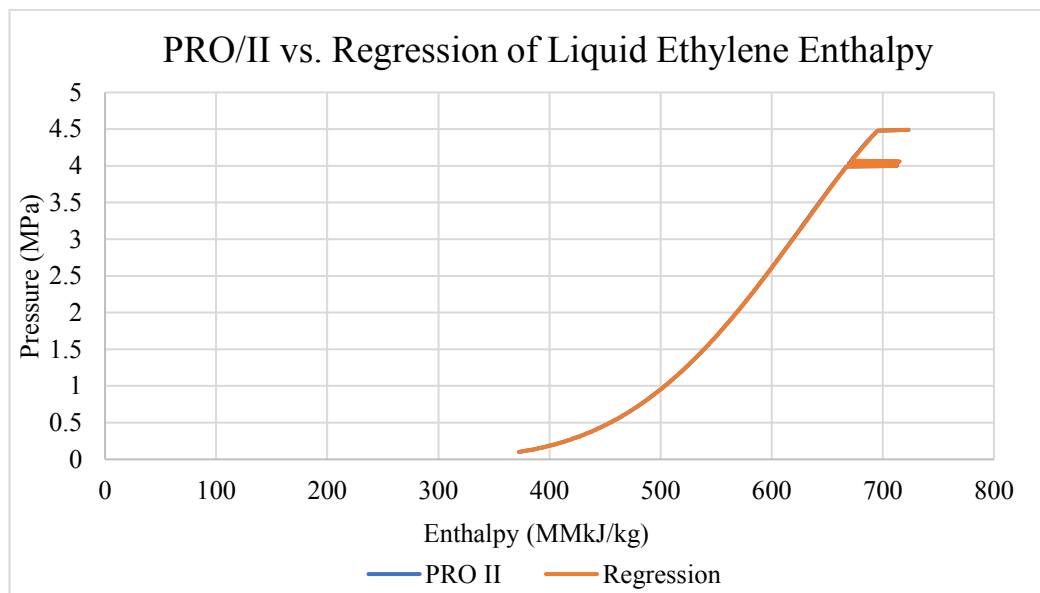
Figure A7 Comparison between PRO/II and regressed enthalpy of liquid ethylene.

Equation:

$$H^{2,3} = 1019.77P^{2,3} + 41.50T^{2,3} - 3349.31 + 6.33(P^{2,3})^2 - 0.01186(T^{2,3})^2 - 2.4482P^{2,3}T^{2,3}$$
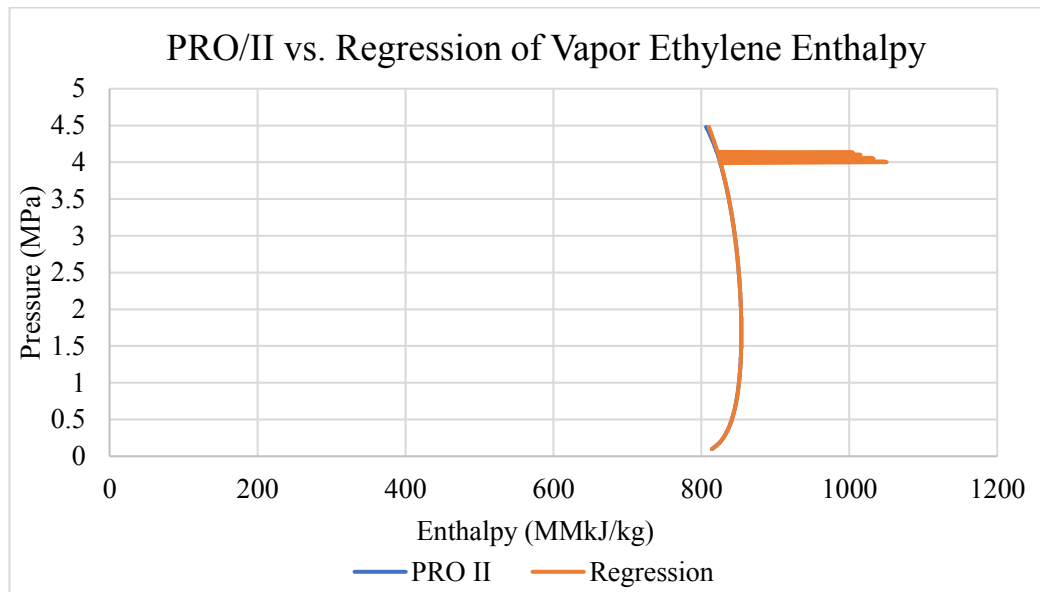
Figure A8 Comparison between PRO/II and regressed enthalpy of vapor ethylene.

Equation:

$$H^{2,1} = -1369.6P^{2,1} - 49.63T^{2,1} + 4935.76 - 8.949(P^{2,1})^2 + 0.1538(T^{2,1})^2 + 3.322P^{2,1}T^{2,1}$$
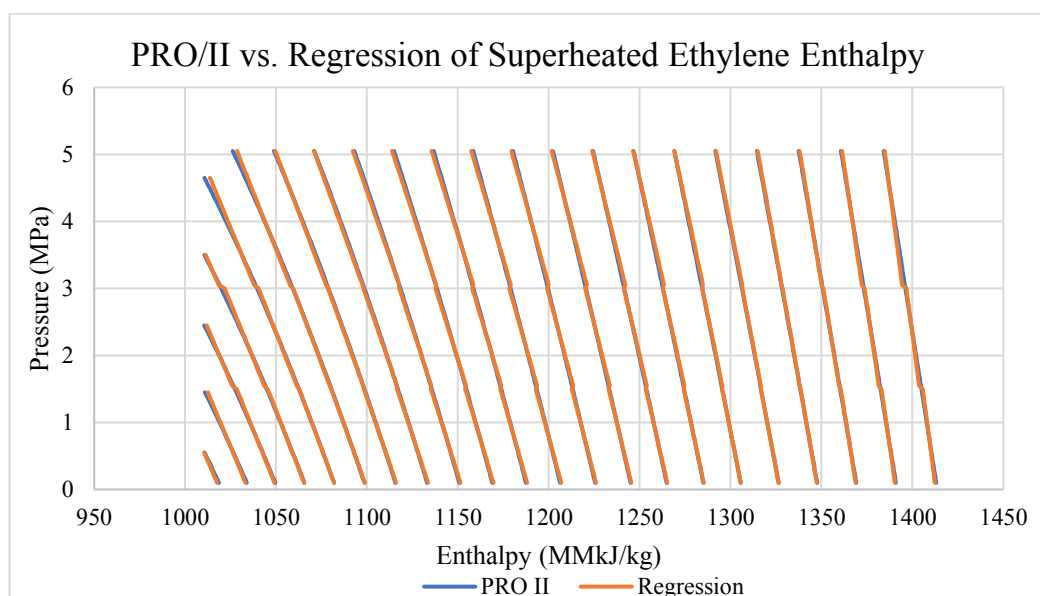
Figure A9 Comparison between PRO/II and regressed enthalpy of superheated ethylene.

Equation:

$$H^{2,2} = -32.817P^{2,2} + 0.884T^{2,2} + 654.923 - 0.0841(P^{2,2})^2 + 0.00125(T^{2,2})^2 + 0.0568P^{2,2}T^{2,2}$$
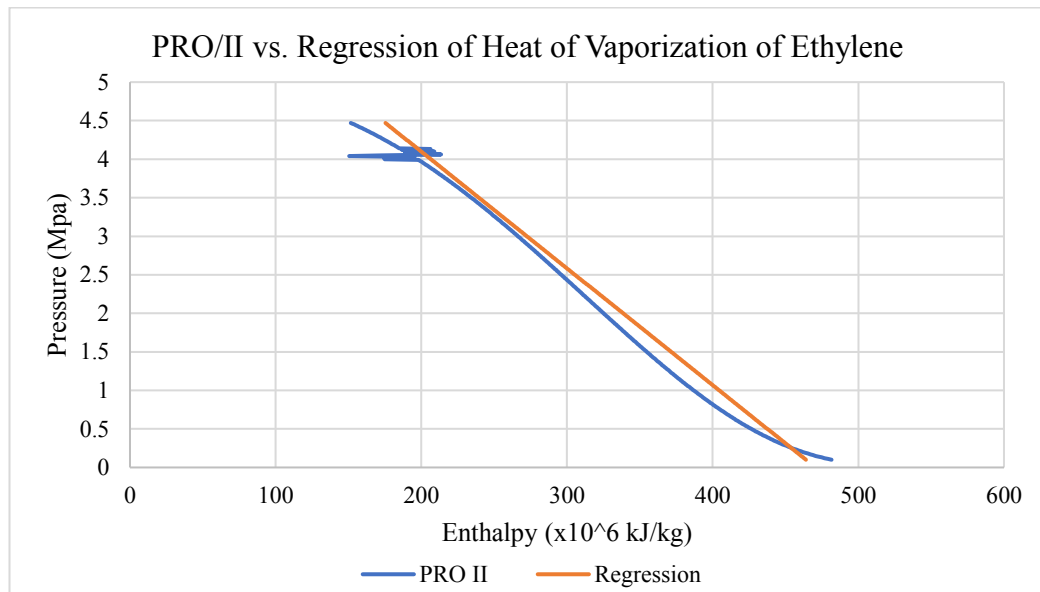
Figure A10 Comparison between PRO/II and regressed heat of vaporization of ethylene.

Equation:

$$H^{V,C2} = -66.04219P^{2,2} + 470.60916$$
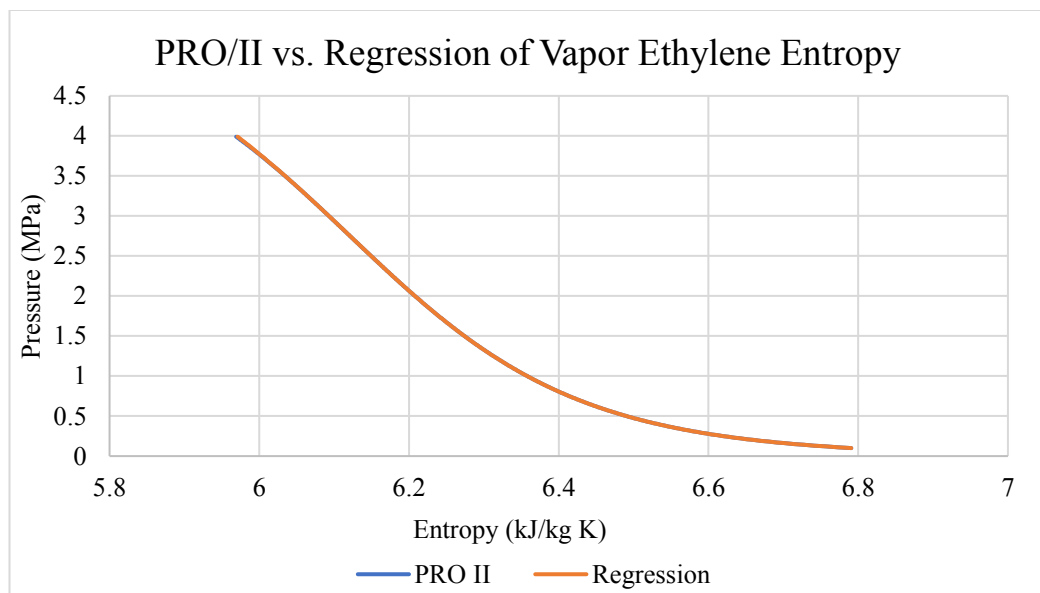
Figure A11 Comparison between PRO/II and regressed entropy of vapor ethylene.

Equation:

$$S^{2,1} = -1.359P^{2,1} - 0.0626T^{2,1} + 12.77 - 0.023(P^{2,1})^2 + 0.000164(T^{2,1})^2 + 0.00358P^{2,1}T^{2,1}$$
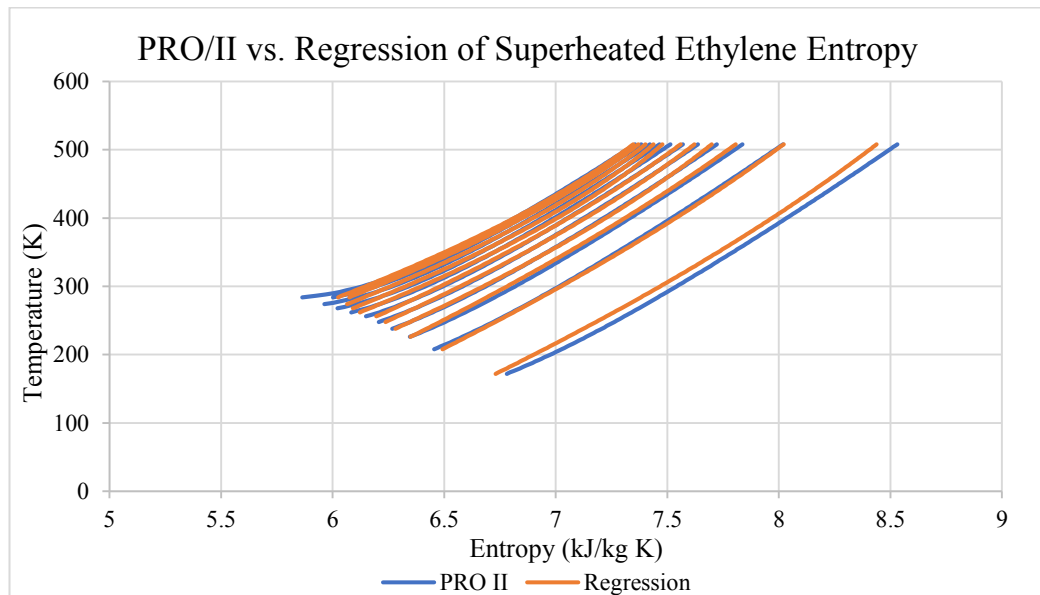
Figure A12 Comparison between PRO/II and regressed entropy of superheated ethylene.

Equation:

$$S^{2,2} = -0.39P^{2,2} + 0.00876T^{2,2} + 4.95 + 0.0288(P^{2,2})^2 - 0.0000052(T^{2,2})^2 + 0.000254P^{2,2}T^{2,2}$$
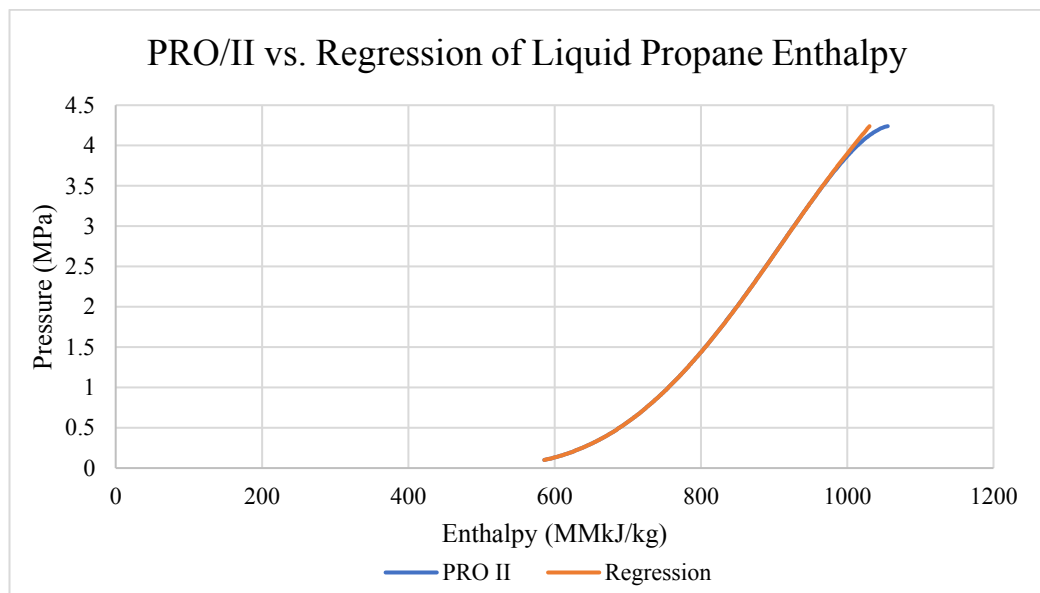
Figure A13 Comparison between PRO/II and regressed enthalpy of liquid propane.

Equation:

$$H^{1,3} = 87.36P^{1,3} + 1.776T^{1,3} + 148.55 + 4.175(P^{1,3})^2 + 0.00044(T^{1,3})^2 - 0.1897P^{1,3}T^{1,3}$$
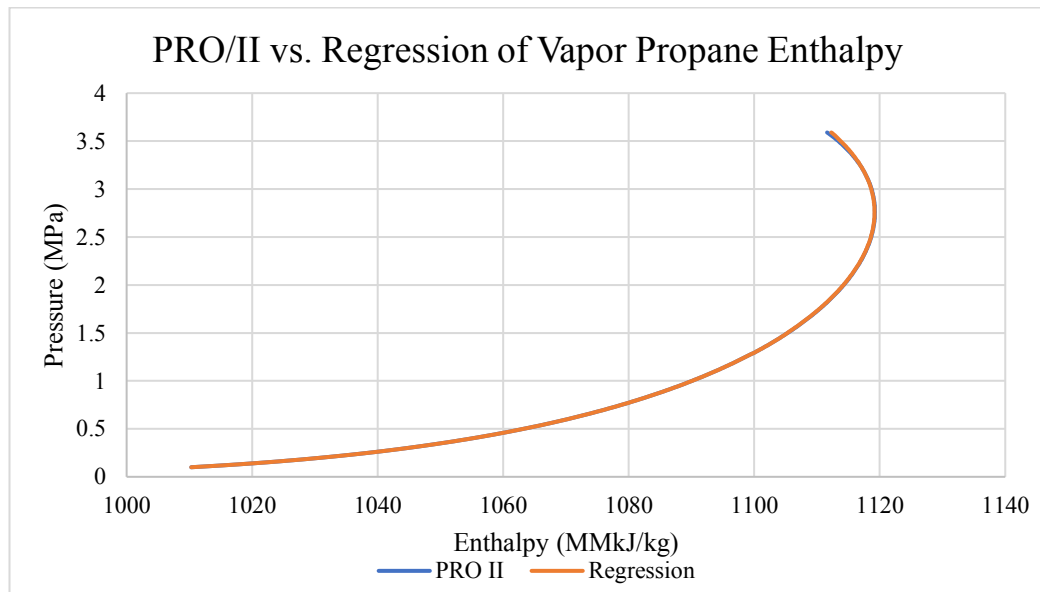
Figure A14 Comparison between PRO/II and regressed enthalpy of vapor propane.

Equation:

$$H^{1,1} = -59.375P^{1,1} + 0.618T^{1,1} + 786.314 - 3.855(P^{1,1})^2 + 0.001586(T^{1,1})^2 + 0.1288P^{1,1}T^{1,1}$$
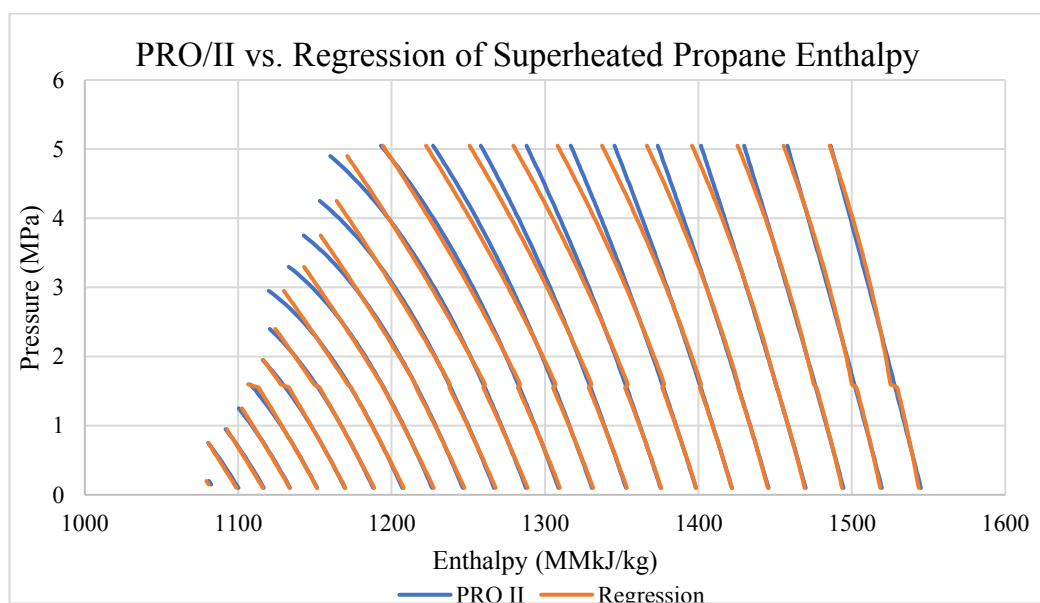
Figure A15 Comparison between PRO/II and regressed enthalpy of superheated propane.

Equation:

$$H^{1,2} = -54.36P^{1,2} + 0.52T^{1,2} + 781.689 - 1.023(P^{1,2})^2 + 0.00201(T^{1,2})^2 + 0.9269P^{1,2}T^{1,2}$$
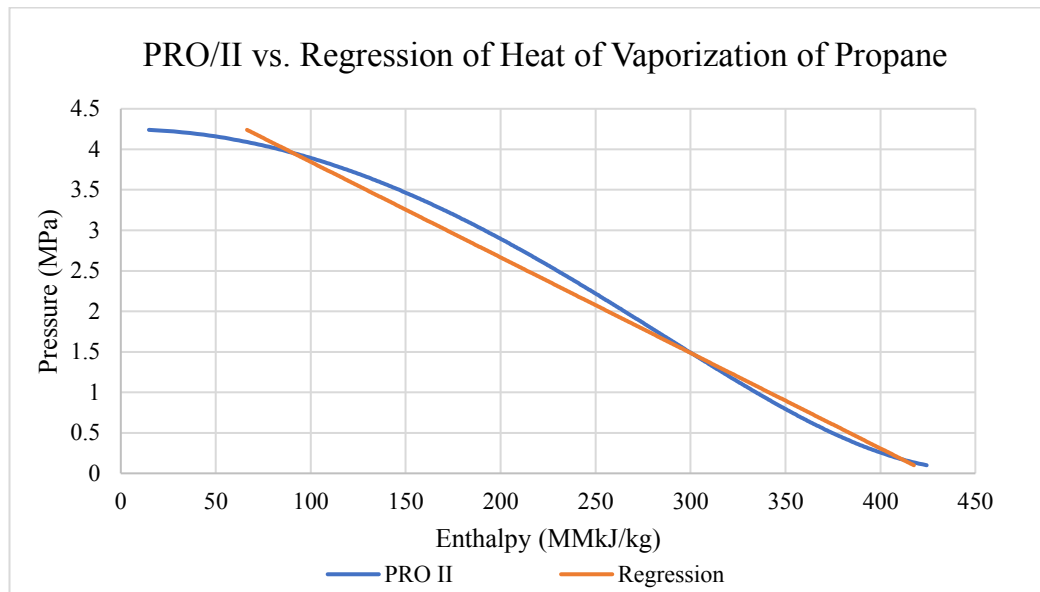
Figure A16 Comparison between PRO/II and regressed of heat of vaporization of vapor methane.

Equation:

$$H^{V,C3} = -84.8199P^{1,V} + 426.913979$$
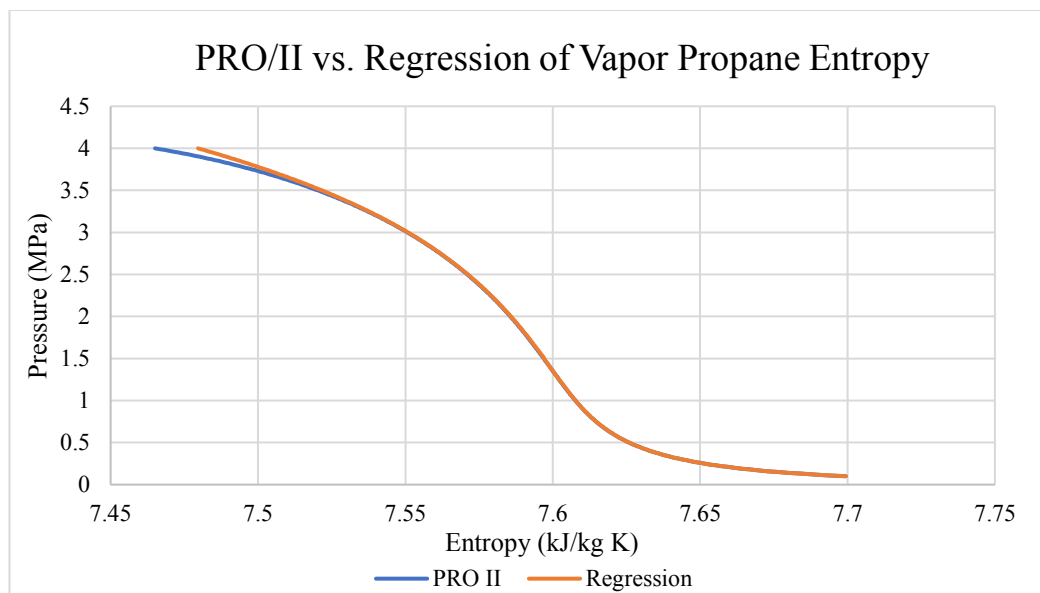
Figure A17 Comparison between PRO/II and regressed entropy of vapor propane.

Equation:

$$S^{1,1} = -0.896P^{1,1} - 0.0275T^{1,1} + 10.99 - 0.019(P^{1,1})^2 + 0.0000578(T^{1,1})^2 + 0.00183P^{1,1}T^{1,1}$$
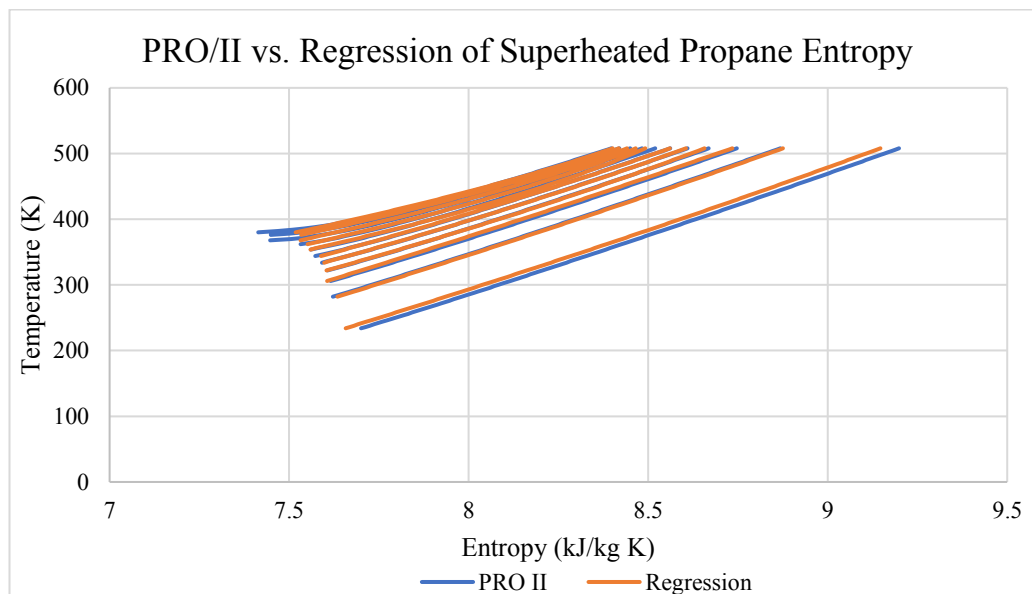
Figure A18 Comparison between PRO/II and regressed entropy of superheated propane.

Equation:

$$S^{1,2} = -0.866P^{1,2} + 0.00663T^{1,2} + 6.28 + 0.260(P^{1,2})^2 - 0.0000016(T^{1,2})^2 + 0.000266P^{1,2}T^{1,2}$$

Appendix B GAMS Optimization Result

Table B1 Optimization result of base case model

	PRO/II	GAMS	%Error
F1	6881.224	6874.372	0.10
F2	1541.560	1549.164	0.49
F3	520.155	521.309	0.22
H11	332.952	331.485	0.44
H12	480.550	479.203	0.28
H13	110.873	109.199	1.51
H1V	110.873	109.199	1.51
H21	176.978	176.980	0.00
H22	430.401	429.105	0.30
H23	-119.381	-118.233	0.96
H2V	-119.381	-118.233	0.96
H31	-156.274	-156.908	0.41
H32	202.783	201.331	0.72
H33	62.209	62.007	0.32
H34	-382.011	-382.146	0.04
H3V	-382.011	-382.146	0.04
P11	0.110	0.110	0.00
P12	1.340	1.340	0.00
P13	1.340	1.340	0.00
P1V	0.110	0.110	0.00
P21	0.110	0.110	0.00
P22	2.126	2.126	0.00
P23	2.126	2.126	0.00
P2V	0.110	0.110	0.00
P31	0.110	0.110	0.00
P32	3.077	3.077	0.00
P33	3.077	3.077	0.00
P34	3.077	3.077	0.00
P3V	0.110	0.110	0.00
q11	1.000	1.000	0.00
q12	1.000	1.000	0.00
q13	0.000	0.000	0.00
q1V	0.474	0.470	0.85
q21	1.000	1.000	0.00
q22	1.000	1.000	0.00
q23	0.000	0.000	0.00
q2V	0.376	0.376	0.10
q31	1.000	1.000	0.00

q32	1.000	1.000	0.00
q33	1.000	1.000	0.00
q34	0.000	0.000	0.00
q3V	0.557	0.557	0.04
QB11	1528176	1528080	0.01
QB12	847522	847915	0.05
QB13	73120	72630	0.67
QB22	456855	457333	0.10
QB23	231063	231541	0.21
QB33	117418	117418	0.00
Qout	2543829	2543548	0.01
S11	7.693	7.694	0.01
S12	7.693	7.694	0.01
S21	6.778	6.775	0.05
S22	6.778	6.775	0.05
S31	10.955	10.917	0.35
S32	10.955	10.917	0.35
T11	232.849	232.850	0.00
T12	341.146		0.00
T13	312.136	311.200	0.30
T1V	232.849	232.850	0.00
T21	170.546	170.500	0.03
T22	361.750		0.00
T23	239.850	239.850	0.00
T2V	170.546	170.500	0.03
T31	112.594	112.500	0.08
T32	297.060		0.00
T33	239.850	239.850	0.00
T34	177.500	177.500	0.00
T3V	112.594	112.500	0.08
W1	282.126	282.075	0.02
W2	108.518	108.495	0.02
W3	51.879	51.876	0.01
W total	442.524	442.446	0.02

Table B2 Optimization result of variable model compare with PRO/II optimizer at minimum temperature approach equal to 3 K

	Initial PRO/II	GAMS	% Error	Optimizer PRO/II	% Error
F1	6216.104	6252.178	0.58	6224.981	0.43
F2	1415.464	1419.043	0.25	1426.000	0.49
F3	487.116	493.173	1.24	510.155	3.44
H11	333.723	333.421	0.09	333.452	0.01
H12	476.387	474.760	0.34	476.489	0.36
H13	104.202	104.602	0.38	103.633	0.92
H1V	104.202	104.602	0.38	103.633	0.92
H21	179.542	180.261	0.40	180.783	0.29
H22	405.777	405.623	0.03	400.222	1.33
H23	-129.986	-129.589	0.30	-130.466	0.67
H2V	-129.986	-129.589	0.30	-130.466	0.67
H31	-155.889	-155.596	0.18	-156.274	0.43
H32	199.594	200.665	0.53	200.939	0.13
H33	53.927	53.763	0.30	53.757	0.01
H34	-387.795	-388.262	0.12	-382.709	1.43
H3V	-387.795	-388.262	0.12	-382.709	1.43
HL1	1223.286	1223.673	0.03	1223.286	0.03
HL2	59.771	59.919	0.24	59.344	0.95
HL3	-373.626	-371.032	0.69	-370.596	0.11
HL4	-593.200	-594.081	0.14	-595.147	0.17
P11	0.113	0.114	0.88	0.112	1.81
P12	1.270	1.253	1.33	1.266	1.04
P13	1.270	1.253	1.33	1.266	1.04
P1V	0.113	0.114	0.88	0.112	1.81
P21	0.127	0.123	3.15	0.136	10.61
P22	1.884	1.882	0.10	1.880	0.10
P23	1.884	1.882	0.10	1.880	0.10
P2V	0.127	0.123	3.15	0.136	10.61
P31	0.110	0.110	0.00	0.110	0.00
P32	3.053	3.029	0.78	3.041	0.39
P33	3.053	3.029	0.78	3.041	0.39
P34	3.053	3.029	0.78	3.041	0.39
P3V	0.110	0.110	0.00	0.110	0.00
q11	1.000	1.000	0.00	1.000	0.01
q12	1.000	1.000	0.00	1.000	0.00
q13	0.000	0.000	0.00	0.000	0.00
q1V	0.455	0.452	0.70	0.455	0.70
q21	1.000	1.000	0.00	1.000	0.01
q22	1.000	1.000	0.00	1.000	0.00

q23	0.000	0.000	0.00	0.000	0.00
q2V	0.324	0.328	1.14	0.338	3.18
q31	1.000	1.000	0.00	1.000	0.01
q32	1.000	1.000	0.00	1.000	0.00
q33	1.000	1.000	0.00	1.000	0.00
q34	0.000	0.000	0.00	0.000	0.00
q3V	0.545	0.554	1.68	0.556	0.33
QB11	1426726	1430614	0.27	1430619	0.00
QB12	758353	759489	0.15	756761	0.35
QB13	70956	72448	2.10	75085	3.64
QB1L	598527	598676	0.02	598746	0.01
QB22	438125	439690	0.35	443842	0.94
QB23	215169	217994	1.31	222665	2.14
QB2L	222945	221696	0.56	221166	0.23
QB33	112965	114744	1.57	115517	0.67
QB3L	112951	114744	1.58	115512	0.66
Qout	2313540	2314294	0.03	2321024	0.29
S11	7.692	7.612	1.04	7.693	1.05
S12	7.692	7.612	1.04	7.693	1.05
S21	6.753	6.719	0.49	6.740	0.31
S22	6.753	6.719	0.49	6.740	0.31
S31	10.951	10.831	1.09	10.956	1.15
S32	10.951	10.831	1.09	10.956	1.15
T11	233.477	233.256	0.09	233.256	0.00
T12	338.174		0.00	338.171	0.00
T13	309.857	310.000	0.04	309.728	0.08
T1V	233.447	233.256	0.08	233.256	0.00
T21	173.101	174.355	0.72	174.355	0.00
T22	346.784		0.00	343.723	0.00
T23	236.411	236.256	0.06	236.256	0.00
T2V	173.101	174.355	0.72	174.355	0.00
T31	112.881	112.595	0.25	112.595	0.00
T32	295.634		0.00	296.131	0.00
T33	236.411	236.256	0.06	236.256	0.00
T34	176.713	177.355	0.36	177.355	0.00
T3V	112.818	112.595	0.19	112.595	0.00
TL1	661.200	661.200	0.00	661.200	0.00
TL2	236.411	236.256	0.06	236.256	0.00
TL3	176.713	177.355	0.36	177.355	0.00
TL4	116.200	115.595	0.52	115.597	0.00
W1	246.337	245.467	0.35	247.335	0.76
W2	88.952	88.833	0.13	86.922	2.15
W3	48.100	48.805	1.46	50.621	3.72
W total	383.389	383.105	0.07	384.878	0.38

Table B3 Optimization result of variable model compare with PRO/II optimizer at minimum temperature approach equal to 5 K

	Initial PRO/II	GAMS	% Error	Optimizer PRO/II	% Error
F1	6329.359	6340.582	0.18	6270.562	1.10
F2	1478.485	1471.722	0.46	1473.484	0.12
F3	518.298	513.696	0.89	518.109	0.86
H11	333.723	333.625	0.03	333.599	0.01
H12	475.254	474.659	0.13	475.039	0.08
H13	101.729	102.281	0.54	101.028	1.23
H1V	101.729	102.281	0.54	101.028	1.23
H21	178.674	178.007	0.37	179.643	0.92
H22	414.718	414.640	0.02	409.591	1.22
H23	-123.891	-125.573	1.36	-123.866	1.36
H2V	-123.891	-125.573	1.36	-123.866	1.36
H31	-156.274	-156.602	0.21	-156.274	0.21
H32	204.868	206.094	0.60	205.279	0.40
H33	57.720	58.418	1.21	57.570	1.45
H34	-376.885	-378.986	0.56	-376.974	0.53
H3V	-376.885	-378.986	0.56	-376.974	0.53
HL1	1223.286	1223.673	0.03	1223.286	0.03
HL2	65.154	65.215	0.09	65.154	0.09
HL3	-366.549	-366.506	0.01	-366.535	0.01
HL4	-588.817	-588.572	0.04	-588.811	0.04
P11	0.113	0.113	0.00	0.113	0.43
P12	1.247	1.247	0.00	1.240	0.56
P13	1.247	1.247	0.00	1.240	0.56
P1V	0.113	0.113	0.00	0.113	0.43
P21	0.121	0.121	0.00	0.128	5.55
P22	1.976	1.976	0.00	1.960	0.81
P23	1.976	1.976	0.00	1.960	0.81
P2V	0.121	0.121	0.00	0.128	5.55
P31	0.110	0.110	0.00	0.110	0.00
P32	3.118	3.118	0.00	3.126	0.26
P33	3.118	3.118	0.00	3.126	0.26
P34	3.118	3.118	0.00	3.126	0.26
P3V	0.110	0.110	0.00	0.110	0.00
q11	1.000	1.000	0.01	1.000	0.01
q12	1.000	1.000	0.00	1.000	0.00
q13	0.000	0.000	0.00	0.000	0.00
q1V	0.450	0.446	0.84	0.449	0.57
q21	1.000	1.000	0.01	1.000	0.01
q22	1.000	1.000	0.00	1.000	0.00

q23	0.000	0.000	0.00	0.000	0.00
q2V	0.361	0.358	0.70	0.357	0.31
q31	1.000	1.000	0.01	1.000	0.01
q32	1.000	1.000	0.00	1.000	0.00
q33	1.000	1.000	0.00	1.000	0.00
q34	0.000	0.000	0.00	0.000	0.00
q3V	0.567	0.571	0.65	0.567	0.68
QB11	1468376	1466855	0.10	1458354	0.58
QB12	796325	795043	0.16	786040	1.13
QB13	76266	75860	0.53	76529	0.88
QB1L	595758	595951	0.03	595758	0.03
QB22	447338	446785	0.12	447216	0.10
QB23	225254	224693	0.25	225140	0.20
QB2L	222073	222092	0.01	222066	0.01
QB33	114342	114238	0.09	114346	0.10
QB3L	114337	114238	0.09	114341	0.09
Qout	2364171	2361089	0.13	2345259	0.67
S11	7.692	7.612	1.04	7.692	1.05
S12	7.692	7.612	1.04	7.692	1.05
S21	6.761	6.715	0.69	6.752	0.55
S22	6.761	6.715	0.69	6.752	0.55
S31	10.956	11.011	0.50	10.956	0.50
S32	10.956	11.011	0.50	10.956	0.50
T11	233.477	233.376	0.04	233.376	0.00
T12	337.305		0.00	337.104	0.00
T13	309.089	310.000	0.29	308.853	0.37
T1V	233.477	233.376	0.04	233.376	0.00
T21	172.231	173.203	0.56	173.203	0.00
T22	352.318		0.00	349.433	0.00
T23	238.376	238.376	0.00	238.376	0.00
T2V	172.231	173.203	0.56	173.203	0.00
T31	112.595	112.595	0.00	112.595	0.00
T32	298.110		0.00	298.317	0.00
T33	238.376	238.376	0.00	238.376	0.00
T34	178.200	178.203	0.00	178.203	0.00
T3V	112.595	112.595	0.00	112.595	0.00
TL1	661.200	661.200	0.00	661.200	0.00
TL2	238.376	238.376	0.00	238.376	0.00
TL3	178.200	178.203	0.00	178.203	0.00
TL4	117.595	117.595	0.00	117.597	0.00
W1	248.832	248.398	0.17	246.363	0.82
W2	96.941	96.738	0.21	94.118	2.71
W3	51.994	51.754	0.46	52.034	0.54
W total	397.767	396.891	0.22	392.515	1.10

Table B4 Optimization result of variable model compare with PRO/II optimizer at minimum temperature approach equal to 7 K

	Initial PRO/II	GAMS	% Error	Optimizer PRO/II	% Error
F1	6560.091	6524.316	0.55	6557.107	0.50
F2	1492.063	1483.545	0.57	1492.024	0.57
F3	485.713	479.850	1.21	485.685	1.22
H11	332.953	333.103	0.05	333.059	0.01
H12	479.147	480.053	0.19	479.031	0.21
H13	107.956	106.868	1.01	107.956	1.02
H1V	107.956	106.868	1.01	107.956	1.02
H21	176.978	177.769	0.45	176.976	0.45
H22	426.891	429.802	0.68	426.901	0.67
H23	-118.990	-119.149	0.13	-118.990	0.13
H2V	-118.990	-119.149	0.13	-118.990	0.13
H31	-156.274	-155.602	0.43	-156.274	0.43
H32	202.375	204.426	1.01	202.426	0.98
H33	62.571	63.378	1.29	62.553	1.30
H34	-381.561	-384.955	0.89	-381.573	0.88
H3V	-381.561	-384.955	0.89	-381.573	0.88
HL1	1223.286	1223.673	0.03	1223.286	0.03
HL2	69.394	69.111	0.41	69.394	0.41
HL3	-369.697	-368.959	0.20	-369.697	0.20
HL4	-582.405	-582.894	0.08	-582.405	0.08
P11	0.110	0.110	0.00	0.110	0.37
P12	1.310	1.310	0.00	1.310	0.00
P13	1.310	1.310	0.00	1.310	0.00
P1V	0.110	0.110	0.00	0.110	0.37
P21	0.110	0.110	0.00	0.110	0.01
P22	2.060	2.060	0.00	2.060	0.00
P23	2.060	2.060	0.00	2.060	0.00
P2V	0.110	0.110	0.00	0.110	0.01
P31	0.110	0.110	0.00	0.110	0.00
P32	3.069	3.069	0.00	3.070	0.03
P33	3.069	3.069	0.00	3.070	0.03
P34	3.069	3.069	0.00	3.070	0.03
P3V	0.110	0.110	0.00	0.110	0.00
q11	1.000	1.000	0.01	1.000	0.01
q12	1.000	1.000	0.00	1.000	0.00
q13	0.000	0.000	0.00	0.000	0.00
q1V	0.467	0.458	1.95	0.467	1.99
q21	1.000	1.000	0.01	1.000	0.01
q22	1.000	1.000	0.00	1.000	0.00

q23	0.000	0.000	0.00	0.000	0.00
q2V	0.377	0.371	1.64	0.377	1.67
q31	1.000	1.000	0.01	1.000	0.01
q32	1.000	1.000	0.00	1.000	0.00
q33	1.000	1.000	0.00	1.000	0.00
q34	0.000	0.000	0.00	0.000	0.00
q3V	0.558	0.558	0.02	0.558	0.02
QB11	1475997	1476023	0.00	1476021	0.00
QB12	814489	814393	0.01	814483	0.01
QB13	67904	67682	0.33	67934	0.37
QB1L	593602	593947	0.06	593602	0.06
QB22	441604	440491	0.25	441589	0.25
QB23	215720	215132	0.27	215705	0.27
QB2L	225883	225358	0.23	225883	0.23
QB33	109424	110055	0.58	109424	0.57
QB3L	109424	110055	0.58	109424	0.57
Qout	2435043	2434772	0.01	2433175	0.07
S11	7.694	7.614	1.04	7.693	1.04
S12	7.694	7.614	1.04	7.693	1.04
S21	6.779	6.774	0.07	6.779	0.07
S22	6.779	6.774	0.07	6.779	0.07
S31	10.956	11.001	0.41	10.956	0.41
S32	10.956	11.001	0.41	10.956	0.41
T11	232.850	232.936	0.04	232.936	0.00
T12	340.062		0.00	340.006	0.00
T13	311.170	310.000	0.38	311.170	0.38
T1V	232.850	232.936	0.04	232.936	0.00
T21	170.546	170.744	0.12	170.544	0.12
T22	359.431		0.00	359.437	0.00
T23	239.936	239.936	0.00	239.936	0.00
T2V	170.546	170.744	0.12	170.544	0.12
T31	112.595	112.595	0.00	112.595	0.00
T32	296.854		0.00	296.880	0.00
T33	239.936	239.936	0.00	239.936	0.00
T34	177.544	177.744	0.11	177.544	0.11
T3V	112.595	112.595	0.00	112.595	0.00
TL1	661.200	661.200	0.00	661.200	0.00
TL2	239.936	239.936	0.00	239.936	0.00
TL3	177.544	177.744	0.11	177.544	0.11
TL4	119.610	119.595	0.01	119.610	0.01
W1	266.402	266.319	0.03	265.876	0.17
W2	103.579	103.862	0.27	103.582	0.27
W3	48.389	47.989	0.83	48.393	0.84
W total	418.370	418.169	0.05	417.851	0.08

Table B5 Optimization result of variable model compare with PRO/II optimizer at minimum temperature approach equal to 9 K

	Initial PRO/II	GAMS	% Error	Optimizer PRO/II	% Error
F1	6715.637	6761.240	0.68	6727.381	0.50
F2	1555.485	1546.116	0.60	1540.320	0.37
F3	527.851	520.301	1.43	518.953	0.26
H11	332.953	332.998	0.01	332.953	0.01
H12	478.671	477.674	0.21	478.670	0.21
H13	106.977	109.062	1.95	106.977	1.91
H1V	106.977	109.062	1.95	106.977	1.91
H21	176.978	177.128	0.08	177.027	0.06
H22	432.485	434.377	0.44	435.135	0.17
H23	-112.885	-112.273	0.54	-112.993	0.64
H2V	-112.885	-112.273	0.54	-112.993	0.64
H31	-156.274	-156.602	0.21	-156.274	0.21
H32	212.171	213.598	0.67	223.349	4.57
H33	63.908	64.393	0.76	59.678	7.32
H34	-367.117	-367.278	0.04	-370.732	0.94
H3V	-367.117	-367.278	0.04	-370.732	0.94
HL1	1223.286	1223.673	0.03	1223.286	0.03
HL2	74.470	73.916	0.74	74.470	0.75
HL3	-359.717	-359.274	0.12	-359.717	0.12
HL4	-576.059	-577.047	0.17	-576.059	0.17
P11	0.110	0.110	0.00	0.110	0.00
P12	1.300	1.300	0.00	1.300	0.00
P13	1.300	1.300	0.00	1.300	0.00
P1V	0.110	0.110	0.00	0.110	0.00
P21	0.110	0.110	0.00	0.110	0.27
P22	2.166	2.163	0.14	2.222	2.74
P23	2.166	2.163	0.14	2.222	2.74
P2V	0.110	0.110	0.00	0.110	0.27
P31	0.110	0.110	0.00	0.110	0.00
P32	3.265	3.260	0.15	3.500	7.36
P33	3.265	3.260	0.15	3.500	7.36
P34	3.265	3.260	0.15	3.500	7.36
P3V	0.110	0.110	0.00	0.110	0.00
q11	1.000	1.000	0.01	1.000	0.01
q12	1.000	1.000	0.00	1.000	0.00
q13	0.000	0.000	0.00	0.000	0.00
q1V	0.465	0.464	0.17	0.465	0.17
q21	1.000	1.000	0.01	1.000	0.01
q22	1.000	1.000	0.00	1.000	0.00

q23	0.000	0.000	0.00	0.000	0.00
q2V	0.390	0.387	0.78	0.390	0.68
q31	1.000	1.000	0.01	1.000	0.01
q32	1.000	1.000	0.00	1.000	0.00
q33	1.000	1.000	0.00	1.000	0.00
q34	0.000	0.000	0.00	0.000	0.00
q3V	0.586	0.585	0.25	0.579	0.96
QB11	1517566	1514292	0.22	1520222	0.39
QB12	848314	845184	0.37	844294	0.11
QB13	78260	77631	0.80	84937	9.41
QB1L	590965	591476	0.09	590965	0.09
QB22	450878	447447	0.76	446724	0.16
QB23	227516	224598	1.28	223362	0.55
QB2L	223351	222848	0.23	223351	0.23
QB33	111293	112029	0.66	111293	0.66
QB3L	111289	112029	0.67	111289	0.66
Qout	2496156	2492276	0.16	2500518	0.33
S11	7.694	7.614	1.04	7.694	1.05
S12	7.694	7.614	1.04	7.694	1.05
S21	6.779	6.775	0.06	6.778	0.05
S22	6.779	6.775	0.06	6.778	0.05
S31	10.956	11.011	0.50	10.956	0.50
S32	10.956	11.011	0.50	10.956	0.50
T11	232.850	232.859	0.00	232.850	0.00
T12	339.696		0.00	339.696	0.00
T13	310.845	312.000	0.37	310.845	0.37
T1V	232.850	232.859	0.00	232.850	0.00
T21	170.546	170.546	0.00	170.594	0.03
T22	363.124		0.00	364.899	0.00
T23	241.850	241.859	0.00	241.850	0.00
T2V	170.546	170.546	0.00	170.594	0.03
T31	112.595	112.595	0.00	112.595	0.00
T32	301.780		0.00	307.375	0.00
T33	241.850	241.859	0.00	241.850	0.00
T34	179.594	179.546	0.03	179.594	0.03
T3V	112.595	112.595	0.00	112.595	0.00
TL1	661.200	661.200	0.00	661.200	0.00
TL2	241.850	241.859	0.00	241.850	0.00
TL3	179.594	179.546	0.03	179.594	0.03
TL4	121.595	121.595	0.00	121.595	0.00
W1	271.831	271.721	0.04	272.305	0.21
W2	110.399	110.483	0.08	110.436	0.04
W3	54.023	53.504	0.96	54.724	2.28
W total	436.253	435.708	0.12	437.465	0.40

Table B6 Optimization result of heat load variation at 12% LNG heat load on methane loop

	12%load on Methane		
	64%load on propane	60%load on propane	58%load on propane
F1	6252.178	7054.832	8739.712
F2	1419.043	2576.226	4694.326
F3	493.173	505.401	497.599
H11	333.421	353.214	387.015
H12	474.760	416.146	426.209
H13	104.602	80.451	82.318
H1V	104.602	80.451	82.318
H21	180.261	179.848	176.776
H22	405.623	494.951	507.776
H23	-129.589	-21.409	58.888
H2V	-129.589	-21.409	58.888
H31	-155.596	-155.596	-155.596
H32	200.665	195.418	194.120
H33	53.763	129.364	166.458
H34	-388.262	-380.457	-382.590
H3V	-388.262	-380.457	-382.590
HL1	1223.673	1223.673	1223.673
HL2	59.919	133.829	170.157
HL3	-371.032	-373.169	-374.516
HL4	-594.081	-594.081	-594.081
P11	0.114	0.342	0.538
P12	1.253	1.050	1.050
P13	1.253	1.050	1.050
P1V	0.114	0.342	0.538
P21	0.123	0.110	0.110
P22	1.882	3.517	5.010
P23	1.882	3.517	5.010
P2V	0.123	0.110	0.110
P31	0.110	0.110	0.110
P32	3.029	2.992	2.966
P33	3.029	2.992	2.966
P34	3.029	2.992	2.966
P3V	0.110	0.110	0.110
q11	1.000	1.000	1.000
q12	1.000	1.000	1.000
q13	0.000	0.000	0.000
q1V	0.452	0.256	0.179

q21	1.000	1.000	1.000
q22	1.000	1.000	1.000
q23	0.000	0.000	0.000
q2V	0.328	0.514	0.647
q31	1.000	1.000	1.000
q32	1.000	1.000	1.000
q33	1.000	1.000	1.000
q34	0.000	0.000	0.000
q3V	0.554	0.563	0.560
QB11	1430615	1924298	2662960
QB12	759490	1330260	2107229
QB13	72448	33384	13765
QB1L	598677	560654	541966
QB22	439691	518482	553405
QB23	217994	257664	273206
QB2L	221696	260818	280199
QB33	114744	113645	112952
QB3L	114744	113645	112952
Qout	2314294	2368269	3005508
S11	7.612	7.596	7.581
S12	7.612	7.596	7.581
S21	6.719	6.746	6.747
S22	6.719	6.746	6.747
S31	10.831	10.831	10.831
S32	10.831	10.831	10.831
T11	233.256	262.840	277.377
T13	310.000	301.000	302.000
T1V	233.256	262.840	277.377
T21	174.355	173.953	173.698
T23	236.256	265.840	280.377
T2V	174.355	173.953	173.698
T31	112.595	112.595	112.595
T33	236.256	265.840	280.377
T34	177.355	176.953	176.698
T3V	112.595	112.595	112.595
TL1	661.200	661.200	661.200
TL2	236.256	265.840	280.377
TL3	177.355	176.953	176.698
TL4	115.595	115.595	115.595
W1	245.467	123.326	95.152
W2	88.833	225.494	431.618
W3	48.805	49.279	48.339
W total	383.105	398.098	575.109

Table B7 Optimization result of heat load variation at 14% LNG heat load on methane loop

	14%load on Methane		
	64%load on propane	60%load on propane	58%load on propane
F1	7936.129	8335.830	9793.560
F2	1839.129	3509.836	7700.209
F3	1405.308	1491.590	1530.127
H11	316.241	370.464	388.402
H12	440.924	432.847	381.310
H13	82.318	82.318	33.676
H1V	82.318	82.318	33.676
H21	192.863	192.130	178.877
H22	370.567	417.801	408.355
H23	-128.440	-20.591	61.153
H2V	-128.440	-20.591	61.153
H31	-155.596	-158.596	-154.596
H32	267.447	275.743	269.824
H33	25.026	106.762	145.671
H34	-281.984	-278.830	-268.306
H3V	-281.984	-278.830	-268.306
HL1	1223.673	1223.673	1223.673
HL2	61.173	133.829	170.157
HL3	-253.457	-253.456	-253.456
HL4	-594.081	-594.081	-594.081
P11	0.110	0.340	0.520
P12	1.050	1.050	0.667
P13	1.050	1.050	0.667
P1V	0.110	0.340	0.520
P21	0.198	0.258	0.245
P22	1.646	3.507	4.929
P23	1.646	3.507	4.929
P2V	0.198	0.258	0.245
P31	0.110	0.110	0.110
P32	4.457	4.426	4.428
P33	4.457	4.426	4.428
P34	4.457	4.426	4.428
P3V	0.110	0.110	0.110
q11	1.000	1.000	1.000
q12	1.000	1.000	1.000
q13	0.000	0.000	0.000
q1V	0.398	0.261	0.074
q21	1.000	1.000	1.000

q22	1.000	1.000	1.000
q23	0.000	0.000	0.000
q2V	0.298	0.527	0.723
q31	1.000	1.000	1.000
q32	1.000	1.000	1.000
q33	1.000	1.000	1.000
q34	0.000	0.000	0.000
q3V	0.699	0.773	0.770
QB11	1856444	2396104	3405468
QB12	917737	1583400	2673531
QB13	340676	252050	189971
QB1L	598031	560654	541966
QB22	590916	770269	852598
QB23	403338	545314	608955
QB2L	187578	224955	243643
QB33	149508	149508	149508
QB3L	149508	149508	149508
Qout	2845942	2953548	3531889
S11	7.651	7.596	7.424
S12	7.651	7.596	7.424
S21	6.645	6.701	6.562
S22	6.645	6.701	6.562
S31	10.831	10.831	10.831
S32	10.831	10.831	10.831
T11	233.758	262.840	277.377
T13	302.000	302.000	284.500
T1V	233.758	262.840	277.377
T21	186.474	186.474	186.474
T23	236.758	265.840	280.377
T2V	186.474	186.474	186.474
T31	112.595	112.595	112.595
T33	236.758	265.840	280.377
T34	189.474	189.474	189.474
T3V	112.595	112.595	112.595
TL1	661.200	661.200	661.200
TL2	236.758	265.840	280.377
TL3	189.474	189.474	189.474
TL4	115.595	115.595	115.595
W1	274.860	154.846	35.117
W2	90.784	225.870	505.815
W3	165.141	179.960	180.394
W total	530.785	560.675	721.326

Table B8 Optimization result of heat load variation at 16% LNG heat load on methane loop

	16%load on Methane		
	64%load on propane	60%load on propane	58%load on propane
F1	6449.213	7323.160	9297.685
F2	1598.125	2827.130	5130.433
F3	777.370	777.370	777.370
H11	328.141	355.245	382.046
H12	459.678	421.516	422.816
H13	91.144	87.127	87.127
H1V	91.144	87.127	87.127
H21	186.458	187.026	186.274
H22	383.469	452.267	484.196
H23	-130.506	-21.148	59.450
H2V	-130.506	-21.148	59.450
H31	-172.596	-172.596	-172.596
H32	185.641	185.641	185.641
H33	45.399	120.970	158.663
H34	-340.881	-340.881	-340.881
H3V	-340.881	-340.881	-340.881
HL1	1223.673	1223.673	1223.673
HL2	61.173	133.829	170.157
HL3	-339.784	-339.784	-339.784
HL4	-594.081	-594.081	-594.081
P11	0.110	0.338	0.497
P12	1.105	1.102	1.102
P13	1.105	1.102	1.102
P1V	0.110	0.338	0.497
P21	0.278	0.188	0.185
P22	2.008	3.568	5.006
P23	2.008	3.568	5.006
P2V	0.278	0.188	0.185
P31	0.110	0.110	0.110
P32	3.633	3.633	3.633
P33	3.633	3.633	3.633
P34	3.633	3.633	3.633
P3V	0.110	0.110	0.110
q11	1.000	1.000	1.000
q12	1.000	1.000	1.000
q13	0.000	0.000	0.000
q1V	0.439	0.288	0.206
q21	1.000	1.000	1.000

q22	1.000	1.000	1.000
q23	0.000	0.000	0.000
q2V	0.270	0.512	0.709
q31	1.000	1.000	1.000
q32	1.000	1.000	1.000
q33	1.000	1.000	1.000
q34	0.000	0.000	0.000
q3V	0.608	0.608	0.608
QB11	1528449	1963471	2742069
QB12	821397	1352543	2179131
QB13	109020	50273	20972
QB1L	598031	560654	541966
QB22	506549	602673	650662
QB23	300282	359029	388330
QB2L	206266	243643	262332
QB33	130819	130819	130819
QB3L	130819	130819	130819
Qout	2376758	2448791	3121136
S11	7.686	7.466	7.466
S12	7.686	7.466	7.466
S21	6.619	6.648	6.636
S22	6.619	6.648	6.636
S31	10.831	10.831	10.831
S32	10.831	10.831	10.831
T11	233.758	262.840	277.377
T13	310.000	304.000	304.000
T1V	233.758	262.840	277.377
T21	180.098	180.098	180.098
T23	236.758	265.840	280.377
T2V	180.098	180.098	180.098
T31	112.595	112.595	112.595
T33	236.758	265.840	280.377
T34	183.098	183.098	183.098
T3V	112.595	112.595	112.595
TL1	661.200	661.200	661.200
TL2	236.758	265.840	280.377
TL3	183.098	183.098	183.098
TL4	115.595	115.595	115.595
W1	235.641	134.811	105.296
W2	87.458	208.297	424.575
W3	77.356	77.356	77.356
W total	400.456	420.465	607.227

Table B9 Optimization result of up scaled variable model compare with PRO/II optimizer at minimum temperature approach equal to 3 K

	Initial PRO/II	GAMS	% Error	Optimizer PRO/II	% Error
F1	6252177	6252177	0.00	6000000	4.03
F2	1419042	1419042	0.00	1424208	0.36
F3	493172	493172	0.00	509067	3.22
H11	333.42	333.06	0.11	341.46	2.41
H12	474.76	475.40	0.13	488.05	2.80
H13	104.60	104.02	0.55	103.02	1.51
H1V	104.60	104.02	0.55	103.02	1.51
H21	180.26	180.65	0.22	180.78	0.29
H22	405.62	408.08	0.61	400.22	1.33
H23	-129.59	-129.99	0.31	-130.46	0.68
H2V	-129.59	-129.99	0.31	-130.46	0.68
H31	-155.60	-158.50	1.87	-156.10	0.33
H32	200.67	195.54	2.55	202.70	1.02
H33	53.76	53.93	0.31	53.27	0.90
H34	-388.26	-387.80	0.12	-383.02	1.35
H3V	-388.26	-387.80	0.12	-383.02	1.35
HL1	1223.67	1223.34	0.03	1223.28	0.03
HL2	59.92	59.77	0.25	59.34	0.96
HL3	-371.03	-373.65	0.70	-370.59	0.12
HL4	-594.08	-593.47	0.10	-595.14	0.18
P11	0.11	0.11	0.88	0.11	1.81
P12	1.25	1.27	1.36	1.26	0.56
P13	1.25	1.27	1.36	1.26	0.56
P1V	0.11	0.11	0.88	0.11	1.81
P21	0.14	0.13	11.19	0.13	4.86
P22	1.88	1.88	0.11	1.88	0.11
P23	1.88	1.88	0.11	1.88	0.11
P2V	0.14	0.13	11.19	0.13	4.86
P31	0.11	0.11	0.00	0.11	0.00
P32	3.03	3.05	0.79	3.06	1.24
P33	3.03	3.05	0.79	3.06	1.24
P34	3.03	3.05	0.79	3.06	1.24
P3V	0.11	0.11	0.00	0.11	0.00
q11	1.00	1.00	0.00	1.00	0.00
q12	1.00	1.00	0.00	1.00	0.00
q13	0.00	0.00	0.00	0.00	0.00
q1V	0.45	0.46	0.71	0.45	0.39
q21	1.00	1.00	0.00	1.00	0.00
q22	1.00	1.00	0.00	1.00	0.00

q23	0.00	0.00	0.00	0.00	0.00
q2V	0.33	0.34	4.97	0.34	3.18
q31	1.00	1.00	0.00	1.00	0.00
q32	1.00	1.00	0.00	1.00	0.00
q33	1.00	1.00	0.00	1.00	0.00
q34	0.00	0.00	0.00	0.00	0.00
q3V	0.55	0.55	1.46	0.55	0.23
QB11	1430615000	1431959427	0.09	1430653693	0.00
QB12	759490000	763537766.2	0.53	755809922	0.48
QB13	72448460	69841400.51	3.60	76069111	5.00
QB1L	598676500	598554117.9	0.02	598746506	0.01
QB22	439690600	440809891.4	0.25	443284282	0.82
QB23	217994400	217845286.5	0.07	222107681	1.89
QB2L	221696200	222954867.1	0.57	221166941	0.24
QB33	114744300	113082984.2	1.45	115517145	0.67
QB3L	114744300	113078045.5	1.45	115512091	0.67
Qout	2314294000	2321898115	0.33	2310147823	0.18
S11	7.61	7.69	1.01	7.72	1.50
S12	7.61	7.69	1.01	7.72	1.50
S21	6.72	6.76	0.59	6.74	0.31
S22	6.72	6.76	0.59	6.74	0.31
S31	10.83	10.94	0.97	10.95	1.17
S32	10.83	10.94	0.97	10.95	1.17
T11	233.26	233.48	0.09	238.87	2.41
T12		337.69	0.00	343.73	0.00
T13	310.00	309.86	0.05	309.52	0.15
T1V	233.26	233.48	0.09	233.25	0.00
T21	174.36	173.95	0.23	174.35	0.00
T22		348.04	0.00	343.72	0.00
T23	236.26	236.41	0.07	236.25	0.00
T2V	174.36	173.1	0.72	174.35	0.00
T31	112.60	112.59	0.00	112.65	0.05
T32		293.97	0.00	296.98	0.00
T33	236.26	236.41	0.07	236.25	0.00
T34	177.36	176.71	0.36	177.35	0.00
T3V	112.60	112.59	0.00	112.59	0.00
TL1	661.20	661.20	0.00	661.20	0.00
TL2	236.26	236.41	0.07	236.25	0.00
TL3	177.36	176.71	0.36	177.35	0.00
TL4	115.60	116.14	0.47	115.59	0.00
W1	245466.52	247205.22	0.71	244304.19	0.47
W2	88833.16	89646.63	0.92	86812.68	2.27
W3	48805.15	48501.03	0.62	50738.72	3.96
W total	383104.83	385352.88	0.59	381855.60	0.33

Table B10 Optimization result of up scaled variable model compare with PRO/II optimizer at minimum temperature approach equal to 5 K

	Initial PRO/II	GAMS	% Error	Optimizer PRO/II	% Error
F1	6340326	6340326	0.00	6304113	0.57
F2	1472595	1472595	0.00	1473678	0.07
F3	513733	513733	0.00	518309	0.89
H11	333.68	333.08	0.18	333.60	0.03
H12	474.64	474.30	0.07	475.54	0.19
H13	102.28	101.73	0.54	102.03	0.25
H1V	102.28	101.73	0.54	102.03	0.25
H21	178.03	178.54	0.28	179.64	0.91
H22	414.73	414.43	0.07	410.63	0.99
H23	-125.43	-123.89	1.23	-123.90	1.23
H2V	-125.43	-123.89	1.23	-123.90	1.23
H31	-156.60	-154.31	1.46	-156.27	0.21
H32	206.10	210.22	2.00	204.97	0.55
H33	58.50	57.72	1.34	57.68	1.40
H34	-378.97	-376.89	0.55	-376.89	0.55
H3V	-378.97	-376.89	0.55	-376.89	0.55
HL1	1223.67	1223.29	0.03	1223.29	0.03
HL2	65.30	65.15	0.23	65.15	0.23
HL3	-366.50	-366.55	0.01	-366.53	0.01
HL4	-588.57	-588.82	0.04	-588.81	0.04
P11	0.11	0.11	0.00	0.11	0.43
P12	1.25	1.25	0.00	1.25	0.24
P13	1.25	1.25	0.00	1.25	0.24
P1V	0.11	0.11	0.00	0.11	0.43
P21	0.12	0.12	0.00	0.13	5.55
P22	1.98	1.98	0.10	1.98	0.05
P23	1.98	1.98	0.10	1.98	0.05
P2V	0.12	0.12	0.00	0.13	5.55
P31	0.11	0.11	0.00	0.11	0.00
P32	3.12	3.12	0.00	3.12	0.06
P33	3.12	3.12	0.00	3.12	0.06
P34	3.12	3.12	0.00	3.12	0.06
P3V	0.11	0.11	0.00	0.11	0.00
q11	1.00	1.00	0.00	1.00	0.00
q12	1.00	1.00	0.00	1.00	0.00
q13	0.00	0.00	0.00	0.00	0.00
q1V	0.45	0.45	0.85	0.45	1.10
q21	1.00	1.00	0.00	1.00	0.00
q22	1.00	1.00	0.00	1.00	0.00

q23	0.00	0.00	0.00	0.00	0.00
q2V	0.36	0.36	0.71	0.36	0.33
q31	1.00	1.00	0.00	1.00	0.00
q32	1.00	1.00	0.00	1.00	0.00
q33	1.00	1.00	0.00	1.00	0.00
q34	0.00	0.00	0.00	0.00	0.00
q3V	0.57	0.57	0.65	0.57	0.65
QB11	1467170000	1466853677	0.02	1459845809	0.50
QB12	795437500	792725940	0.34	787721799	0.97
QB13	75825480	78343615	3.32	76339892	0.68
QB1L	595906800	595758100	0.02	595758100	0.02
QB22	446880600	445354698	0.34	447318476	0.10
QB23	224747000	223271283	0.66	225242515	0.22
QB2L	222133700	222073715	0.03	222066261	0.03
QB33	114242500	114342582	0.09	114346763	0.09
QB3L	114242500	114337583	0.08	114341769	0.09
Qout	2360901000	2362251817	0.06	2354635563	0.27
S11	7.61	7.69	1.05	7.69	1.05
S12	7.61	7.69	1.05	7.69	1.05
S21	6.72	6.76	0.69	6.75	0.55
S22	6.72	6.76	0.69	6.75	0.55
S31	11.01	10.97	0.34	11.73	6.54
S32	11.01	10.97	0.34	13.36	21.36
T11	233.41	233.48	0.03	233.38	0.01
T12		336.84	0.00	337.48	0.00
T13	310.00	309.09	0.29	309.19	0.26
T1V	233.41	233.48	0.03	233.38	0.01
T21	173.20	172.23	0.56	173.20	0.00
T22		352.16	0.00	350.14	0.00
T23	238.41	238.38	0.01	238.38	0.01
T2V	173.20	172.23	0.56	173.20	0.00
T31	112.60	113.49	0.79	112.59	0.00
T32		300.31	0.00	298.16	0.00
T33	238.41	238.38	0.01	238.38	0.01
T34	178.20	178.20	0.00	178.20	0.00
T3V	112.60	112.59	0.00	112.59	0.00
TL1	661.20	661.20	0.00	661.20	0.00
TL2	238.41	238.38	0.01	238.38	0.01
TL3	178.20	178.20	0.00	178.20	0.00
TL4	117.60	117.60	0.00	117.60	0.00
W1	248258.76	248721.56	0.19	248552.88	0.12
W2	96821.37	96492.01	0.34	94556.50	2.34
W3	51758.33	52020.09	0.51	52009.91	0.49
W total	396838.45	397233.66	0.10	395119.29	0.43

Table B11 Optimization result of up scaled variable model compare with PRO/II
optimizer at minimum temperature approach equal to 7 K

	Initial PRO/II	GAMS	% Error	Optimizer PRO/II	% Error
F1	6524276	6524276	0.00	6557105	0.50
F2	1484540	1484540	0.00	1492024	0.50
F3	479884	479884	0.00	485685	1.21
H11	333.16	333.86	0.21	333.06	0.03
H12	480.03	480.50	0.10	479.03	0.21
H13	106.87	107.96	1.02	107.96	1.02
H1V	106.87	107.96	1.02	107.96	1.02
H21	177.78	176.73	0.59	176.98	0.45
H22	429.90	426.36	0.82	426.90	0.70
H23	-119.00	-118.99	0.01	-118.99	0.01
H2V	-119.00	-118.99	0.01	-118.99	0.01
H31	-155.60	-153.54	1.32	-156.27	0.44
H32	204.43	209.81	2.63	202.43	0.98
H33	63.47	62.57	1.41	62.55	1.44
H34	-384.94	-381.56	0.88	-381.57	0.88
H3V	-384.94	-381.56	0.88	-381.57	0.88
HL1	1223.67	1223.29	0.03	1223.29	0.03
HL2	69.20	69.39	0.28	69.39	0.28
HL3	-368.95	-369.70	0.20	-369.70	0.20
HL4	-582.89	-582.41	0.08	-582.41	0.08
P11	0.11	0.11	0.00	0.11	0.37
P12	1.31	1.31	0.00	1.31	0.00
P13	1.31	1.31	0.00	1.31	0.00
P1V	0.11	0.11	0.00	0.11	0.37
P21	0.11	0.11	0.00	0.11	0.01
P22	2.06	2.06	0.10	2.06	0.10
P23	2.06	2.06	0.10	2.06	0.10
P2V	0.11	0.11	0.00	0.11	0.01
P31	0.11	0.11	0.00	0.11	0.00
P32	3.07	3.07	0.00	3.07	0.03
P33	3.07	3.07	0.00	3.07	0.03
P34	3.07	3.07	0.00	3.07	0.03
P3V	0.11	0.11	0.00	0.11	0.00
q11	1.00	1.00	0.00	1.00	0.00
q12	1.00	1.00	0.00	1.00	0.00
q13	0.00	0.00	0.00	0.00	0.00
q1V	0.46	0.47	1.99	0.47	1.91
q21	1.00	1.00	0.00	1.00	0.00
q22	1.00	1.00	0.00	1.00	0.00

q23	0.00	0.00	0.00	0.00	0.00
q2V	0.37	0.38	1.40	0.38	1.40
q31	1.00	1.00	0.00	1.00	0.00
q32	1.00	1.00	0.00	1.00	0.00
q33	1.00	1.00	0.00	1.00	0.00
q34	0.00	0.00	0.00	0.00	0.00
q3V	0.56	0.56	0.02	0.56	0.02
QB11	1476406000	1473851968	0.17	1476020640	0.03
QB12	814857800	809591476	0.65	814483438	0.05
QB13	67647510	70657462	4.45	67934199	0.42
QB1L	593901000	593602466	0.05	593602466	0.05
QB22	440586000	439015634	0.36	441589484	0.23
QB23	215184600	213131991	0.95	215705842	0.24
QB2L	225401500	225883437	0.21	225883437	0.21
QB33	110059500	109424842	0.58	109424840	0.58
QB3L	110059500	109424741	0.58	109424741	0.58
Qout	2434632000	2430607641	0.17	2433175337	0.06
S11	7.61	7.70	1.10	7.69	1.04
S12	7.61	7.70	1.10	7.69	1.04
S21	6.77	6.78	0.07	6.78	0.07
S22	6.77	6.78	0.07	6.78	0.07
S31	11.00	10.98	0.19	10.96	0.41
S32	11.00	10.98	0.19	10.96	0.41
T11	232.97	233.46	0.21	232.94	0.02
T12		340.72	0.00	340.01	0.00
T13	310.00	311.17	0.38	311.17	0.38
T1V	232.97	232.85	0.05	232.94	0.02
T21	170.75	170.55	0.12	170.54	0.12
T22		359.15	0.00	359.44	0.00
T23	239.97	239.94	0.02	239.94	0.02
T2V	170.75	170.55	0.12	170.54	0.12
T31	112.60	113.85	1.12	112.59	0.00
T32		299.91	0.00	296.88	0.00
T33	239.97	239.94	0.02	239.94	0.02
T34	177.75	177.54	0.11	177.54	0.11
T3V	112.60	112.59	0.00	112.59	0.00
TL1	661.20	661.20	0.00	661.20	0.00
TL2	239.97	239.94	0.02	239.94	0.02
TL3	177.75	177.54	0.11	177.54	0.11
TL4	119.60	119.61	0.01	119.61	0.01
W1	266173.92	265765.84	0.15	265876.48	0.11
W2	103964.38	102937.74	0.99	103581.66	0.37
W3	47992.38	48434.61	0.92	48393.11	0.83
W total	418130.67	417138.20	0.24	417851.24	0.07

Table B12 Optimization result of up scaled variable model compare with PRO/II optimizer at minimum temperature approach equal to 9 K

	Initial PRO/II	GAMS	% Error	Optimizer PRO/II	% Error
F1	6784782	6784782	0.00	6706159	1.16
F2	1551579	1551579	0.00	1553471	0.12
F3	527697	527697	0.00	526547	0.22
H11	332.90	331.60	0.39	332.95	0.01
H12	477.70	477.13	0.12	478.67	0.20
H13	109.06	107.96	1.01	106.98	1.91
H1V	109.06	107.96	1.01	106.98	1.91
H21	177.30	177.68	0.21	176.99	0.17
H22	434.01	433.72	0.07	431.16	0.65
H23	-112.59	-112.87	0.25	-112.84	0.22
H2V	-112.59	-112.87	0.25	-112.84	0.22
H31	-156.60	-156.21	0.25	-156.27	0.21
H32	213.89	212.34	0.72	213.94	0.03
H33	64.09	63.91	0.28	63.26	1.29
H34	-366.43	-367.12	0.19	-367.67	0.34
H3V	-366.43	-367.12	0.19	-367.67	0.34
HL1	1223.67	1223.29	0.03	1223.29	0.03
HL2	73.73	74.47	1.01	74.47	1.01
HL3	-359.00	-359.72	0.20	-359.69	0.19
HL4	-577.05	-576.06	0.17	-576.06	0.17
P11	0.11	0.11	0.00	0.11	0.00
P12	1.30	1.31	0.77	1.30	0.00
P13	1.30	1.31	0.77	1.30	0.00
P1V	0.11	0.11	0.00	0.11	0.00
P21	0.11	0.11	0.00	0.11	0.09
P22	2.16	2.16	0.05	2.14	0.79
P23	2.16	2.16	0.05	2.14	0.79
P2V	0.11	0.11	0.00	0.11	0.09
P31	0.11	0.11	0.00	0.11	0.00
P32	3.27	3.27	0.00	3.30	1.11
P33	3.27	3.27	0.00	3.30	1.11
P34	3.27	3.27	0.00	3.30	1.11
P3V	0.11	0.11	0.00	0.11	0.00
q11	1.00	1.00	0.00	1.00	0.00
q12	1.00	1.00	0.00	1.00	0.00
q13	0.00	0.00	0.00	0.00	0.00
q1V	0.46	0.47	0.67	0.46	0.17
q21	1.00	1.00	0.00	1.00	0.00
q22	1.00	1.00	0.00	1.00	0.00

q23	0.00	0.00	0.00	0.00	0.00
q2V	0.39	0.39	1.05	0.39	1.06
q31	1.00	1.00	0.00	1.00	0.00
q32	1.00	1.00	0.00	1.00	0.00
q33	1.00	1.00	0.00	1.00	0.00
q34	0.00	0.00	0.00	0.00	0.00
q3V	0.59	0.59	0.08	0.59	0.11
QB11	1518716000	1517397395	0.09	1515425417	0.22
QB12	848092200	848077981	0.00	845091151	0.35
QB13	79050030	78328093	0.91	79342946	0.37
QB1L	591573700	590965511	0.10	590965511	0.10
QB22	449790000	450811898	0.23	450247724	0.10
QB23	227179600	227450483	0.12	226901671	0.12
QB2L	222610400	223351658	0.33	223336298	0.33
QB33	112169900	111293940	0.78	111309280	0.77
QB3L	112169900	111289058	0.79	111304418	0.77
Qout	2501115000	2504747562	0.15	2492637583	0.34
S11	7.61	7.69	1.05	7.69	1.05
S12	7.61	7.69	1.05	7.69	1.05
S21	6.78	6.78	0.11	6.78	0.05
S22	6.78	6.78	0.11	6.78	0.05
S31	11.01	10.96	0.50	10.96	0.50
S32	11.01	10.96	0.50	10.96	0.50
T11	232.78	232.85	0.03	232.85	0.03
T12		339.08	0.00	339.70	0.00
T13	312.00	311.17	0.27	310.84	0.37
T1V	232.78	232.85	0.03	232.85	0.03
T21	170.60	171.07	0.28	170.56	0.02
T22		363.73	0.00	362.26	0.00
T23	241.78	241.85	0.03	241.85	0.03
T2V	170.60	170.55	0.03	170.56	0.02
T31	112.60	112.60	0.00	112.59	0.00
T32		301.85	0.00	302.67	0.00
T33	241.78	241.85	0.03	241.85	0.03
T34	179.60	179.59	0.00	179.60	0.00
T3V	112.60	112.59	0.00	112.59	0.00
TL1	661.20	661.20	0.00	661.20	0.00
TL2	241.78	241.85	0.03	241.85	0.03
TL3	179.60	179.59	0.00	179.60	0.00
TL4	121.60	121.60	0.00	121.60	0.00
W1	272888.56	274263.98	0.50	271447.89	0.53
W2	110639.51	110351.70	0.26	109678.79	0.87
W3	54306.37	54023.52	0.52	54148.71	0.29
W total	437834.45	438639.20	0.18	435275.39	0.58

Table B13 Equipment cost of scaled up case minimum temperature approach equal to 3 K

	Heat Transfer [kJ/h]	LMTD	Area [m²]	Work [kW]	Log C	Cost [$]
1st Heat Exchanger	1430615000	18.721	23585.067		8.92944	850043834
2nd Heat Exchanger	439690600	9.687	14008.895		8.44599	279252750
3rd Heat Exchanger	114744300	22.287	1589.017		6.69511	4955768
Cooler	2314294000	4.453	360873.158		6.86952	7404929
Compressor 1				245466.52	6.63860	4351143
Compressor 2				88833.16	6.50678	3212057
Compressor 3				48805.15	6.41036	2572569
Total Equipment Cost						1151793053
Total Equipment Cost after consider Cost index						5492794600

Table B14 Equipment cost of scaled up case minimum temperature approach equal to 5 K

	Heat Transfer [kJ/h]	LMTD	Area [m²]	Work [kW]	Log C	Cost [$]
1st Heat Exchanger	1467170000	22.278	20325.885		8.78888	615014360
2nd Heat Exchanger	446880600	12.261	11249.173		8.24982	177757664
3rd Heat Exchanger	114242500	25.046	1407.788		6.61045	4078037
Cooler	2360901000	3.549	461913.163		6.95440	9003463
Compressor 1				248258.76	6.63984	4363602
Compressor 2				96821.37	6.51950	3307520
Compressor 3				51758.33	6.42043	2632930
Total Equipment Cost						816157578
Total Equipment Cost after consider Cost index						3892180051

Table B15 Equipment cost of scaled up case minimum temperature approach equal to 7 K

	Heat Transfer [kJ/h]	LMTD	Area [m^2]	Work [kW]	Log C	Cost [$]
1st Heat Exchanger	1476406000	26.628	17112.715		8.62878	425388925
2nd Heat Exchanger	440586000	14.346	9478.700		8.09977	125828164
3rd Heat Exchanger	110059500	27.476	1236.296		6.52113	3319945
Cooler	2434632000	6.873	245976.091		6.73997	5495102
Compressor 1				266173.92	6.64738	4440026
Compressor 2				103964.38	6.52980	3386881
Compressor 3				47992.38	6.40746	2555425
Total Equipment Cost						570414471
Total Equipment Cost after consider Cost index						2720253889

Table B16 Equipment cost of scaled up case minimum temperature approach equal to 9 K

	Heat Transfer [kJ/h]	LMTD	Area [m^2]	Work [kW]	Log C	Cost [$]
1st Heat Exchanger	1518716000	29.815	15721.178		8.55087	355527808
2nd Heat Exchanger	449790000	16.812	8257.341		7.98086	95689178
3rd Heat Exchanger	112169900	30.498	1135.141		6.46327	2905873
Cooler	2501115000	5.890	294867.142		6.80090	6322737
Compressor 1				272888.56	6.65003	4467205
Compressor 2				110639.51	6.53864	3456540
Compressor 3				54306.37	6.42857	2682742
Total Equipment Cost						471052086
Total Equipment Cost after consider Cost index						2246403856

Table B17 Annual operating cost of scaled up all cases

	3K	5K	7K	9K
Compressor 1	568251	575184	616691	632248
Compressor 2	205815	224323	240872	256337
Compressor 3	113075	119917	111192	125821
Total [$/h]	887142	919425	968756	1014407
Total [$/y]	7771369421	8054163937	8486307108	8886211173

Appendix C Total Annual Cost Calculation

CAPCOST equation is used to calculate capital cost (CAPEX).

$$\log_{10} C_P^0 = K_1 + K_2 \log_{10}(A) + K_3 [\log_{10}(A)]^2$$

C_P^0 is capital cost of equipment in USD

K   is constant

A   is a size parameter of the equipment

LNG heat exchanger of case 3K is used as case study. K of LNG heat exchanger is selected as follows.

$$
\begin{array}{lcl}
K_1 & = & 3.9912 \\
K_2 & = & 0.0668 \\
K_3 & = & 0.2430 \\
\end{array}
$$

Size parameter of LNG heat exchanger is area which is calculated as follows.

$$Q = UA\Delta T_{lm}$$

Q   is heat transfer in the box

U   is overall heat transfer coefficient

ΔT_{lm} is log mean temperature difference

$$1430615000 = 3240 \; x \; A \; x \; 18.72$$

$$A = 23585.06 \; m^2$$

So, cost of LNG heat exchanger is calculated as follows.

$$\log_{10} C_P^0 = 3.9912 + 0.0668 \log_{10}(23585.06) + 0.2430[\log_{10}(23585.60)]^2$$

$$C_P^0 = 850043834 \; USD$$

Chemical engineering plant cost index is used to correct value.

$$C_{present} = C_{old} \frac{I_{present}}{I_{old}}$$

$$C_{present} = 850043834 \frac{119}{567.5}$$

$$C_{present} = 178247077$$

Operating cost consider only electricity bill of compressor. The electricity bill per kilo watt is referred from the Metropolitan Electricity Authority of Thailand.

$$C_{elect} = 2.316875 \; [USD/kW]$$

Operating cost is calculated from following equation.

$$OPEX = 8760 C_{elect} W^k$$
$$OPEX = 8760(2.316875)(245266.52)$$
$$OPEX = 568251.8685 \; [USD/h]$$
$$OPEX = 4977886368 \; [USD/y]$$

When assumption is applied, total annual cost can be calculated as follows.

$$TAC = CAPEX + OPEX$$
$$TAC = \left(\frac{178247077 \times 0.015}{1 - (1 + 0.015)^{-20}} \right) + 4977886368$$
$$TAC = 4980734070 \; [USD/y]$$

CURRICULUM VITAE

Name: Mr. Naken Saetang

Date of Birth: August 21, 1993

Nationality: Thai

University Education:

2016-2018 Master Degree of Petroleum Technology, The Petroleum and Petrochemical College, Chulalongkorn University, Bangkok, Thailand

2012-2015 Bachelor Degree of Chemical Technology, Faculty of Science, Chulalongkorn University, Bangkok, Thailand

Work Experience:

2014 Position: Process Engineer Trainee

Company name: Thai Beverage Plc.

Proceedings:

1. Saetang, N., Bagajewicz, M.J., and Suriyapraphadilok, U., (2018, June 5) Optimization of Single Refrigerant in Commercial LNG Cascade Process. Proceedings of The 24th PPC Symposium on Petroleum, Petrochemicals, and Polymers and The 9th Research Symposium on Petrochemicals and Materials Technology, Bangkok, Thailand.

2. Saetang, N., Bagajewicz, M.J., and Suriyapraphadilok, U., (2017, Oct 18-20) Optimization of the Single Refrigerant ConocoPhillips LNG Cascade Process. Proceedings of The 7th International Thai Institute of Chemical Engineering and Applied Chemistry Conference 2017 (ITChE 2017), Bangkok, Thailand.